A STRATIGRAPHIC AND GEOCHEMICAL ANALYSIS OF THE OJINAGA FORMATION, WEST TEXAS

A Thesis

by

BRONWYN TAYS MOORE

Submitted to the Office of Graduate and Professional Studies of
Texas A&M University
in partial fulfillment of the requirements for the degree of

MASTER OF SCIENCE

Chair of Committee,	Michael Pope
Committee Members,	Art Donovan
	Zoya Heidari
Head of Department,	Michael Pope

August 2016

Major Subject: Geology

ABSTRACT

Stratigraphic, biostratigraphic and geochemical analysis yields a greater understanding of the depositional environment of the Upper Cretaceous Ojinaga Formation in West Texas. A detailed measured section of the Ojinaga Formation in Hudspeth County can be correlated to the coeval Boquillas Formation in the Big Bend Region (Brewster County, West Texas) and prolific unconventional Eagle Ford Group in Terrell County (West Texas), providing a better understanding of the Cenomanian-Turonian depositional system in west Texas.

A high-resolution study of two outcrops in Mule Canyon in Hudspeth County, West Texas, documents this unit's lithology, composition, sedimentary structures, and gamma ray response on a local scale. Three distinct lithostratigraphic facies, termed facies 1-3 from the base up were identified in the Ojinaga Formation based on significant lithological and geochemical changes. The most notable change in facies is the transition from facies 1 to facies 2, indicating a depositional shift from storm-influenced sediments on a carbonate ramp to deep ramp sediments as the result of an increase in accommodation. Facies 2 represents the greatest thickness observed in the section, suggesting an extended period of marine transgression and high accommodation. Facies 2 gradationally transitions into facies 3, noted by increasing carbonate-dominated deposits and decreasing pelagic mudstone. The increase in frequency of carbonate beds interbedded with mudstone may suggest a marine regression and decrease in accommodation.

Geochemical analysis supports the interpretation of three facies within the Ojinaga Formation in Mule Canyon. It is the geochemical observations derived from spectral gamma ray response used to correlate the Ojinaga with the Boquillas and Eagle Ford formations. From this work it is evident that the Ojinaga Formation at Mule Canyon correlates almost entirely to the Lower Eagle Ford Formation in Terrell County. Only a few meters of the uppermost portion of the section at Mule Canyon can be correlated to the Upper Eagle Ford Formations. Biostratigraphic data, indicating that the Mule Canyon Ojinaga Formation strata are Cenomanian in age, supports the gamma ray correlations.

The Ojinaga Formation records a shift in depositional environment from lower ramp carbonate tempestite deposits to more basinal sediments. A change from hummocky to swaley cross-stratification with bedding scour bases, to organic rich carbonate-dominated mudstones are the lithological reflections of this shift. Geochemical analysis indicates the Ojinaga Formation was deposited during euxinic (likely episodic) periods due to basin restriction with increasing marine circulation and oxygenation occurring over time toward the top of the section. Unique environmental conditions in the Western Interior Seaway during portions of the Middle to Late Cenomanian allowed for more total organic carbon preservation in the lowermost portions of the Ojinaga Formation.

ACKNOWLEDGEMENTS

I would like to thank my committee chair, Dr. Pope, and my committee members, Dr. Donovan, and Dr. Heidari, for their guidance and support throughout the course of this research.

I also want to extend my gratitude to the BP America Corporation, which provided the funds, equipment, and logistical support for this study. Field assistance was generously provided by Trey Lyons, Andrew Philbin and Eric Peavey. I would also like to thank Matthew Wehner and Scott Staerker for their valuable contributions and technical guidance.

I have been blessed with unwavering support from my friends and peers during my time at Texas A&M University, including Rachael Bouwmeester, Matt Jackson, Robert Grajeda, Lauren Holder, Michelle Chrpa, Drew Davis, Philipp Lithos and Pat Wagner.

Finally, I must express my very profound gratitude to my parents and my brother for believing in me and encouraging me throughout my eight years of university studies. I am so fortunate to have such an amazing group of family and friends; this would not have been possible without them. Thank you!

TABLE OF CONTENTS

Page

LIST OF FIGURES

Page

LIST OF TABLES

Page

1. INTRODUCTION

The Eagle Ford Group in South Texas is currently one of the most active unconventional source rock plays in the United States. In 2013 over $30 billion was spent developing this play in South Texas (Pickett, 2013). Production from the Eagle Ford Group in South Texas comes from marine organic-rich carbonate mudstones that are both horizontally and laterally extensive as well as productive through the oil to dry gas windrow (EIA, 2012). Previous work (Neybert, 1985) suggested that the Ojinaga strata exposed in the southern Quitman Mountains (Hudspeth County) of northwest Texas was equivalent to the Eagle Ford Group of South Texas. Coeval Eagle Ford strata in the Big Bend area are often referred to as the Boquillas Formation (REF). It is the comparison of the Ojinaga Formation in the Quitman Mountains of northwest Texas, to the Boquillas Formation in the Big Bend region of West Texas, and the Eagle Ford Formation in West Texas (Terrell County), as well as South Texas that is the focus of this study.

The Ojinaga Formation outcrop section at Mule Canyon is 229 m thick. At this locality it consists primarily of black, organic-rich, calcareous mudstones with abundant interbedded carbonate beds near the base of the unit. The lower boundary with the Buda Formation is interpreted as an unconformity based on the irregular nature of the contact, as well as the abrupt change in lithologies across it. The upper boundary with the overlying San Carlos Formation is not exposed in the study area.

The coeval Ojinaga, Boquillas and Eagle Ford formations in West Texas (Figure. 1) were deposited during a major first-order epicontinental marine transgression and subsequent maximum highstand within the Upper Cretaceous seaway that extended across North America (Sloss, 1963). During the Cenomanian, marine waters transgressed north from the Gulf of Mexico and south from the Arctic to form the Western Interior Seaway, and merged into one continuous seaway in the earliest Turonian (Cantu-Chapa, 1993). The thickness and lithological changes observed within these formations reflect the facies, physiographic, and accommodations variations across the paleo-floor of the epicontinental seaway of present day Texas, where these strata were deposited. The Eagle Ford in West Texas was deposited on the seafloor of the flooded Comanche Platform, as well as on the seafloor of a submarine plateau to the east in South Texas (Donovan et al., 2012). The Boquillas Formation in West Texas was deposited on the seafloor along the southwest margin of the Comanche Platform, while the Ojinaga Formation was deposited on a deeper portion of the seafloor off the Comanche Platform to the northwest (Cantu-Chapa., 1993)

The last extensive work on the Ojinaga Formation in West Texas (Neybert, 1985) focused on its petrography and the depositional environment. This study of the Ojinaga Formation provides a more detailed characterization of the Ojinaga Formation utilizing petrophysical, biostratigraphic and geochemical data. Based on this information a regional sequence stratigraphic framework, depositional environment, and chronostratigraphy are also proposed. The detailed

characterization of the Ojinaga Formation of this study also provides a data point which allows correlations to the coeval Boquillas Formation in Big Bend National Park and the Eagle Ford Formation in Lozier Canyon (Terrell County).

2. GEOLOGIC SETTING

The Late Cretaceous Ojinaga Formation is comprised of marine mudstone that was deposited on the floor of the Western Interior Seaway (WIS) in what is now present day northwest Texas and northeast Mexico. The Ojinaga Formation is exposed within the Cordilleran Mountain system of western North American. The Cordilleran Mountain system consists of three tectonic provinces; Sierra Madre Occidental, Mesa Central and Sierra Madre Oriental (Neybert 1985). The Ojinaga Formation of this study is located within the Quitman Mountains in the Sierra Madre Oriental tectonic province in present day Hudspeth County (Figure. 2A).

A major structural element in northeastern Mexico and western Texas is the Chihuahua Trough (Cordoba et al., 1970). The Diablo Platform bounds the Chihuahua Trough to the northeast and the Aldama Platform borders it to the southwest (Figure. 2A). Throughout the late Jurassic and Cretaceous an estimated 6000 m of sediment accumulated in the Chihuahua Trough (Neybert 1985). The Late Cretaceous through Early Cenozoic Laramide Orogeny produced the faulted mountains of the Chihuahua tectonic belt and Chihuahua trough. The Ojinaga Formation outcrops in the southern Cieneguilla-Quitman Mountain range, a northwest trending 4-6 mi wide and more than 60 mi long mountain range within the Chihuahua Tectonic Belt (Reaser and Underwood, 1982). In Texas the Chihuahua Tectonic Belt is comprised of four mountain ranges; Campo Grande Mountains, the Malone Mountains, the Southern Quitman Mountains, and Devil Ridge (Berge, 1982). During the Late Triassic to Late Jurassic normal faulting

formed the Chihuahua Trough as intracontinental marine basins expanded from the Jurassic opening of the Gulf of Mexico (Dickinson 1981, Dickinson et al., 1986, Berge, 1982). The Late Cretaceous and Paleogene Laramide Orogeny caused extensive compression, folding and thrusting towards the northeast (Berge, 1982). Lastly, during the Neogene this area was split into isolated ranges by Basin-and-Range extension. The Ojinaga Formation within the southern Quitman Mountains is characterized by folds, thrusts and overturned stratigraphic sections directed east or northeast towards the Diablo Platform (Jones and Reaser, 1970).

The Jurassic magmatic arc in the western U.S. originated from a subduction zone that continued into the Cretaceous (Cantu -Chapa, 1993). The magmatic arc affected sedimentation in the Chihuahua basin by depositing numerous bentonite beds. In the northern part of the Chihuahua tectonic belt there is evidence of tectonic activity in the Neocomian and Early Aptian (Cantu-Chapa et al., 1985), which is correlated to the Sevier Orogeny (Heller and Paola, 1989). From the Aptian through to the Turonian a relatively stable tectonic environment persisted in southern North America resulting in large amounts of carbonate being deposited in the shallow intracratonic basins in Texas and Mexico. During the early Cenomanian the Ojinaga Formation was deposited unconformably above the Buda Limestone in the southern Quitman Mountains. The Ojinaga Formation developed was deposited in a lower shoreface to offshore setting on the floors of an epicontinental seaway following a period of subaerial exposure of the top of the underlying Buda Formation. The unconformity marks a break in sedimentation

and change in depositional environment from highly bioturbated marine skeletal wackstone deposited on a well-oxygenated seafloor during Buda time to relatively un-bioturbated organic-rich carbonate mudstone deposited on an oxygenic depleted euxinic seafloor during Ojinaga time (Neybert, 1985).

3. PREVIOUS WORK

The Ojinaga Formation outcrops of Hudspeth County previously were analyzed by Powell (1964) Neybert (1985) and Purcell (1987). Powell's (1964) work on the Ojinaga Formation developed a lithological and paleontological correlation of the Ojinaga Formation, Chispa Summit Formation and Boquillas Formation (Powell, 1964). Neybert (1995) provided a detailed petrographic analysis and interpretation of the Ojinaga Formation depositional environments, while Purcell (1987) determined the structural history of the Ojinaga Formation. The coeval Eagle Ford Group and Boquillas Formation were studied by a number of authors including Hazzard (1959), Freeman (1961,1968), Trevino (1988) and Lock and Peschier (2006). Important biostratigraphy work on these units was completed by Pessagno (1969) and Smith (1981). Donovan and Staerker (2010), Donovan and others (2012), and Donovan and others (2015) provided additional geochemical, paleontological and petrographic information to refine lithological, biostratigraphic, geochemical, sedimentological properties as well as define depositional sequences and mappable units.

4. METHODOLOGY

This study of the Ojinaga Formation in Mule Canyon (Hudspeth County), northwest Texas (Figure. 2B) was focused on the sedimentology, organic geochemistry, inorganic geochemistry, biostratigraphy, chemostratigraphy and sequence stratigraphy. Data collection and fieldwork was conducted during two two-week periods in June 2014 and a two-week period in May 2015. The fieldwork involved measuring two sections bed-by-bed and sampling each geological section. A complete Ojinaga Formation section does not occur in the area due to isoclinal folds in its upper part and extensive Cenozoic erosion (Neybert 1985). One 229 m thick section and a 45 m thick section were measured of the lower Ojinaga Formation in this study (Figure, 2B).

4.1 Measured Section

The two outcrops sections (Figure. 2B) were measured with the aid of a Brunton Compass and a Jacob's Staff. Mule Canyon 1 (MC1) is an incomplete 229 m outcrop section whose top occurs at the hinge of the first isoclinal fold on the most prominent topographic knob in the area (Figure3). The Mule Canyon 2 (MC2) outcrop is a well-exposed 46 m section recording the basal Ojinaga Formation. MC2 is located approximately 244 m southeast from MC1 (Figure. 1). Carbonate rocks in these sections were classified using Dunham's (1962) classification. Sedimentary structures were classified using Campbell's (1967) classification. The two measured sections incorporated descriptions of lithology, bed thickness, color,

fossil type and abundance and sedimentary structures. The criterion used to distinguish between wave and current related sedimentary structures are outlined in Table 1. Hand samples were collected approximately every 75 cm from both sections. The Ojinaga Formation measured section MC1 was informally sub-divided into three local facies 1, 2 & 3 (Figure. 8).

4.2 Gamma Ray Scintillometer

A Terraplus RS-230 hand-held gamma-ray Scintillometer collected spectral gamma-ray (SGR) values every 30 cm at MC1. Total gamma ray response (Figure. 8)was estimated using the empirical formula GR (API) = 8*U(ppm)+4*Th(ppm)+16*K(%) from Herron and Herron (1996).

Multiple variables may have affected the SGR readings collected during this study. The SGR values were collected over five days on two separate trips. Section MC1 has varying degrees of weathering; fresh rock surfaces were created where possible. In areas of overburden (marked by X's on stratigraphic column, Figure. 8), small trenches were dug to expose fresh rock surfaces.

The SGR was used to create a spectral gamma-ray (GR) profile that can be used to correlate with subsurface wells and coeval formation outcrops. The GR profile displays the variability of uranium (U), thorium (Th) and potassium (K) content within the MC1 section. These elements are used as generalized respective proxies for organic-matter, the occurrence of bentonite beds and clay content, respectively.

4.3 Thin-Section Petrography

Twelve standard size (27 x 36 mm) thin section and twenty-four large size (50 x 75 mm) thin-sections were prepared from MC1 and MC2 hand samples. The thin-sections were impregnated with blue dye to detect porosity. Thin sections were analyzed using a petrographic microscope equipped with camera and computer software capable of measuring grain and pore size. Photos of each thin-section were taken to accompany the thin-section descriptions. All photographs and thin-section descriptions are included in Appendix C.

Thin-sections were analyzed for lithology, fossil content, composition, pore characteristics, depositional texture and fabric, and digenetic alterations. Pore characteristics were classified as depositional, diagenetic, or fracture related using Ahr's (2008) classification scheme that categorizes pores.

4.4 Stable Isotope Analysis

Stable Isotope Analysis of $\delta^{13}C$ and $\delta^{18}0$ was determined on 65 samples collected from MC1 and MC2 at Texas A&M University's Stable Isotope Geoscience Facility. Of the 65 samples 44 carbonate samples from MC1 and MC2 were collected and analyzed for inorganic carbon, 21 samples of calcareous mudstone were decarbonated and analyzed for organic carbon $\delta^{13}C$. Approximately 1 mg of the powdered carbonate samples were analyzed for $\delta^{13}C$ using a Carlo Erba NA1500 elemental analyzer (EA) coupled to a Thermo Finnigan Delta XP isotope ratio mass spectrometer (IRMS). Every fifth sample or more was run in duplicate.

Carbon and nitrogen isotope values were calibrated with USGS 40 (-26.39‰ and -4.52‰) and USGS 41 (37.63‰ and 47.57‰) L-glutamic acid standards, and reported versus VPDB and air respectively. Analytical precision of 0.13‰ was obtained for $\delta^{13}C$ based on replicates of standards. This stable isotope analysis was conducted for comparison to the geochemical signature at the Cenomanian-Turonian (C-T) boundary global strata-type section and point (GSSP) located near Pueblo, Colorado (Ogg and Hinov, 2012). This method supplements the biostratigraphic markers and lithological ages.

4.5 Total Organic Carbon Analysis

Total organic carbon analysis was completed by GeoMark research on 17 samples (Figure2). 11 samples were collected over the 229 m MC1 section. The remaining 6 samples were collected from the 46 m MC2 section. The methods by which GeoMark laboratories extracted the TOC measurements are described in Appendix A. The results indicate vertical variations of the organic content within the Ojinaga Formation. The TOC also provides an understanding of the paleodepositional environment and organic matter preservation.

4.6 X-ray Fluorescence

A Thermo Scientific Niton XL3t GOLDD+ handheld x-ray fluorescence (XRF) tool, calibrated with x-ray diffraction data, was used on seventy-eight samples in the Texas A&M University rock physics laboratory. The samples were collected from the 229 m Mule Canyon Section 1. The analysis provides compositional

information to determine the major and trace element chemostratigraphy of the Ojinaga Formation. The hand-held XRF analysis from thin section samples and powered samples provided major element oxide concentrations for 7 elements and trace element concentrations for 16 elements. Element concentrations are interpreted as a measurement of specific lithological facies or paleodepositional environment indicators. The XRF measurement of aluminum (Al) is used as a proxy for the content of clay, calcium (Ca) for carbonate content and silica (Si) for quartz, respectively (Ratcliffe et al., 2012). Molybdenum (Mo) is used to determine paleoredox conditions and thus paleodepositional environment. Sediments deposited within anoxic and euxinic conditions in modern and ancient marine environments, sediments deposited create major trace element sinks (such as Molybdenum (Mo) and nickel (Ni)) (Calvert and Pedersen, 1993). Trace elements can indicate and be predictors for oxygen-poor conditions and preservation of organic matter.

4.7 Biostratigraphy

Twenty-two Ojinaga Formation samples for biostratigraphy (foraminiferal, calcareous nannofossils and palynology) were collected approximately every 9 m in MC1. Biostratigraphic analysis also was performed on 25 samples collected from Mule Canyon Section 1 (Figure2). Dr. James Pospichal at BugWare Inc completed the biostratigraphic analysis. The microfossil biostratigraphy provided information for correlation of lithological units to the Eagle Ford and Boquillas Formation. The

biostratigraphic age markers incorporated the first and last occurrence of key age defining foraminiferal, nannofossils and palynological assemblage.

5. RESULTS

The Ojinaga Formation in the study area is unconformably bounded below by the Buda Formation and its upper contact is not exposed in this area (Neybert, 1985). Erosional surfaces, bentonite beds and biostratigraphic data, provide a chronostratigraphic framework for correlating the Ojinaga Formation to the coeval Boquillas Platform sequence and the Eagle Ford Formation.

5.1 Buda-Ojinaga Contact

The contact of the Buda Formation and the Ojinaga Formation is unconformity exposed within the study area. At the base of Mule Canyon Section 1 the Buda Formation is exposed as a steeply dipping west facing flank of an anticline. The Buda Formation forms an eastern side of the canyon at the base of MC1, with the Ojinaga Formation exposed on the western side of the canyon. The eroded and highly bioturbated Buda Limestone lies abruptly below the dark, thinly bedded mudstone of the Ojinaga Formation.

5.2 Lithological Units

Detailed facies descriptions are illustrated in Table 1. Significant facies characteristics are presented here.

The Ojinaga Formation at Mule Canyon is sub-divided into a vertical succession of three facies (units);

1. Facies 1: Interbedded foraminiferal packstone, siltstone and mudstone with wavy laminations and/ or hummocky cross stratification.
2. Facies 2: Interbedded parallel laminated calcareous siltstone and mudstone.
3. Faces 3: Interbedded parallel laminated foraminiferal packstone and mudstone.

Faces 1 consists of approximately 38 m of hummocky cross-stratified and wavy laminated foraminiferal packstone interbedded with wavy to parallel laminated calcareous stilstone and thinly bedded mudstone. The foraminiferal packstone commonly contains very low-angle laminations with areas of truncations. Many of the calcareous siltstone and foraminiferal packstone beds have an erosional base (Figure. 6B) that grades upward into low angle convex/concave ripple laminae that thicken on the crest and thin towards the trough of the ripple (Figure. 6D). The bottom scour of some of the beds disrupt the preservation of underlying beds. Facies 1 contains the most organic matter with approximately 30% in mudstone (Figure. 7B) and siltstone (Figure. 7C) with slightly lower values in the foraminiferal packstone (Figure. 7A). Bentonite beds are common throughout the lower Ojinaga Formation, occurring approximately every 1.5-3m.

Facies 2 consists of approximately 170 m of dark brown to black calcareous mudstone with occasional calcareous siltstone interbeds and bentonite beds.

Bentonite beds occur throughout facies 2 and increase in frequency towards the upper part of this facies. Although most of facies 2 commonly is eroded or covered by wash from surrounding topography, approximately 85% of the unit is estimated to be mudstone.

Facies 3 is approximately 21 m of wavy laminated calcareous siltstone interbedded with thinly bedded calcareous mudstone and parallel laminated foraminiferal packstone. The uppermost bed at 229 m is a dolomitized spiculitic packstone (Figure.7 D), it is the only bed of its kind observed in the study area.

5.3 Spectral Gamma Ray Logs

Hand-held spectral gamma ray (SGR) logs provide a record of vertical changes in the gamma ray signatures of the rocks in the Ojinaga Formation. The SGR determines the enrichment of K, Th, and U, which are interpreted to be proxies for clay, bentonite and organic matter (Figure. 8). The K, Th and U content are lower within the foraminiferal packstone and siltstone but increases within mudstone and bentonite beds in the section (Figure. 8).

5.3.1 Facies and Sub-Facies

The facies units and sub-units of the Ojinaga Formation were defined as mappable members for correlation to related time coeval equivalent strata. (Figure. 8) Facies were determined from outcrop and lithological interpretation; sub-units were defined based on lithology (if present) in the measured section and/or spectral gamma ray response.

The more notable differences of GR response changes within facies are presented here. Each sub-facies has a GR of decreasing values from the base of the sub-facies to the middle and increasing values towards the top, with the exception of facies 1a and facies 3. In general the lower half of the Ojinaga Formation section (facies 1- facies 2b) is noticeably richer in U and has less Th than the upper portion of the section (facies 2b-facies 3).

From the base of the Ojinaga Formation to the top of facies 1a there is a sharp decrease in GR, K, Th and U indicating an abrupt facies change. Above this, sub-facies 1B records a decrease in GR corresponding to lower K and Th values. A smaller decline is noted in U content over this interval. In the middle of facies 1, total GR, K and Th are at the lowest values recorded in the entire measured section. From the middle of facies 1 to the top of this unit there is an increase in total GR, K, Th and U.

Throughout facies 2 the total GR and K content remain fairly consistent with small 10's of meters variations. Within each of the facies 2 subfacies the GR response records an increase and decrease in mudstone content. Facies 3a shows a distinct decrease in GR, K, Th and U within the section. Many of the Th spikes within the section correspond directly with bentonite beds.

5.4 Total Organic Carbon

The samples for total organic carbon (TOC) within the 229 m tick Mule Canyon Section 1 show a wide range (0.88-3.05 wt%) of TOC values (Figure. 8).

Facies 1 TOC reaches the highest values (0.88-3.05 wt%) in the Ojinaga Formation, decreasing towards the top of the unit. In facies 2 TOC content reaches the second highest enrichment of 1.47 wt% in the middle of facies 2A, decreasing to as little as 0.54 wt% in facies 2C. The TOC values increase again to 1.16 wt% within facies 3. Additional TOC samples were selected from the less weathered Mule Canyon Section 2, 9 m above the Buda Formation contact to the top (38 m) of the section (Table 2). The samples range from 1.38 wt% to 2.71 wt% with the highest concentration of organic content between 23 and 35 m. In both sections the TOC content is highest within facies 1.

5.5 Stable Isotope Geochemistry

The global burial of organic carbon during the Ocean Anoxic Event 2 (OAE2) caused a distinct +2 to +4% positive excursion of the $\delta^{13}C$ ratio of marine sediments (Schlanger and Jenkyns, 1976; Schlanger et al., 1987). The end of the excursion lies just above the Cenomanian-Turonian boundary (Pratt and Threlkeld 1984, Sageman et al., 2006). $\delta^{13}C$ data from the MC1 of the Ojinaga Formation indicate the OAE2 event is not recorded in this section (Figure. 8). The organic isotopes remain around 0.5 ‰ throughout the section, but increase to close to 2.0 ‰ in the middle of facies 1 and at the boundary of facies 2B and 2C.

5.6 Biostratigraphy

The biostratigraphic analysis, in addition to geochemical and sedimentological data provide a framework for key stratal surfaces and

partitioning geologic time within the Ojinaga Formation. Two prominent biostratigraphic changes occur in section MC1: one between facies 1 and facies 2A and the second near the top of facies 3. Calcareous nannofossils are relatively abundant and are poor to moderately preserved in this section. The biostratigraphy indicates that the 229 m thick Ojinaga Formation section MC1 is entirely within the Middle-Upper Cenomanian. Key Cenomanian markers in the section are: *Corollithion kennedyi*, *Helenea chiastia*, *Axopodorhabdus albianus*, *Rhagodiscus asper*, and *Lithraphidites acutus* (Figure. 10) Within the age ranges determined most nannofossils marker species occur, but not consistent in all samples analyzed due to poor preservation, facies changes or environmental factors.

Based on the nannofossils bioevents the Ojinaga Formation section was deposited during one CC (Perch-Nielsen, 1985) and four UC (Burnett, 1998) zonations (Figure. 10). Near the base of the Ojinaga Formation the first occurrence of *L. acutus* is used to approximate the Middle Cenomanian/Lower Cenomanian boundary. The lowest sample (<1.5 m) however, contains questionable nannofossils fragments that may be basal Cenomanian. The top of UC3c (94.79 Ma) is determined by *Gartnerago nanum* , though there is only one partial fragment. *Corollithion kennedyi* marks the end of UC3d, however, due to frequency and preservation it is possible this is not its last occurrence. The range of UC4a-5c was determined to represent the last age within the Ojinaga Formation based on the last occurrence of *Helenea chiastia.* The sample containing *Helenea chiastia* has very

low diversity and abundance; therefore the age of rock may be as low as UC3d or as high as UC5c (top of the Cenomanian).

The last sample at 229 m is dated at a minimum age event at 93.9 million years, putting it below the C-T boundary. This sample was determined to be at or below the top of *Helenea chiastia* occurrence. Lower in the Ojinaga Formation at 54 m above the Buda Formation the biostratigraphy gives a minimum age of 94.79 million years old as determined by the presence of *Gartnerago Nanum* and *Lithraphidites acutus*.

5.7 X-Ray Fluorescence

The major concentrations of elements such as Ca, Si, Fe, Al, and K as well as trace elements such as Mo and U, obtained from the hand-held XRF analysis are presented in Figures 11 and 12. From the base of the Ojinaga Formation the concentration of Al increases. Ca and Si increase at the bottom and the top of the section but decrease in the middle of the Ojinaga Formation. To further illustrate the carbonate to clay relationship the ratio of Ca/Al and K/Al are plotted as a function of depth (Figure. 13). More carbonate occurs at the base of the Ojinaga Formation and decrease towards the top of the section. The clay mineral (i.e., detrital input) fraction changes in the area with higher carbonate, the clay minerals become less K-rich with increasing carbonate content. The highest Ca/Al ratio is associated with the highest TOC and lowest K in facies 1.

Plots of redox sensitive trace metals Mo and V (Figure. 12) show a general increase in concentration with increasing TOC, suggesting that they are linked to preservation of organic material in the Lower Ojinaga Formation. When plotted against Al, trace elements Mo, Cr, V and Zn are poorly correlated with Al, indicating that their concentrations are not closely associated with detrital input.

To evaluate the enrichment of trace elements Mo and V of sediments in the Ojinaga Formation relative to typical mudstone, the enrichment factor (EF) was calculated for each sample. The EFs for trace element X were equal $(X/Al)_{sample}$ divided by $(X/Al)_{avg.\ mudstone}$. The average mudstone concentrations were derived from Wedepohl (1991) and also summarized by Tribollivard et al. (2006). Mo and V EFs plotted as a function of depth (Figure14). The results indicate that there is a strong enrichment in Mo in the base of the Ojinaga Formation relative to average mudstone. The enrichment decreases towards the top of the section resembling the concentration of an average mudstone. The V EFs shows a slight enrichment at the base but for the majority of the section its values are similar to average mudstone.

The average uranium (U) content in the Ojinaga Formation is 9.4±1 ppm, it ranges from 1-25 ppm, reaching the highest concentration in the middle of facies 2. The U/Al average ratio is $4.7x10^{-4}$ and is approximately 14 times the uranium content in average mudstone (Wedepohl, 1971,1991). The Ojinaga Formation has an average Mo content of 18±2 ppm, though it reaches above 80 ppm in facies .1 Mo and U increase in the bottom 50 m of the Ojinaga Formation, show a slight decrease in concentration after 50 m but remain fairly consistent around $1.02x10^{-03}$ until

200 m where there is a sharp decrease in their concentration. The Mo/Al ratio (Figure. 14) ranges from $2x10^{-4}$ to $2x10^{-3}$ with an average of $1.2x10^{-3}$. The Mo/Al average is approximately 80 times the enrichment of an average mudstone (Wedepohl, 1971, 1991).

5.8 Sequence Stratigraphic Units and Surfaces

For correlation with the Boquillas Formation in the Big Bend National Park area and the Eagle Formation the Ojinaga Formation was sub-divided into sequence stratigraphic units and surfaces, using depositional sequence nomenclature developed by Donovan et al. (2012). Three depositional sequences were identified, corresponding with facies 1 & 2 and 3. These depositional sequences correlate to the Lower Eagle Ford Formations and the basal of the Upper Eagle Ford Formation (Donovan et al., 2012). The lower two sequences of the Ojinaga Formation are equivalent with the Lower Eagle Ford Formation and the upper sequence is equivalent to the Upper Eagle Ford Formation (Figure. 9).

Four genetically related sequences were defined in the Eagle Ford Formation in Lozier Canyon, two within the Lower Eagle Ford and two in the Upper (Donovan et al., 2012). These sequences were referred to as the K63-Lozier Canyon) member, the K64-Antonio Creek Member, the K65-Scott Ranch- Member and the K70-Langtry Member Donovan et al. (2012). The depositional sequences were determined based on petrophysical, geochemical and chronostratigraphic properties, making them useful for correlation. The K63 and the K64 members

make up the Lower Eagle Ford Formation and the K65 and the K70 members makes up the Upper Eagle Ford Group in this area.

The K63 sequence boundary is defined as the change from the Buda Limestone Formation wackestone with low-GR and low TOC values into an interbedded mudstone/mudstone, calcareous siltstone and packstone facies with moderate-GR and high TOC content of facies 1. The top of faces 1 is the K64sb and it shows a distinct increase in U-, Th- and bentonite-rich-GR mudstone/mudstone with moderate TOC content. The last sequence observed in the Ojinaga Formation is above the K65 boundary at the top of facies 2 and marks a shift into low-GR, U-, Th- and TOC poor interbedded packstone, calcareous siltstone and mudstone. One of the most distinctive properties within K65 sequence is the presence of the positive $\delta^{13}C$ isotope excursion in the Eagle Ford Formation at Lozier Canyon (Donovan et al., 2012). This excursion records OAE2 that occurs immediately below the C-T boundary (Wehner et al., 2015).

The K70 and K72 (Donovan et al., 2012) sequence boundaries were not identified in the Ojinaga Formation section. The K70 boundary is recorded by a change from interbedded packstone and carbonate mudstone to bioturbated mudstone above. This lithologic change accompanies an increase in U and Th values and a relative decrease in overall GR. The K72sb marks the termination of the Eagle Ford Formation and transition to the overlying low U, Th and GR content in the Austin Chalk.

A cross section (Figure. 9) datumed on the interpreted K65 boundary from the Ojinaga Formation to the outcrops of the Eagle Ford Section in Lozier Canyon indicates the same sequences are correlated from the Ojinaga Formation (Mule Canyon) the Boquillas Formation (Hot Spring) and the Eagle Ford Formation (Lozier Canyon). The locations of the sections are noted on Figure2. The sequence boundaries (red lines) are correlated between all three sections. Moving from east to west sequence the K63 sequence maintains fairly consistent thickness across the three sections, only slightly increasing in the Ojinaga Formation. The overlying K64 sequence shows a drastic increase in thickness to the west (Figure. 8) being approximately 15 m thick within the Lozier Canyon and at the Hot Springs locality and increases dramatically westward to approximately 210 m in the Quitman Mountains. The K65 sequence is approximately 13 m thick in the Lozier Canyon section, increasing to 85 m at Hot Springs and this sequence is not complete in the Mule Canyon section.

6. DISCUSSION

6.1 Depositional Environment and Sedimentary Structures

The unconformable contact between the Buda Limestone and the Ojinaga Formation marks a break in sedimentation and change in depositional environment from carbonate shelf sedimentation to a mixed siliciclastic and carbonate sedimentation in an euxinic basin (Neybert, 1985). The basal unit (facies 1) of the Ojinaga Formation contains carbonate dominated sediments with symmetrical ripple bedforms (Figure 5) with convex and concave internal laminate geometry and thickening and thinning of hummocky (Harms et al., 1975) and swaley cross-stratification (Leckie and Walker, 1982). Similar sedimentary features occur in coeval sediments of the Boquillas Formation and Eagle Ford Group (Wehner et al., 2015, Donovan et al., 2012, Gardner et al., 2013). These features form during storms in water depths of 10's of meters (maximum 60-70 m), indicating deposition was commonly within storm wave base during early deposition of the Ojinaga Formation within the WIS. The sedimentary structures in the lower Ojinaga Formation were previously interpreted to form below storm wave base and as the result of bottom water currents Neybert (1985). It should be noted that Facies 1 contains a more mudstone-prone (higher GR) lower portion (1A) and a more grainstone-prone (lower GR) upper portion (1B). Not surprisingly the highest gamma ray values occurs approximately 5m off the base within unit 1b. Thus in terms of facies and log patterns, Facies 1 appears to form a distinct Transgressive-

Regressive cycle, interpreted as a depositional sequence. The maximum flooding surface for this sequence is placed about 5m off the base of the sequence at the maximum gamma ray value within subunit 1a.

A distinct change in environmental conditions on the Cenomanian seafloor occurs across the boundary between facies 1 and faces 2. The contact is marked by a change from organic-rich mudstones and grainstones, which are Uranium, Potasium, Thorium-poor (below), to organic-poor mudstones, which are Uranium-, Potassium, and Thorium-rich (above). At the boundary between facies 2 and 3 another abrupt change occurs, marked by a shift to towards more carbonate dominated sediments and concomitant decrease in marine mudstone. A distinct increase in bioturbation also occurs across this boundary suggesting a distinct change in oxygenation also occurred on the Cenomanian seafloor at this time.

6.2 Stratigraphic Sequence Correlation

A regional east to west cross section (Figure9) has the Mule Canyon passing eastward into the Hot Springs section (Wehner et al., 2015) and furthest east to the Lozier Canyon section (Donovan and Staerker, 2010; Gardner et al., 2013). Using the geochemistry and gamma-ray log signatures associated with the sequences defined in outcrop, the bounding surfaces can be correlated regionally (Figure9). A fundamental difference between the surfaces and sequences of the Ojinaga Formation, Hot Springs and Lozier Canyon is the prominent differences in the thickness of the K64 sequence, whereas the basal K63 sequence remains relatively

consistent. The large increase in sedimentation in the K64 sequence is likely the result of greater accommodation created during deposition and/or erosion by the overlying K65sb. The location of the Ojinaga Formation within the Chihuahua Trough allows for large amounts of sediment to be deposited and very limited periods of erosion and development of unconformities. Much lower rates of accommodation and frequent development of unconformities is evident on the shallower Hot Springs and Lozier Canyon section located on the Comanche Platform. The east to west correlation (Figure. 9) records a transition from the deeper part of the ramp towards the updip shallower ramp.

The Hot Springs, Boquillas Formation and the Lozier Canyon, Eagle Ford Formation sections show some variability in thickness that was interpreted to be the result of less accommodation on the Devil's River Uplift an active paleo-high during deposition (Donovan and Staerker, 2010). The thickness variation could, however, indicate either reactivation of faults from the underlying Ouachita Orogeny near Devil's Uplift or differential subsidence from intrabasinal tectonics (Wehner et al., 2015). Deformed bedding within the Eagle Ford Formation occur near the Devil's River Uplift whereas deformed bedsets are smaller, less frequent, and show less deformation at the Hot Springs section, near the platform margin. This suggests the Devil's River Uplift was likely tectonically active during deposition of the Eagle Ford and Boquillas Formation (Wehner et al., 2015).

6.3 Biostratigraphy Correlation

Within the Ojinaga Formation section MC1 the biostratigraphic markers indicated the entire section is Cenomanian in age. The section has been further divided into nanno zone CC10a and the four other nanno zones (Figure10). The preservation and abundance of nannofossils within the section provides enough information to interpret nannofossil zonations, though the confidence level is low. The four UC nannofossils zonations are used to correlate age equivalent strata in the Hot Springs and the Eagle Ford Formation.

One option for correlating the bottom Ojinaga Formation section is to use the top of *Gartnerago nanum* (G. nanum) as the marker for the top of UC3c and bottom of UC3d. The base of *Corollithion kennedyi* (C. Kennedyi) that would be used to define the bottom of UC3d (observed at 54.1 m) is not honored due to its low fossil abundance. The top of G. nanum is used to correlate to the Hot Springs and Lozier Canyon sections. The top of G. nanum can be correlated to 15 m above the base of the Buda Formation in the Hot Springs section. Moving east to the Lozier Canyon section the Top of G. nanum was not determined but is projected to approximately 13.5 m.

Below the G. nanum occurrence there are no fossils that constrain the age of the lowest 54 m of section. *Rotalipora appenninica* was noted from 0 meters (top of the Buda) to roughly 12 m. (McNulty et al. 1985). The Buda Formation underlying the Ojinaga Formation is early Cenomanian and the presence of R. appenninica indicates a zone in age that spans from the latest Albanian into the middle

Cenomanian (Robaszynski et al., 1979). The undefined base C. Kennedyi leaves the possibility of the lower 54 m of the Ojinaga Formation to be older in age than the nannofossils can constrain based on the samples analyzed.

The second option for dating the base of the Ojinaga Formation is to honor the potential base of C. Kennedyi and co-occurrence of G. nanum. The co-occurrence can only naturally occur in two ways; G. nanum was reworked higher in the section above where it would stratigraphically occur and hence should be disregarded as a correlation point, or there is an erosional surface at 54 m and the section is interpreted to be older than any section reported at Hot Springs or Lozier Canyon. To be confident using this option, more work would be needed to see if there is support for a facies change or other characteristic change in the rocks below 54 m to suggest that it is different stratigraphy than that seen in the bottom of Hot Springs and Lozier Canyon. The addition of more biostratigraphic analysis would help constrain the nanno zonation designations and increase confidence in the picks made here.

The top of UC3d defined by the last occurrence of C. kennedyi can be correlated across both Hot Springs and Lozier Canyon sections (Figure. 10). In Hot Springs the top of UC3d is an erosional surface and the Upper Cenomanian is truncated and there is no basal Turonian strata. An erosional surface in Lozier Canyon also defines the top of UC3d. Above this nanno zonation there is very low confidence to designate correlatable age zonations with in the Ojinaga Formation. The youngest nanno correlation that can be made between Hot Springs and Lozier

Canyon are illustrated in Figure10. Refinements of the upper Ojinaga Formation nanno zonations require future biostratigraphic analysis.

6.4 Stable Isotope Geochemistry

The OAE2 was either present in rocks above those in section MC1 and eroded away or it was never preserved in this area. The increase of isotopic values in the middle of facies 1 may correlate to the Middle Cenomanian Event (MCE) identified by Eldrett et al. (2015) in the Eagle Ford Formation Shell research borehole Iona-1. The MCE event occurs within the Iona-1 well, located in the southern gateway of the Cretaceous Western Interior Seaway containing the Austin Chalk, underlying Eagle Ford Formation and Buda Formation (Eldrett et al., 2015). The MCE of the Iona-1 is located 10 m above the Buda Limestone and spans 96.57 ± 0.12 Ma to 96.36 ± 0.13 Ma. As in the Iona-1 core, the MCE event within the Ojinaga Formation occurs within the highest TOC interval near the base of the section. Some isotopic variability within section MC1 is attributed to formation of authigenic carbonate from early and late diagenetic processes (Schrag et al., 2013) as well as isotopic composition variability of the water column (Eldrett et al., 2015).

6.5 Anoxia and Organic Preservation

In the basal portion of the Ojinaga Formation (facies 1) the Mo/Al ratio approaches that of modern seawater with higher uranium values. This increase in Mo and U content indicates a Mo sink that approached the efficiency of U deposition due to increasing dissolved Mo as a particle-reactive thiomolybdates (Figure 15)

(Algeo and Tribovillard, 2009, Tyson and Pearson, 1991, Tribovillard, et. al., 2006 and Vorlicek, 2002.). The increase in the Mo/Al ratio indicates the presence of free sulfide in the water column during deposition of the lower Ojinaga Formation. At the highest uranium concentrations there is a slight decrease in the Mo/U ratio, most likely a result of increased euxinia waters and a depletion of Mo in the restricted basin relative to normal seawater (Tribovillard et al., 2012). The recorded Ojinaga Formation at section MC1 preserved Mo/U ratios in the upper portion of facies 2 and facies 3 that are similar to those of average upper crust (McLennan, 2001). Facies 2 and 3 contain lower uranium content, indicating sediments are formed in a reducing environment in a sulfide free water column. (Algeo and Tribovillard, 2009).

The highest TOC content in the lower Ojinaga Formation occurs within facies 1. This interval corresponds to the highest Mo/U ratio and suggests greater preservation of organic matter and more reducing conditions than in facies 2 and 3, which contain lower U concentrations. Increased sedimentation rate as well as an increase in water circulation and increase in oxygen in the water column may dilute TOC in facies 2 and 3.

7. CONCLUSIONS

Hand-held GR Scintillometer data and biostratigraphy allow a geochemical correlation from the Ojinaga Formation to the Boquillas Formation and the Eagle Ford Group. The correlation suggests that the first sequence (K63) above the Buda Limestone Formation has relatively consistent thickness across the region. With a consistent thickness and similar sedimentary structures and lithology across the three formations it is inferred that its depositional environment was a storm-dominated shallowly dipping carbonate ramp. The K64 sequence of the Ojinaga Formation is drastically thicker than the coeval Boquillas and Eagle Ford formations. This rapid thickness change likely is the result of a marine transgression and greater accommodation with minimal erosional or unconformity development.

Biostratigraphic and isotopic data indicate that the Ojinaga Formation exposed in Mule Canyon is Cenomanian in age. Nanno fossil data determined chronological zones that were correlated to the Boquillas Formation and Eagle Ford Formation further east. From the correlation it is evident that both the Boquillas and Eagle Ford formations have unconformities and low nannofossils abundance in the lower Eagle Ford, making accurate age correlations by biostratigraphy challenging. The biostratigraphic chorological correlation also illustrates the increase in sediment deposition within the K64 sequence of the Ojinaga Formation.

Overall the lower Ojinaga Formation at Mule Canyon records a shift in depositional environment from more proximal (facies 1) to more distal (facies 2)

strata deposited on the floor of the floor of the Cenomanian seaway in West Texas. Interestingly, however, facies 1 is the more organic-rich chronostratigraphic unit, suggesting that more anoxic seafloor conditions occurred during this specific interval of the Cenomanian.

REFERENCES

Algeo, T.J., and Tribovillard, N., 2009, Environmental Analysis Of Paleoceanographic Systems Based On Molybdenum–Uranium Covariation: Chemical Geology, v. 268, no. 3–4, p. 211-225.

Blakey, R., 2014, North American Paleogeography, https://deeptimemaps.com/?s=western+interior+seaway (accessed January 2016).

Berge, T. B., 1982, Structural Evolution Of The Northeastern Chihuahua Tectonic Belt. Geologic Studies Of The Cordilleran Thrust Belt, Rocky Mountain Association Of Geologists v. 50, p. 451-457.

Burnett, J.A. (with contributions from Gallagher, L.T. and Hampton, M.J.), 1998, Upper Cretaceous. In: Bown, P.R., (Ed.) Calcareous Nannofossil Biostratigraphy, British Micropalaeontological Society Publications Series. London: Chapman and Hall/ Kluwer Academic Publishers, p. 132–199.

Calvert, S.E., and Pedersen, T.F., 1993, Geochemistry Of Recent Oxic And Anoxic Marine Sediments: Implications For The Geologic Record, Marine Geology, v. 113, p. 67-88.

Campbell, C. V., 1967, Lamina, Lamina Set, Bed And Bedset: Sedimentology, v. 8, p. 7- 26.

Cantu-Chapa, C. M., Sandoval, R., and Arenas, R., 1985, Evolution Sedimentaria Del Cretacico Inferior En El Norte De Mexico: Revista Del Instituto Mexicano Del Petroleo, v. 18, n.2, p. l4-37. (Translated)

Cantu-Chapa, C.M., 1993, Sedimentation And Tectonic Subsidence During The Albian-Cenomanian In The Chihuahua Basin, Mexico: In A.J.T. Simo, R.W._Page 93 Scott, and J.P. Masse, eds: AAPG Memoir 56, p. 61-70.

Cordoba, D.A., Rodriguez-Torres, Rafael, and Guerrob Garcia, Jose., 1970, Mesozoic Stratigraphy Of The Northern Portion Of The Chihuahua Trough: *In* The Geologic Framework Of The Chihuahua Tectonic Belt: West Texas Geol. SOC. p. 39-41.

Dickinson, W. R., 1981, Plate Tectonic Evolution Of The Southern Cordillera, In W. R. Dickinson And W. D. Payne, Eds., Relations Of Tectonics To Ore Deposits In The Cordillera: Arizona Geological Society Digest, v. 14, p. 113-135.

Dickinson, W. R., Klute, M. A. and Swift, N. P., 1986, The Bisbee Basin And Its

Bearing On Late Mesozoic Paleogeo- Graphic And Paleotectonic Relations Between The Cordilleran And Caribbean Regions, In P. L. Abbott, Ed., Cretaceous Stratigraphy, Western North America: SEPM Pacific Section, Book 46, p. 51-62.

Donovan, A. D., and Staerker, T.S., 2010, Sequence stratigraphy of the Eagle Ford (Boquillas) Formation in the subsurface of South Texas and the outcrops of West Texas: Gulf Coast Association of Geologic Societies Transactions, v. 60, p. 861-899.

Donovan, A. D., Staerker, T. S., Pramudito, A., Li, W., Corbett, M. J., Lowery, C. M., Romero, A. M., and Gardner, R. D., 2012, The Eagle Ford Outcrops Of West Texas: A Laboratory For Understanding Heterogeneities Within Unconventional Mudstone Reservoirs: GCAGS Journal, v. 1, p. 162-185.

Donovan, A. D., Gardner, R. D., Pramudito, A., Staerker, T. S., Wehner, M., Corbett, M. J., & Rotzien, J. R., 2015, Chronostratigraphic Relationships of the Woodbine and Eagle Ford Groups across Texas. *Transactions / Gulf-Coast Association Of Geological Societies*,v. 655, p. 97-598.

Eldrett, J.S., Ma, C., Bergman, S.C., et al., 2015, Origin Of Limestone–Marlstone Cycles: Astronomic Forcing Of Organic-Rich Sedimentary Rocks From The Cenomanian To Early Coniacian Of The Cretaceous Western Interior Seaway, USA: Earth And Planetary Science Letters, v. 423, p. 98-113.

Eldrett, J. S., Ma, C., Bergman, S. C., Lutz, B., Gregory, F. J., Dodsworth, P., Kelly, A. E., 2015, An Astronomically Calibrated Stratigraphy Of The Cenomanian, Turonian And Earliest Coniacian From The Cretaceous Western Interior Seaway, USA: Implications for global chronostratigraphy v. 56 p. 316-344.

Freeman, V. L., 1961, Contact Of The Boquillas Flags And Austin Chalk In Val Verde And Terrell Counties, Texas: American Association of Petroleum Geologists Bulletin, v. 45, p. 105–107.

Freeman, V. L., 1968, Geology Of The Comstock Indian Wells Area Val Verde, Terrell, And Brewster Counties, Texas: U.S. Geological Society Professional Paper 594, p. 26.

Gardner, R. D., Pope M. C., Wehner M. P., and Donovan A. D., 2013, Lateral continuity of Eagle Ford strata in Lozier Canyon and Antonio Creek, Terrell County, Texas. GCAGS Journal, v. 2, p. 42-52.

Harms, J. C., Southard J. B., Spearing D. R., and Walker R. G., 1975, Depositional Environments As Interpreted From Primary Sedimentary Structures And

Stratification Sequences: Society of Economic Paleontologists and Mineralogists Short Course Notes v. 2, p. 161.

Hazzard, R. T., 1959, Measured section, in R. L. Cannon, R. T. Hazard, A. Young, and K. P. Young, 1959, Geology of the Val Verde Basin: West Texas Geological Society Guidebook, November 5–8, Midland, p. 118.

Heller, P. L., and Paola, C., 1989, The Paradox Of Lower Creta- Ceous Gravels And The Initiation Of Thrusting Of The Sevier Orogenic Belt, United States Western Interior: Geological Society of America Bulletin, v. 101, p. 864-875.

Herron, S. L., and Herron, M. M., 1996, Quantitative lithology: An application for open and cased hole spectroscopy, Trans. SPWLA 37th Annual Logging Symposium, Paper E.

Jones, B. R., and Reaser, D. F., 1970, Geology of southern Quitman Mountains and vicinity, Hudspeth County, Texas: Texas University Bureau of Economic Geology quadrangle map no. 38, P. 24.

Kelly, C.M., 2016, Molybdenum, Vanadium And Nickel Covariation As An Indicator Of Paleo-Redox Conditions And Basin Restriction Within The Eagle Ford Formation- Implications For The Interpretation Of Volcanic Ash Fertilization.

Leckie, D. A., and Walker R. G., 1982, Storm- And Tide-Dominated Shorelines In Cretaceous Moosebar-Lower Gates Interval-Outcrop Equivalents Of Deep Basin Trap In Western Canada: American Association of Petroleum Geologists Bulletin, v. 66, n. 2, p. 138-157.

Lock, B. E., and Peschier L., 2006, Boquillas (Eagle Ford) Upper Slope Sediments, West Texas: Outcrop Analogs For Potential Mudstone Reservoirs: Coast Association of Geological Societies Transactions, v. 56, p. 491-508.

McLennan, S. M., 2001, Relationships Between The Trace Element Compositions Of Sedimentary Rocks And Upper Continental Crust: Geochemistry, Geophysics, Geosystems, v. 2, paper number 2000GC000109.

Neybert R., 1985, Petrography And Depositional Environments Of The Upper Cretaceous (Cenomanian-Turonian) Ojinaga Formation, Southern Quitman Mountains, Hudspeth County, West Texas, [M.S. Thesis] University of Texas at Arlington, Arlington, Texas, p. 275.

EIA (Energy Information Administration) 2012 *Annual Energy Outlook 2012* (Washington, DC: US Department of Energy) (www.eia.gov/forecasts/aeo/pdf/0383(2012).pdf,

Eldrett, J. S., Minisini, D., and Bergman, S. C., 2014, Decoupling Of The Carbon Cycle During Ocean Anoxic Event 2: Geology, v. 42, no. 7, p. 567-570.

Ogg, J. G., and Hinnov, A., 2012, Cretaceous, In F.M. Gradstein, J. G. Ogg, M. Schmitz, And G. Ogg, Eds., The Geologic Time Scale 2012: Elsevier B.V., Amsterdam, The Netherlands, p. 793-853.

Pratt, L. M., and Threlkeld C. N., 1984, Stratigraphic significance of 13C/12C ratios in mid Cretaceous rocks of the western interior: Canadian Society of Petroleum Geologists Memoir 9, Calgary, Alberta, p. 305–312

Perch-Nielsen, K., 1985, Mesozoic calcareous nannofossils. In: Bolli, H.M., Saunders, J.B., Perch-Nielsen, K. (Eds.), Plankton Stratigraphy, v. 1, p. 329–426.

Pessagno, E. A., 1969, Upper Cretaceous stratigraphy of the western Gulf Coast area of Mexico, Texas, and Arkansas: Geological Society of America Memoir 111, Boulder, Colorado, p. 139.

Pickett, A., 2013, Eagle Ford Mudstone Rocketing Forward, v. 56, no. 10; 201428, p. 83-84,86,88-89.

Powell, J.D., 1963, Cenomanian-Turonian (Cretaceous) ammonites from Trans-Pecos Texas and northeastern Chihuahua, Mexico: Jour. Paleont., vol. 37, pp. 309 -322.

Purcell, D.R.J., 1985, Structure of the Upper Cretaceous Ojinaga Formation, southern Quitman Mountains, Hudspeth County, Texas [M.S. Thesis], University of Texas at Arlington.

Ratcliffe, K.T., Wright, A.M., Schmidt, K., 2012, Application Of Inorganic Whole-Rock Geochemistry To Mudstone Resource Plays: An Example From The Eagle Ford Mudstone Formation, Texas. Sedimentary Record, v. 10, p. 4–9.

Reaser, D.F., and Underwood, J.R., Jr., 1981, Tectonic Style And De- Formational Envilonment In The Eagle-Southern Quitman Mountains, ***In*** Western Trans-Pecos, Texas: N.M. Geol. SOC. Guidebook vo. 31, p. 123-135.

Robaszynski, F., and Caron M., 1979, Atlas De Foraminiferes Planctoniques Du Cretace Moyen (Mer Boreale Et Tethys): Cahier de Micropaleontologie, v. 2, no. 181 p. 80 (Translated).

Sageman, B. B., Meyers S. R., and Arthur M. A., 2006, Orbital Time Scale And New C-Isotope Record For Cenomanian-Turonian Boundary Stratotype: Geology, v. 34, p. 125–128.

Schlanger, S. O., and Jenkyns H. C., 1976, Cretaceous Oceanic An- Oxic Sediments: Causes And Consequences: Geologie en Mijnbouw, v. 55, p. 179–84.

Schlanger, S.O., Arthur, M.A., Jenkyns, H.C., and Scholle, RA., 1987, The Cenomanian-Turonian Oceanic Anoxic Event, I. Stratigraphy And Distribution Of Organic Carbon-Rich Beds And The Marine Δ 13C Excursion. In Brooks, J., and Fleet, A.J. (Eds.), Marine Petroleum Source Rocks. Geol. Soc. Spec. Publ. London, v. 26, p. 371-399.

Schrag, D.P., Higgins, J.A., Macdonald, F.A., Johnston, D.T., 2013, Authigenic Carbonate And The History Of The Global Carbon Cycle. Science v. 339, no. 6119, p. 540–543.

Sloss, L.L., 1963, Sequences In The Cratonic Interior Of North America: Geological Society Of America Bulletin, v. 74, p. 93–114.

Smith, C. C., 1981, Calcareous Nannoplankton And Stratigraphy Of Late Turonian, Coniacian, And Early Santonian Age Of The Eagle Ford And Austin Groups Of Texas: U.S. Geological Society Professional Paper v. 1075, p. 96.

Treviño, R. H., 1988, Unit And Depositional Environments Of The Boquillas Formation, Upper Cretaceous Of Southwest Texas: M.S. Thesis, University of Texas at Arlington, p. 135.

Tribovillard, N., Algeo, T. J., Baudin, F. and A. Riboulleau, 2012, Analysis Of Marine Environmental Conditions Based On Covariation – Applications To Mesozoic Paleoceanography, v. 324-325, p. 46-58.

Vorlicek, T.P., Helz, G.R., 2002, Catalysis By Mineral Surfaces: Implications For Mo Geochemistry In Anoxic Environments. Geochim. Cosmochim. v. 66, p. 3679–3692.

Wedepohl, K.H., 1971, Environmental influences on the chemical composition of mudstones and clays. In: Ahrens, L.H., Press, F., Runcorn, S.K., Urey, H.C. (Eds.), Physics and Chemistry of the Earth. Pergamon, Oxford, p. 305–333.

Wedepohl, K.H., 1991, The Composition Of The Upper Earth's Crust And The Natural Cycles Of Selected Metals. In: Merian, E. (Ed.), Metals And Their Compounds In The Environment. VCH-Verlagsge- Sellschaft, Weinheim, p. 3–17.

Wehner, M., Tice, M. M., Pope, M. C., Gardner, R., Donovan, A. D., & Staerker, T. S., 2015. Anoxic, Storm Dominated Inner Carbonate Ramp Deposition Of Lower Eagle Ford Formation, West Texas. Society Of Petroleum Engineers. Doi:10.2118/178607-MS

APPENDIX A

Figure 1. Composite simplified stratigraphic chart. Nomenclature developed for the coeval Eagle Ford Formation equivalent units.

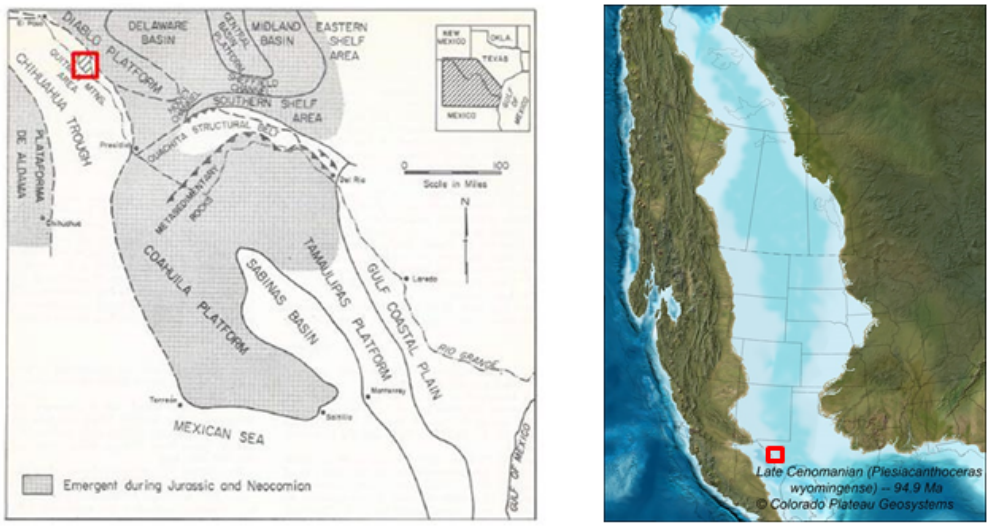

Figure 2A. Paleogeographic and tectonic features of the study area. Late Paleozoic and Mesozoic tectonic features of the study area (Trans-Pecos Texas and northeastern Mexico) modified after Jones and Reaser (1970). Paleogeographic map of the Western Interior Seaway Late Cenomanian (Blakey, 2014), location of study area indicated in red.

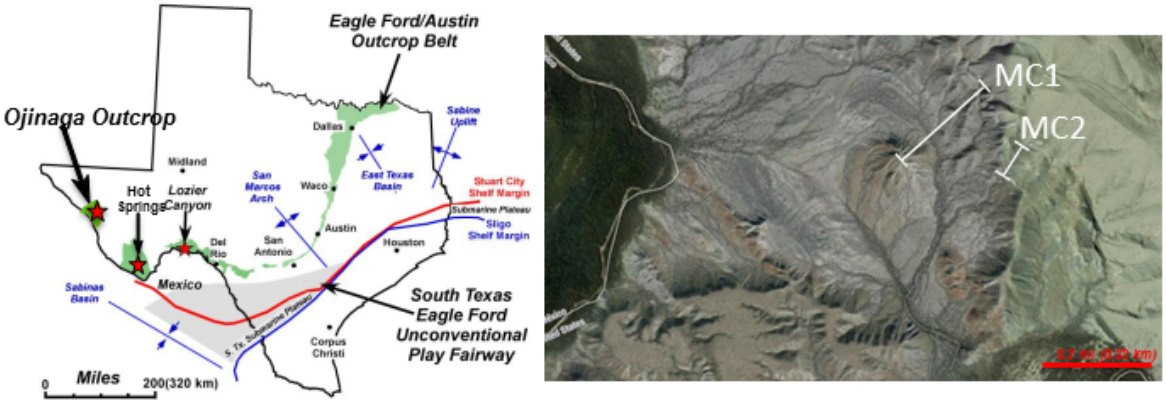

Figure 2B. Deposition map of the study area. Map modified after Donovan et al., 2012. Google Earth map of the study area with locations of the research sections Mule Canyon 1 (MC1) and Mule Canyon 2 (MC2).

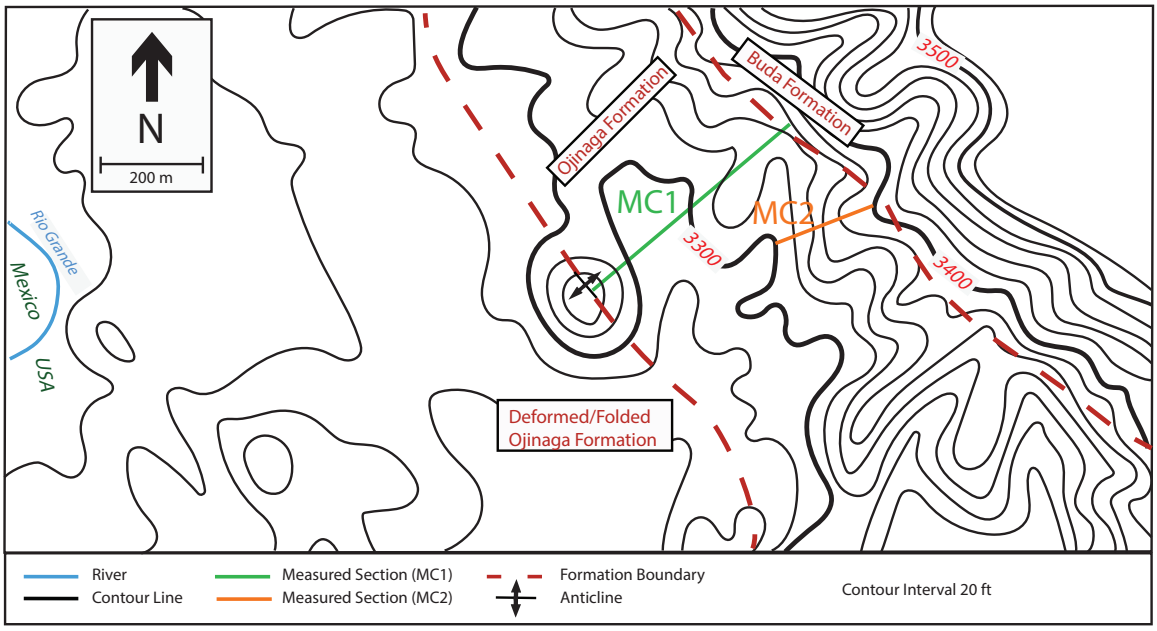

Figure 3. Topographic map showing the Ojinaga Formation measured sections. Mule Canyon 1 (MC1) in green and Mule Canyon 2 (MC2) in orange.

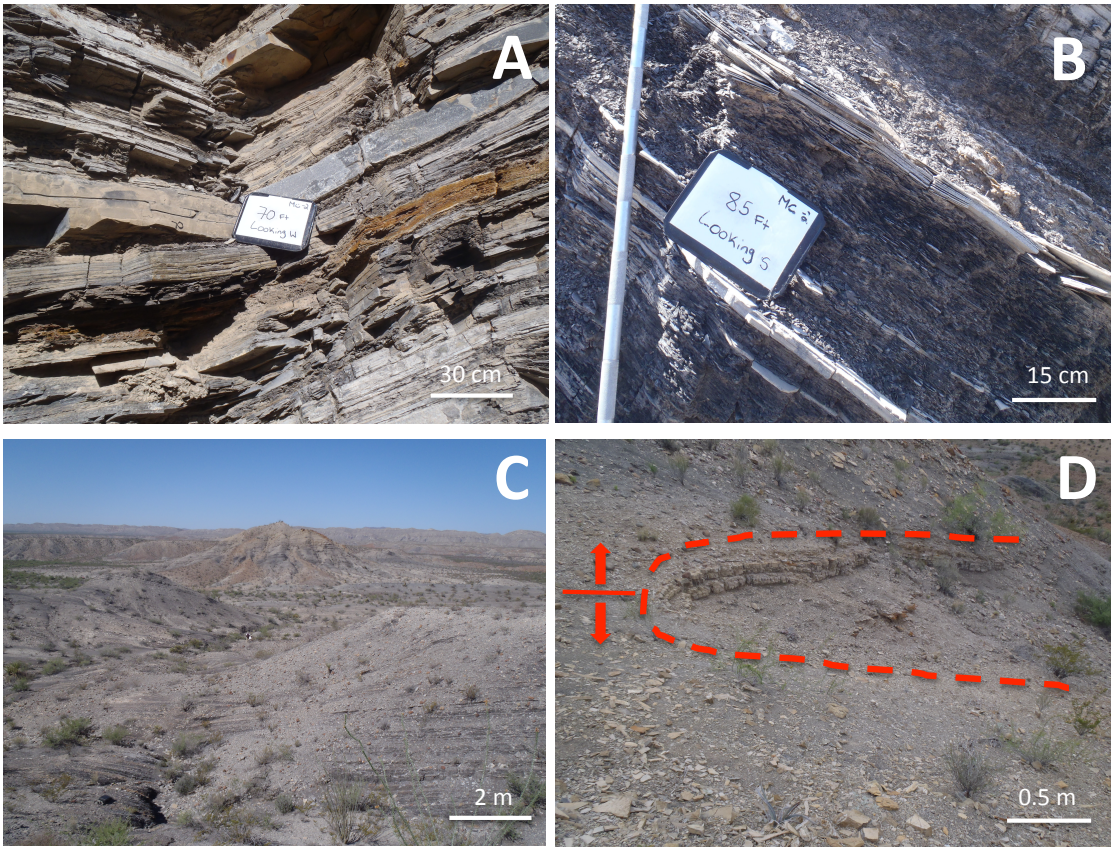

Figure 4. Measured section photographs. (A) Facies 1 interbedded foraminiferal packstone, stilstone and calcareous mudstone. (B) Facies 2 interbedded parallel laminated siltstone and calcareous mudstone (C) Mule Canyon Section 1 (MC1) ~24 m to 229 m at the top of orange hill. (D) Hinge of the anticline at the top (229 m) of MC1.

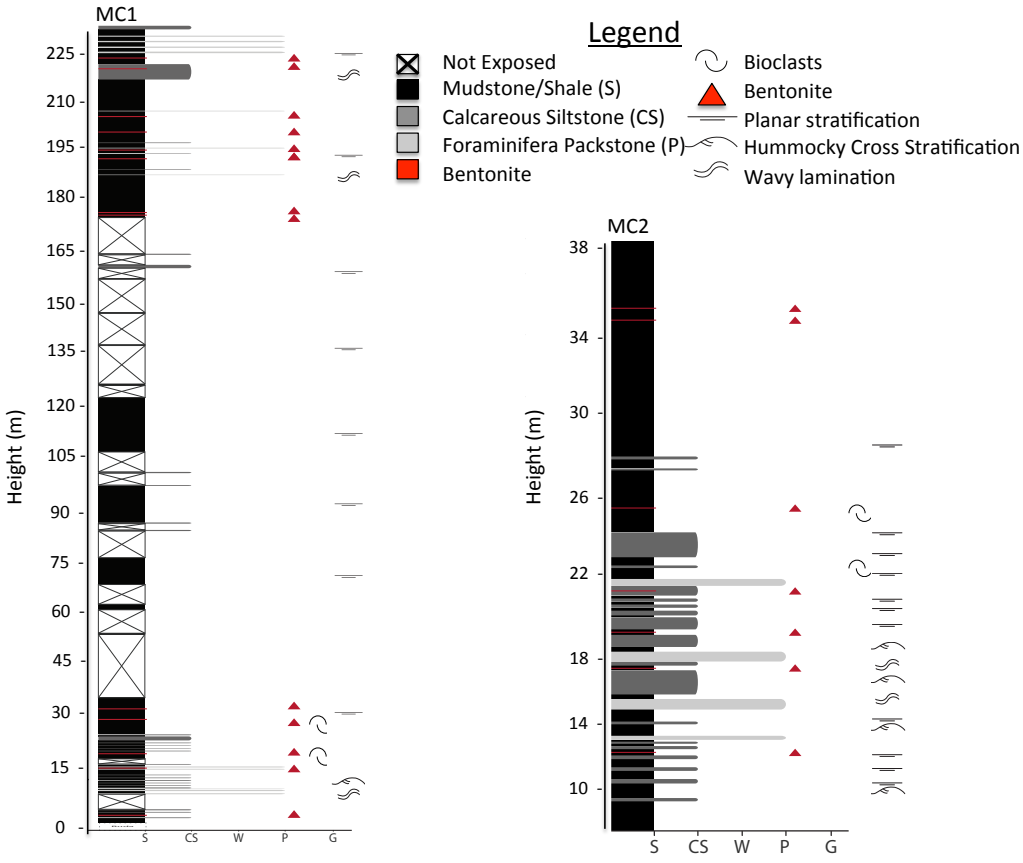

Figure 5. Mule Canyon Ojinaga Formation measured sections. Mule Canyon 1 (MC1) and Mule Canyon 2 (MC2). The horizontal scale is Dunhams (1962) classification for carbonate rocks.

Table 1. Summary Table Of Mule Canyon Ojinaga Formation Facies And Associated Attributes.

Facies	Sub-facies	Thickness (m)	Description	Sedimentary Structures	Composition	Ash Content	Interpretation
Facies 1: Interbedded froaminifera packstone, siltstone and shale, with wavy lamination and hummocky cross stratification	A	6	Interbedded parallel thinly bedded shale and thin (1-5cm) beds of calcareous siltstone	Parallel to wavy lamination, minor wave ripples and cross lamination in upper beds.	50% Planktonic foraminifera, 10% calcispheres 10% skeletal fragments, 30% mud and organic matter	Two 5 cm bentonites	Siltstone beds contain wavy, cross and parallel lamination, indicating deposition near storm wave base. Dominating shale with current related structures indicate sedimentation may have been interrupted by storms and the calcareous stilstone beds were deposited.
	B	32	Interbedded thick ~5-10 cm beds of skeletal packstone and calcareous siltstone with thinner (2-3 cm) mudstone beds	Packstone beds contain wavy laminations, parallel laminations, wave ripples and hummocky cross stratification. Siltstone beds contain wavy lamination to small ripples.	80% Planktonic foraminifera, 20% calcispheres, <5%inoceramid fragments, <5% mollusk fragments and <5% skeletal fragments, 20% mud and organic matter	3 cm thick bentonite beds occurring every 7-10 ft	Storm-related hummocky cross stratification structures and wave ripple like laminations. This suggests this unit was deposited within the storm wave base.
Facies 2: Interbedded parallel laminated calcareous siltstone and shale	A	60	Calcareous shale with occasional siltstone	Calcareous siltstone beds are parallel laminated. Thin bedded shale.	30-50% Planktonic foraminifera,10-20% calcispheres, 40-50% mud and organic matter, <5% skeletal fragments	3 cm thick bentonite beds occurring throughout, increasing towards the top	Parallel lamination and thinly bedded shale with small amounts of siltstone indicate deposition below storm wave base with occasional storms depositing siltstone.
	B	53	Interbedded calcareous shale and siltstone. Increasing carbonate dominated stilstone in the middle of the unit. Small 3 cm bentonites near the top and base of the unit.	Calcareous siltstone beds are parallel laminated. Thin bedded shale.	10-20% Planktonic foraminifera, 20-30% calcispheres, 40-50% mud and organic matter, <5% skeletal fragments	3 cm thick bentonite beds located at the top and the base of the unit	Parallel lamination and thinly bedded shale with small amounts of siltstone indicate deposition below storm wave base with increasing storm activity depositing siltstone.
	C	60	Interbedded calcareous shale, 3 cm thick siltstone, bentonites and thick 5 cm packstone beds	Calcareous siltstone beds are parallel laminated Packstone contains wavy lamination. Thinly bedded shale.	40-50% Planktonic foraminifera, 10-20% calcispheres, 10-20% organic matter	1-3 cm thick bentonite beds occurring throughout, decreasing in frequency from the bottom	Interbedded parallel laminated siltstone and shale with wavy laminated packstone indicate deposition above and below storm wave base.
Facies 3: Interbedded parallel lamination packstone, siltstone and shale		18	Interbedded foraminifera packstone and calcareous shale	Laminated shale (1mm) with increasing parallel laminated packstone beds towards the top of the unit. A wavy laminated silstone package10 ft thick with interbedded shale exists in the middle of the unit. At 750 ft a single dolomitized calcareous spiculitic packstone is present.	50-60% Planktonic foraminifera, 10-20% calcispheres,10% mud and organic matter, calcareous sponge spicules	Very few thin bentonite beds (1-2 cm) beds at the base of the unit	Dominating shale with current related in the lower structures indicate sedimentation below storm wave base. Increasing siltstone and packstone beds with wavy and parallel lamination.

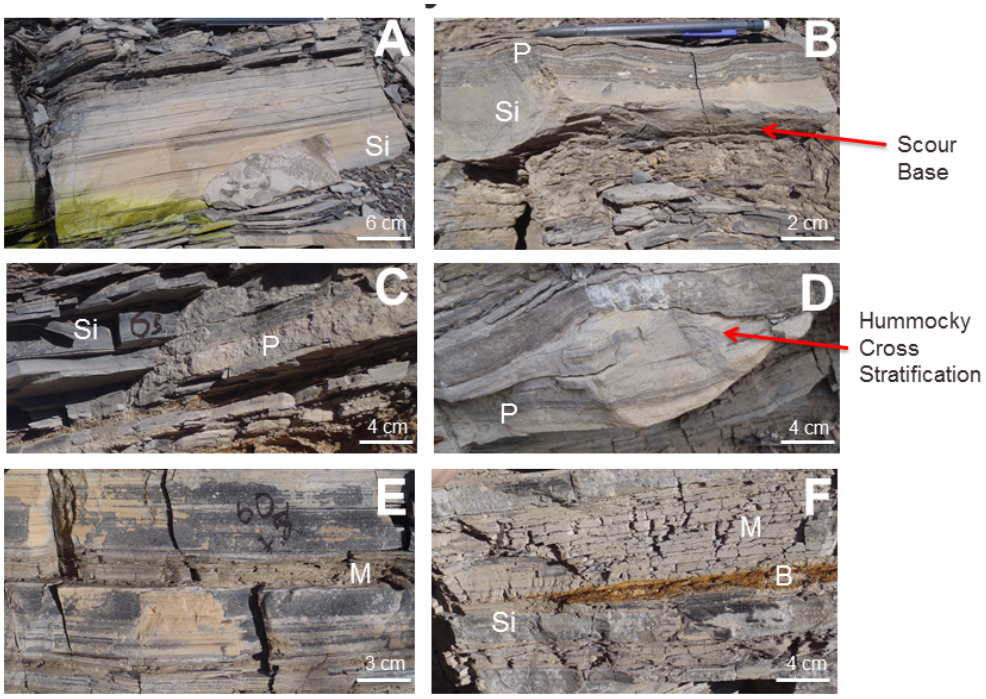

Figure 6. Sedimentary structure photographs. (A) Parallel laminated foraminiferal siltstone (B) Transition from scour based foraminiferal siltstone to a foraminiferal packstone. (C) Parallel laminated foraminiferal packstone to parallel laminated foraminiferal siltstone in facies 1. (D) Foraminiferal packstone Hummocky cross stratification bed in facies 1. (E) Interbedded parallel laminated foraminiferal siltstone and calcareous mudstone. (F) Interbedded parallel laminated mudstone (M) and foraminiferal siltstone (Si).

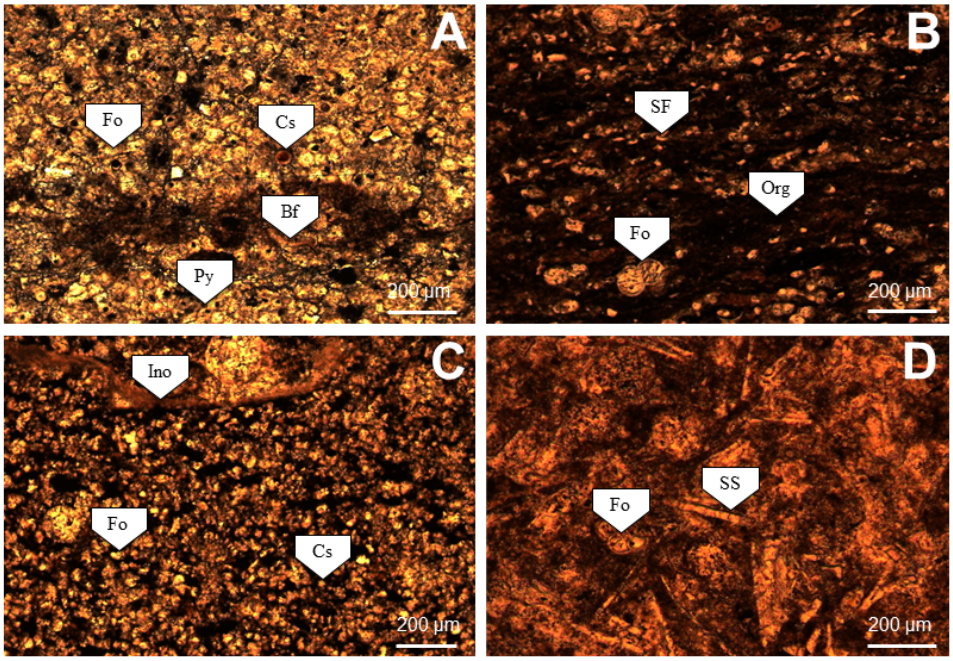

Figure 7. Photomicrographs. Planktonic foraminiferal (Fo), unidentified skeletal fragments (SF), organic matter (Org), calcispheres (Cs), oysters (Mo), inoceramid bivalves (Ino), pyrite (Py), and sponge spicules (SS). (A) Foraminiferal packstone in unit A. (B) Foraminiferal mudstone in unit A (C) Foraminiferal calcareous siltstone in unit A (D) Dolomitized spiculitic packstone in unit C.

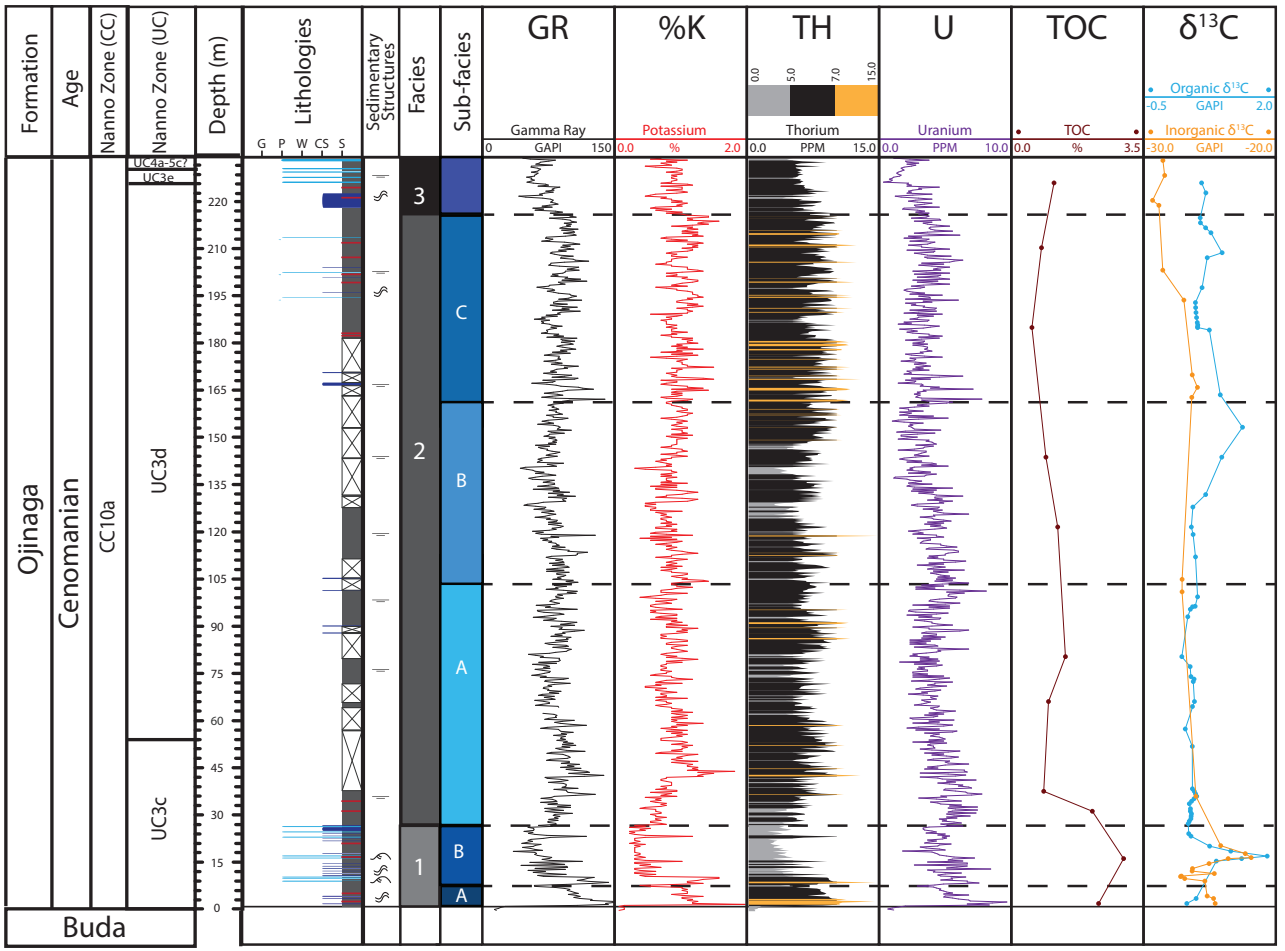

Figure 8. Summary of the lithologic, biostratigraphic and geochemical data. Data collected in Mule Canyon in Hudspeth County, Texas. GR = gamma ray, K = potassium, Th = thorium, U = uranium, TOC = total organic carbon, and ^{13}C = carbon isotopic values.

Table 2. Total Organic Carbon From Mule Canyon Section 2. Sample numbers are the height taken above the Buda Formation Contact.

Sample Height (ft)	TOC (wt%)
MC2-30	1.78
MC2-50	1.42
MC2-75	2.07
MC2-85	2.71
MC2-115	1.38
MC2-125	1.83

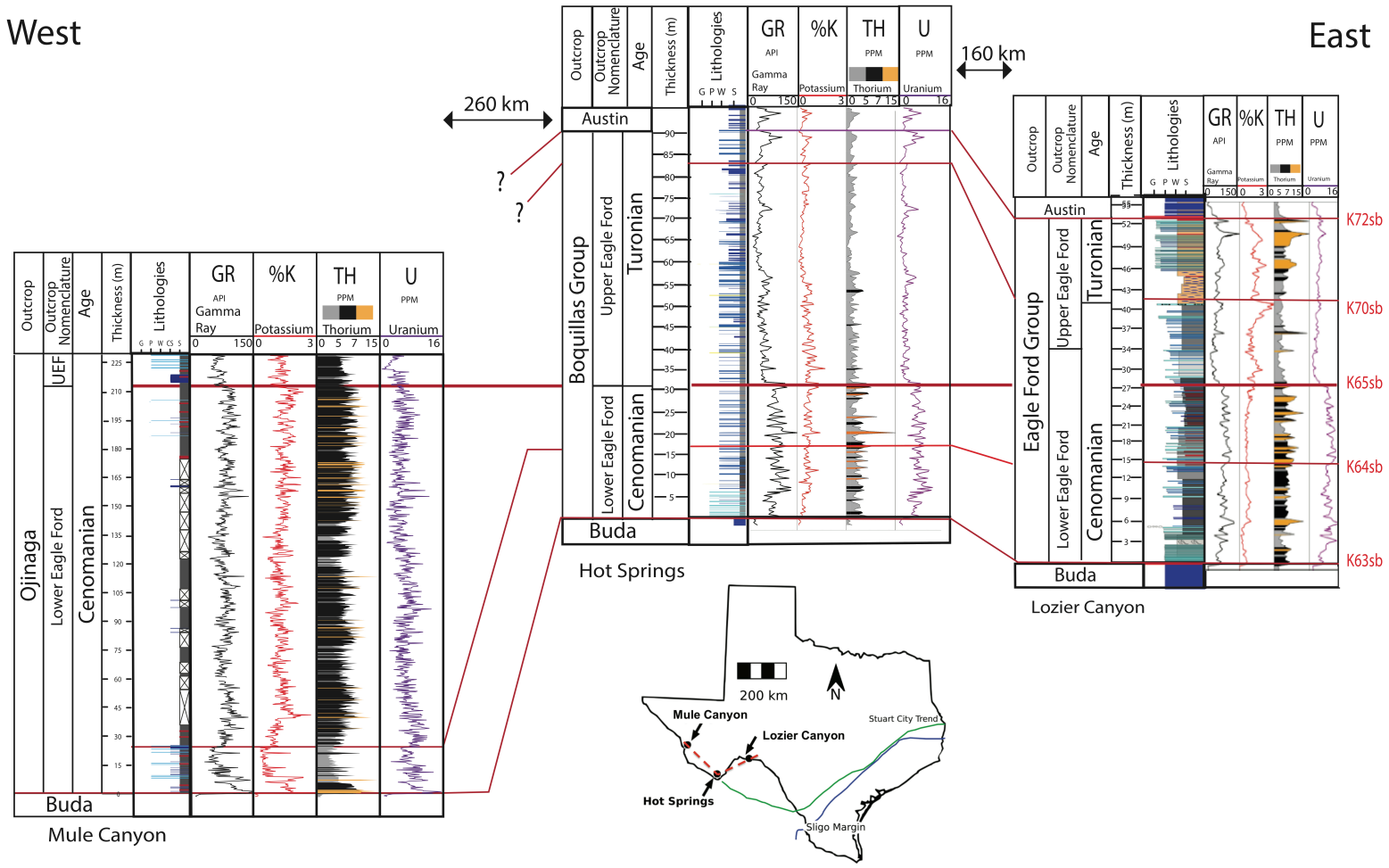

Figure 9. Ojinaga, Boquillas and Eagle Ford Formation correlation based on lithological and geochemical data. Boquillas Formation data (Wehner, 2015), Eagle Ford Formation data (Donovan et al., 2012). Sequence nomenclature developed by Donovan et al. 2012.

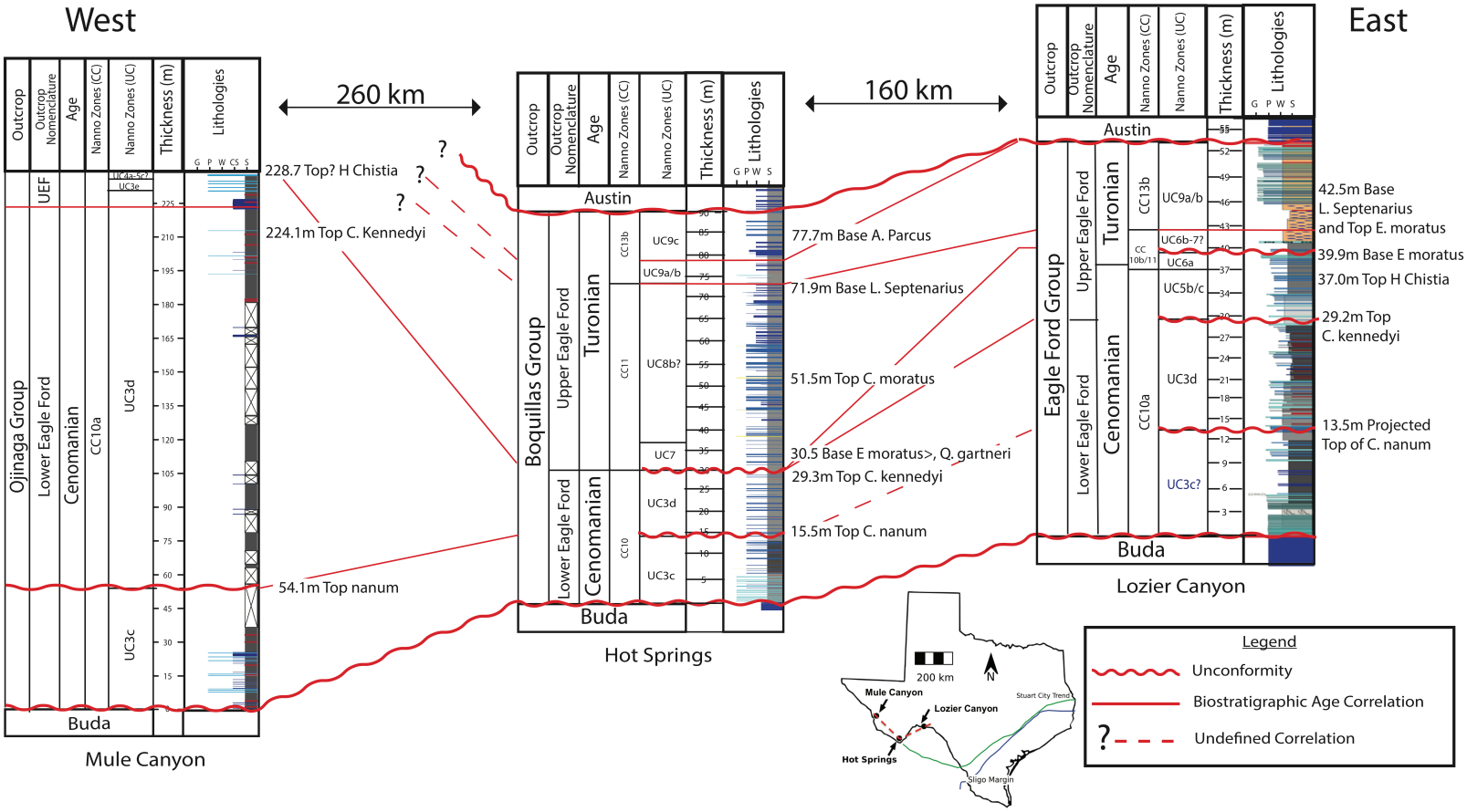

Figure 10. Ojinaga, Boquillas and Eagle Ford Formation correlation based on biostratigraphic data. Boquillas Formation data (Wehner, 2015), Eagle Ford Formation data (Donovan et al., 2012)

Figure 11. XRF major elemental concentrations. The concentrations of Ca (A), Si (A), Al (A), Fe (B), K (B), Mo (C) and U (C) from Mule Canyon Section 1 derived from XRF analysis plotted as a function of depth.

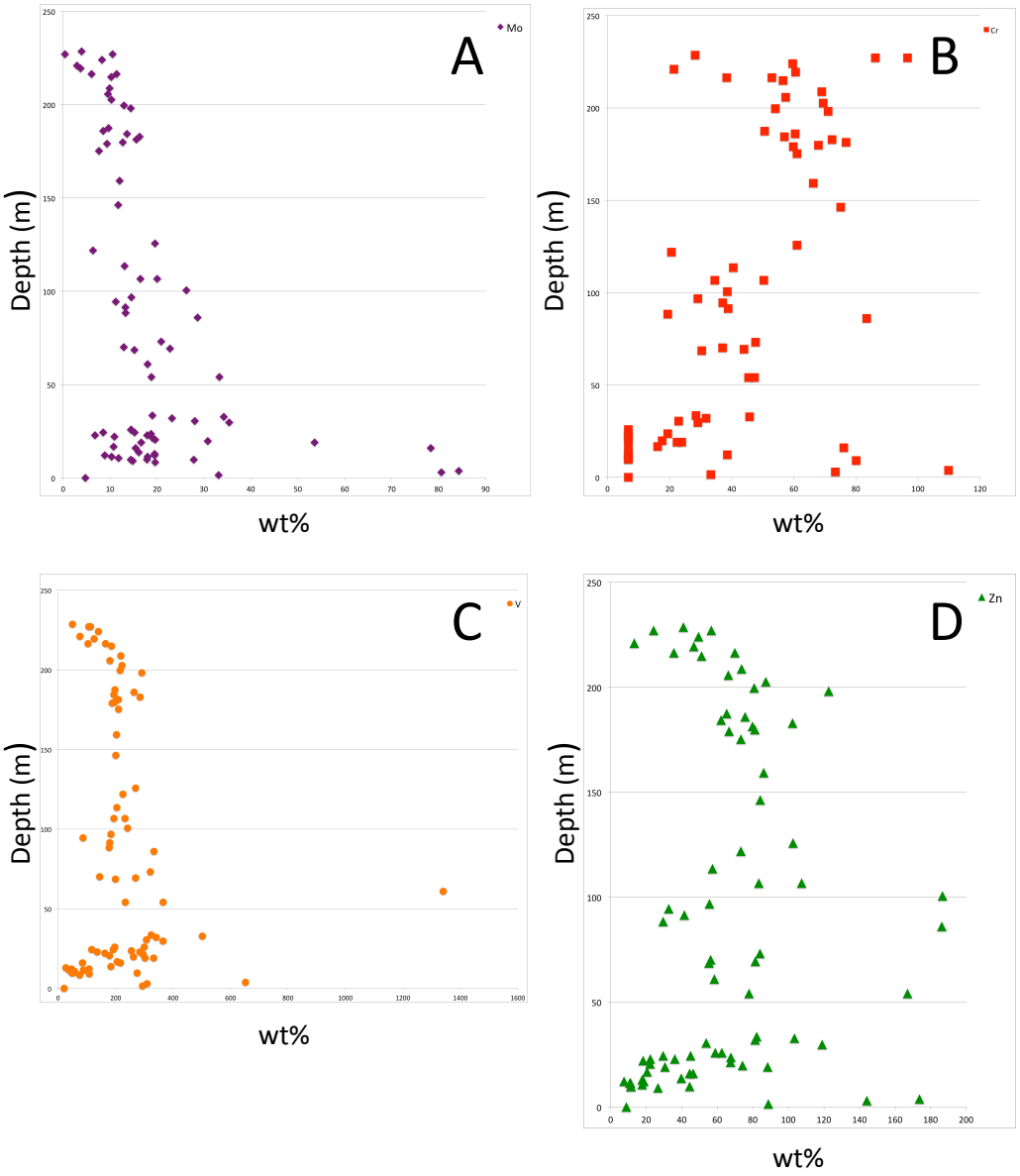

Figure 12. XRF trace elemental concentrations. The concentrations of Mo (A), Cr (B), V (C), and Zn (D) from Mule Canyon Section 1 derived from XRF analysis plotted as a function of depth.

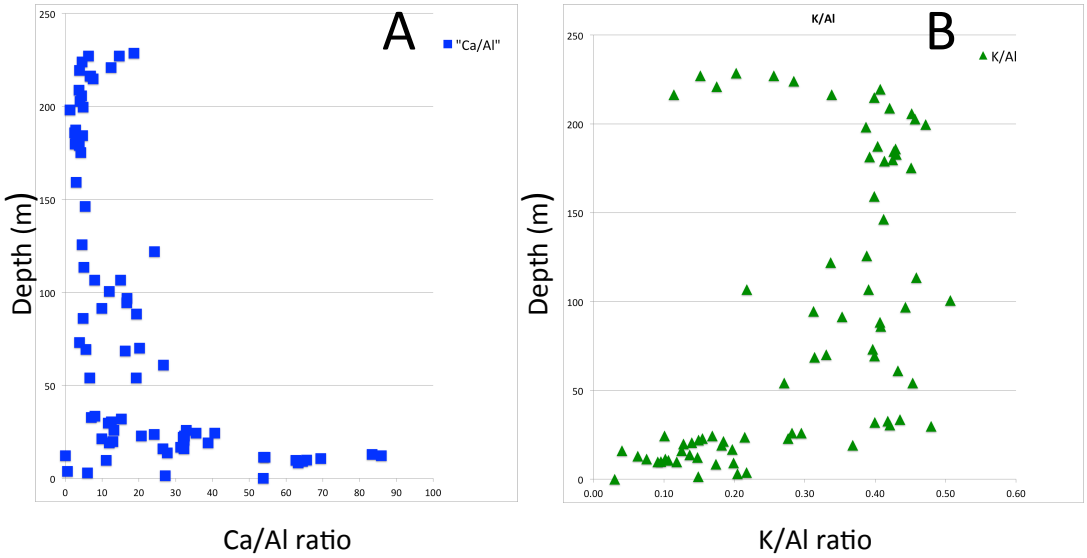

Figure 13. Plots of element ratios. Ca/Al (A), K/Al (B) plotted against depth.

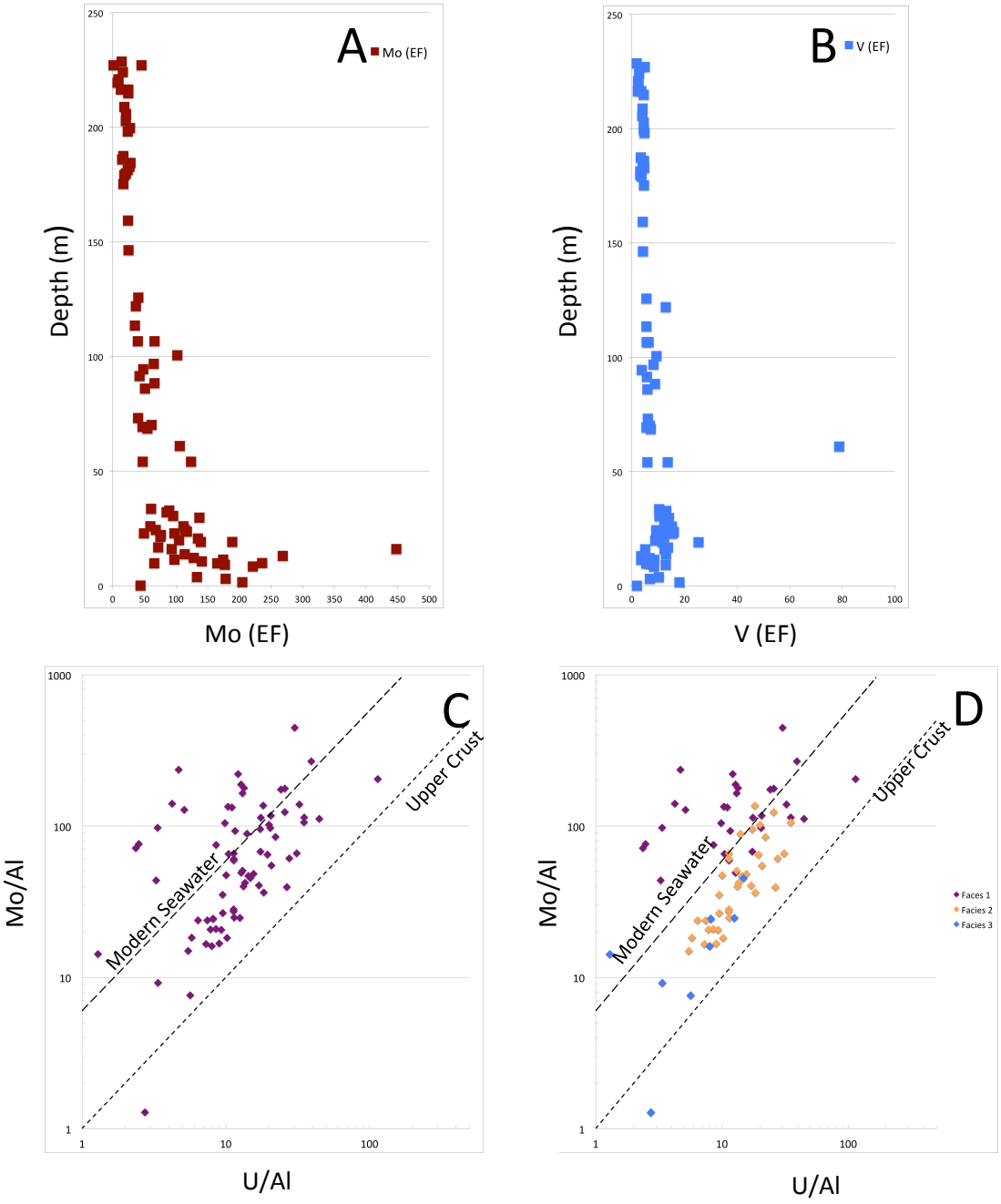

Figure 14. Mo-Enrichment factor plotted against depth. (A). V-Enrichment Factor (EF) plotted against depth (B). Cross-plot of molybdenum and uranium normalized to aluminum (C). Cross-plot of molybdenum and uranium normalized to aluminum with assigned facies (D)

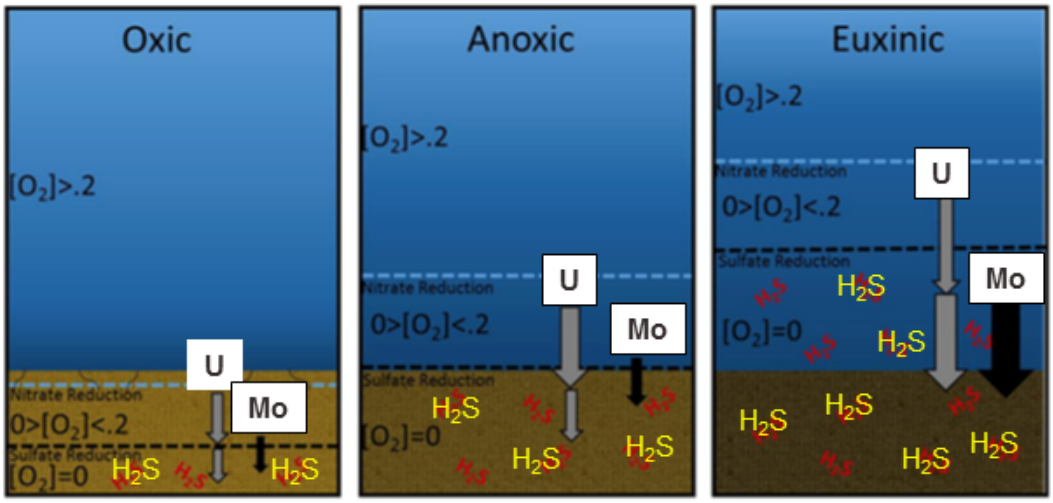

Figure 15. Schematic diagram of oxic, anoxic and euxinic conditions. Classification of depositional environments modified from Kelly, 2016, information derived from Algeo and Tribovillard, 2009 and Tribovillard, et. al., 2006.

APPENDIX B

GeoMark Methodology

1. Sample Requirements for a Typical Geochemical Program For geochemical analysis a teaspoon (ca. 10 g.) of sample material is needed when TOC, RockEval, vitrinite reflectance and residual hydrocarbon fluid fingerprinting is to be completed. If possible, a tablespoon is preferred. However, it is possible to complete a detailed program with even less sample, although there is dependency on the sample characteristics (e.g., organic richness, abundance of vitrinite, amount of staining).

2. Total Organic Carbon (TOC) – LECO C230 instrument Leco TOC analysis requires decarbonation of the rock sample by treatment with hydrochloric acid (HCl). This is done by treating the samples with Concentrated HCL for at least two hours. The samples are then rinsed with water and flushed through a filtration apparatus to remove the acid. The filter is then removed, placed into a LECO crucible and dried in a low temperature oven (110 C) for a minimum of 4 hours. Samples may also be weighed after this process in order to obtain a % Carbonate value based on weight loss.

The LECO C230 instrument is calibrated with standards having known carbon contents. This is completed by combustion of these standards by heating to 1200oC in the presence of oxygen. Both carbon monoxide and carbon dioxide are generated and the carbon monoxide is converted to carbon dioxide by a catalyst. The carbon dioxide is measured by an IR cell. Combustion of unknowns is then completed and the response of unknowns per mass unit is compared to that of the calibration standard, thereby the TOC is determined.

Standards are analyzed as unknowns every 10 samples to check the variation and calibration of the analysis. Random and selected reruns are done to verify the data. The acceptable standard deviation for TOC is 3% variation from established value.

APPENDIX C

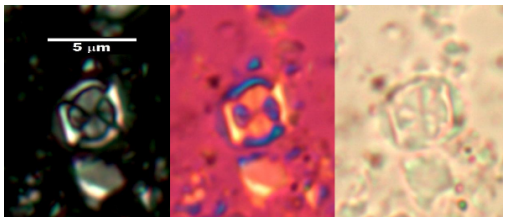

Corollithion kennedyi (Sample 735)

Corollithion kennedyi (Sample 225)

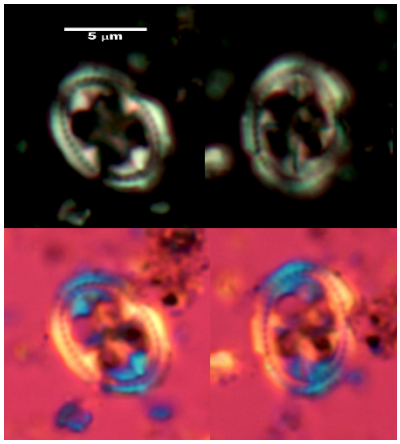

Axopodorhabdus albianus (Sample 177.5)

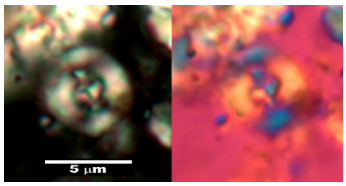

Helenea chiastia (Sample 225)

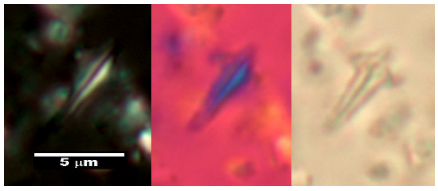

Lithraphidites acutus (Sample 350)

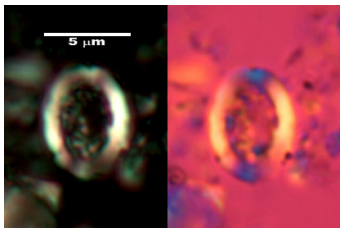

Rhagodiscus asper (Sample 350)

Questionable *L. acutus* specimens from Sample 2.5

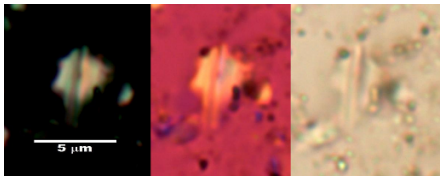

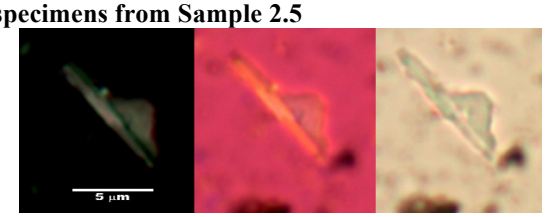

Calcareous Nannofossils from Mule Canyon Section 1. (Courtesy of Bugware Inc.) Light micrographs (x-polarized light, with 530 nm gypsum plate, and plain light; scale bar = 5 um)

APPENDIX D

Petrographic Descriptions

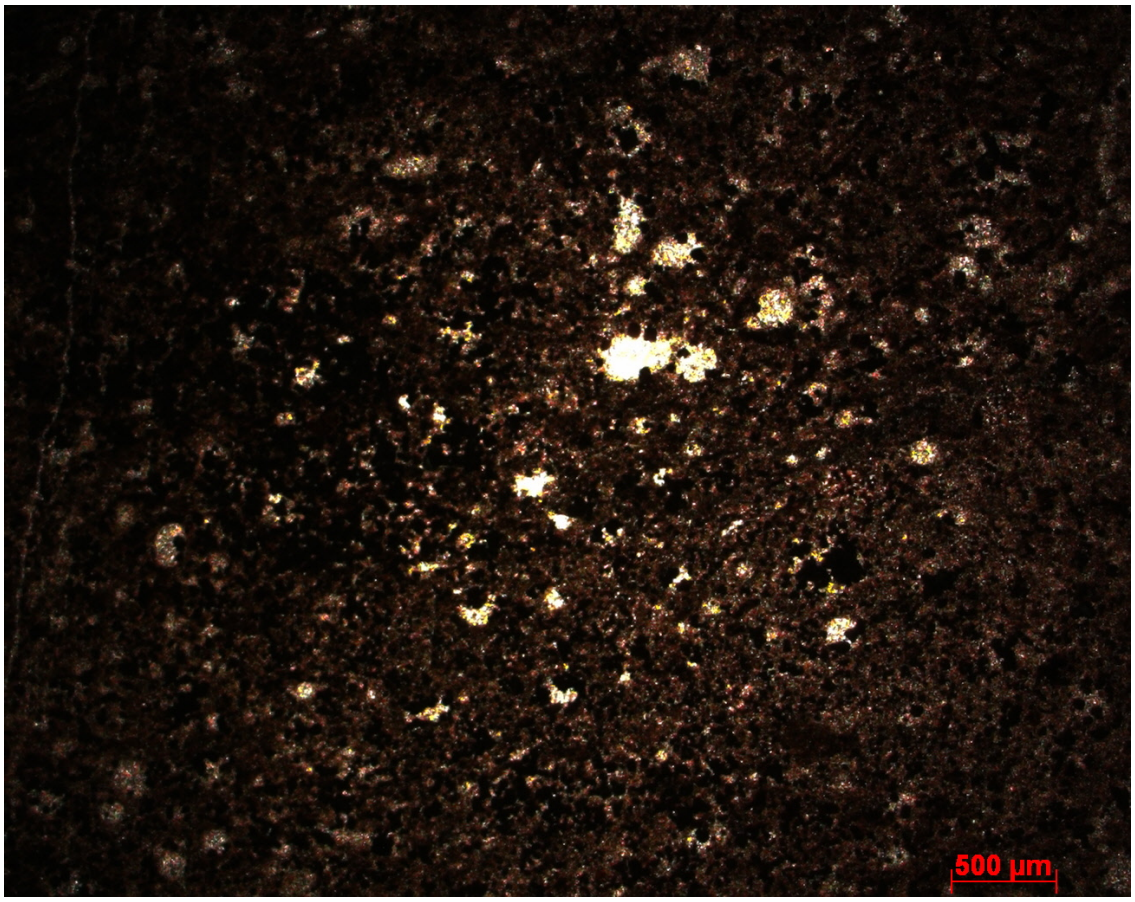

Sample: MC1-30

Height Above Buda: 30 ft

<u>Skeletal Grain Type Abundance</u>

Planktonic Foraminiferal: 70%

Calcispheres: 30%

Pellets: 30%

Pyrite: <5-10%

Organics 50%

Other Diagenetic Features: Some equant calcite in matrix and poikiloitic calcite cement and micrtized calcispheres. Skeletal fragments filled with sparry calcity. Calcite filled fractures. Pyrtie nodules and disseminated pyrite associated with veins and pore space. Porosity 5-10% interparticle. Pellets appear flattened and aligned to bedding indicating compaction. Weak laminations of foraminiferal.

Rock Name: Calcareous wackestone

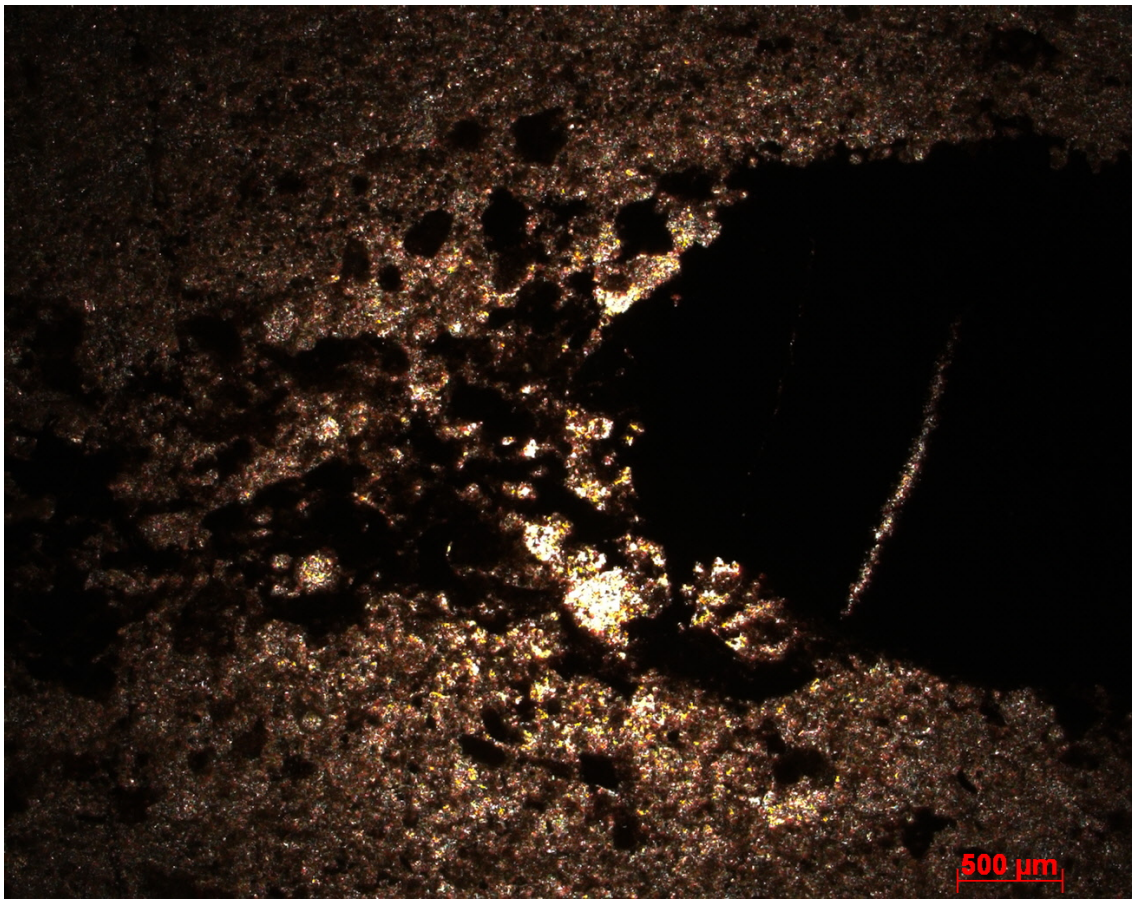

Sample: MC1-32

Height Above Buda: 32 ft

<u>Skeletal Grain Types Abundance</u>

Planktonic Foraminiferal: 15%
Radiolarians: 5%
Inoceramids: 3%
Calcispheres: 50%
Pellets 15%
Organics: 10%
Pyrite: <5%

Other Diagenetic Features: Parallel lamination, syn-depositional pyrite nodules. Calcite cement and micritized skeletal fragments. Sparry calcite, biomicrosparite neomorphosed skeletal grains. Skeletal chambers replaced with sparry calcite, bottom part of sample is unaltered micrite, forams, radiolarians. Calcite veins and highly fractured. Large pyrite nodules.

Rock Name: Foraminiferall calcareous packstone

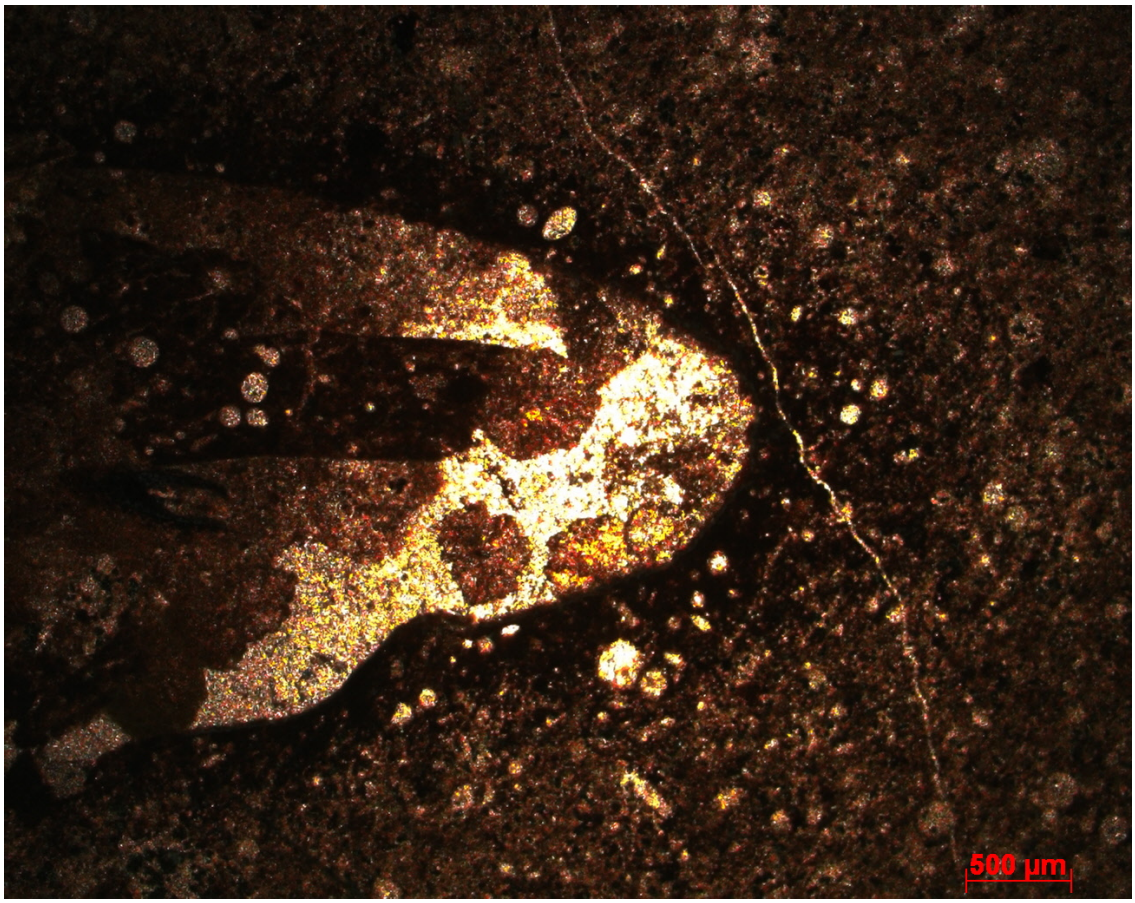

Sample: MC1-32.5

Height Above Buda: 32.5 ft

Skeletal Grain Type Abundance

Planktonic Foraminiferal: 30%

Inoceramids: 30%

Calcispheres: 40%

Pellets 40%

Organics: 30%

Other Diagenetic Features: Micritized biofragments.

Rock Name: Inoceramid foraminiferall calcareous wackestone

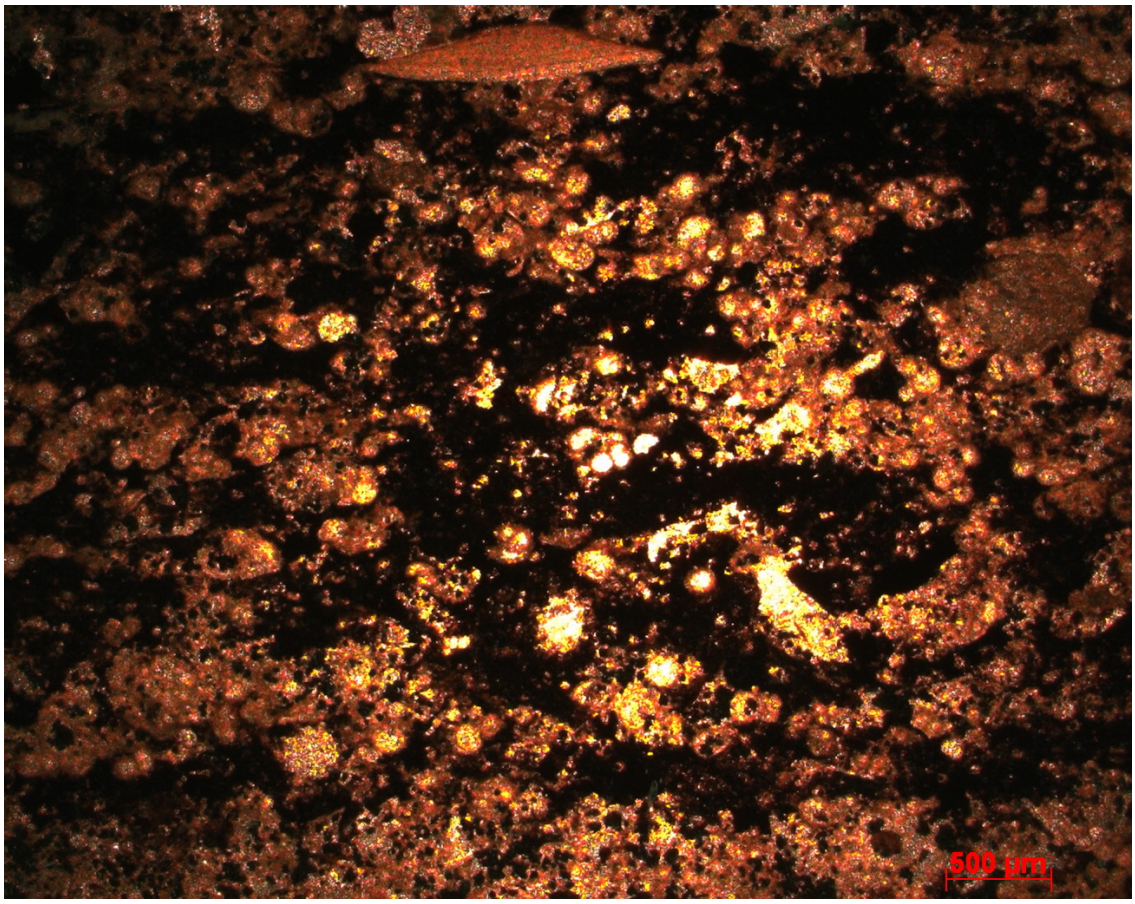

Sample: MC1-35

Height Above Buda: 35 ft.

Skeletal Grain Type Abundance

Planktonic Foraminiferal: 70%

Calcispheres: 30%

Inoceramids: 5%

Pellets 40%

Organics: 30%

Other Diagenetic Features: Some calcite cement in fractures, highly micritized.

Rock Name: Foraminiferall calcareous wackestone

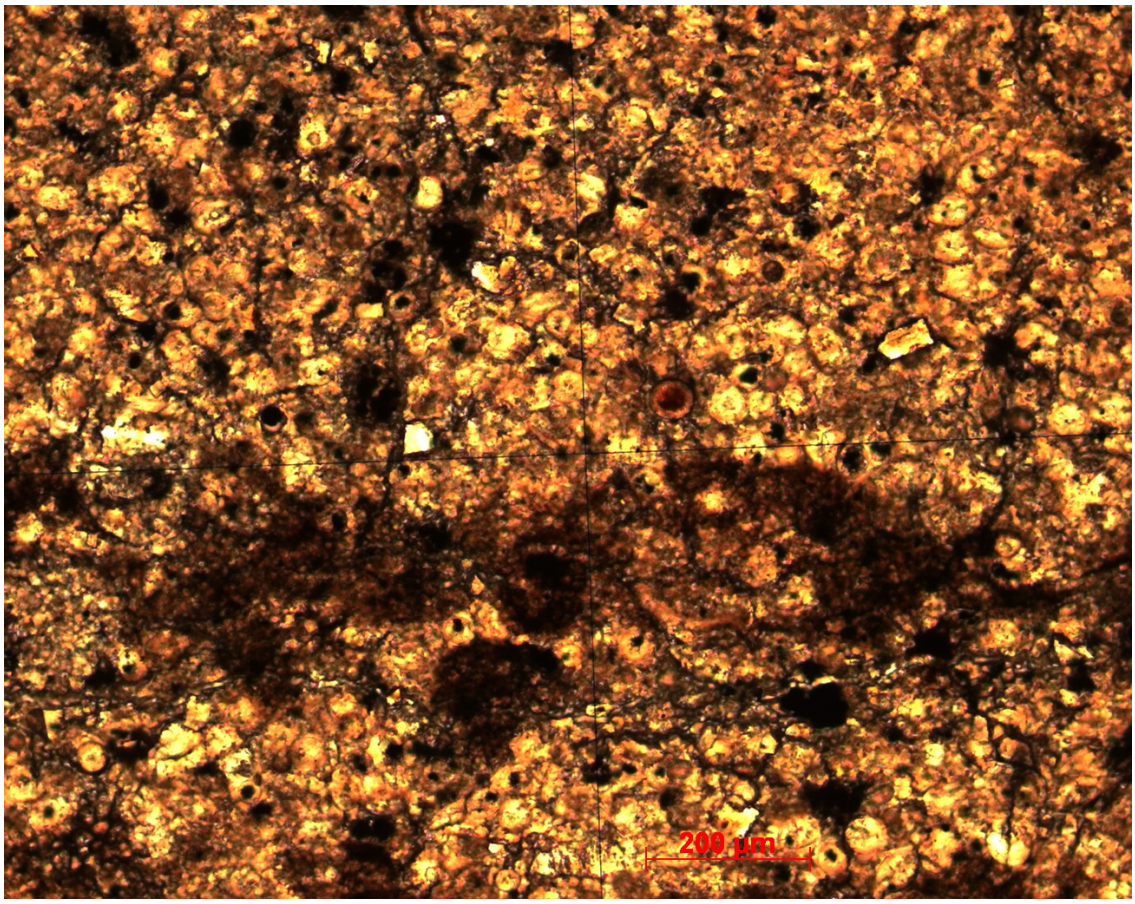

Sample: MC1-37.5

Height Above Buda: 37.5 ft

Skeletal Grain Type Abundance

Planktonic Foraminiferal: 60%
Inoceramids: 5%
Calcispheres: 10%
Unidentified: 25%
Dolomitic Rhombs: 1%
Pyrite: 15%
Organics: 10%

Other Diagenetic Features: Some calcite infilling fractures. Skeletal fragments are micritized. Highly fractured, fractures filled with calcite. Fracture porosity <5%.

Rock Name: Skeletal calcareous siltstone/packstone

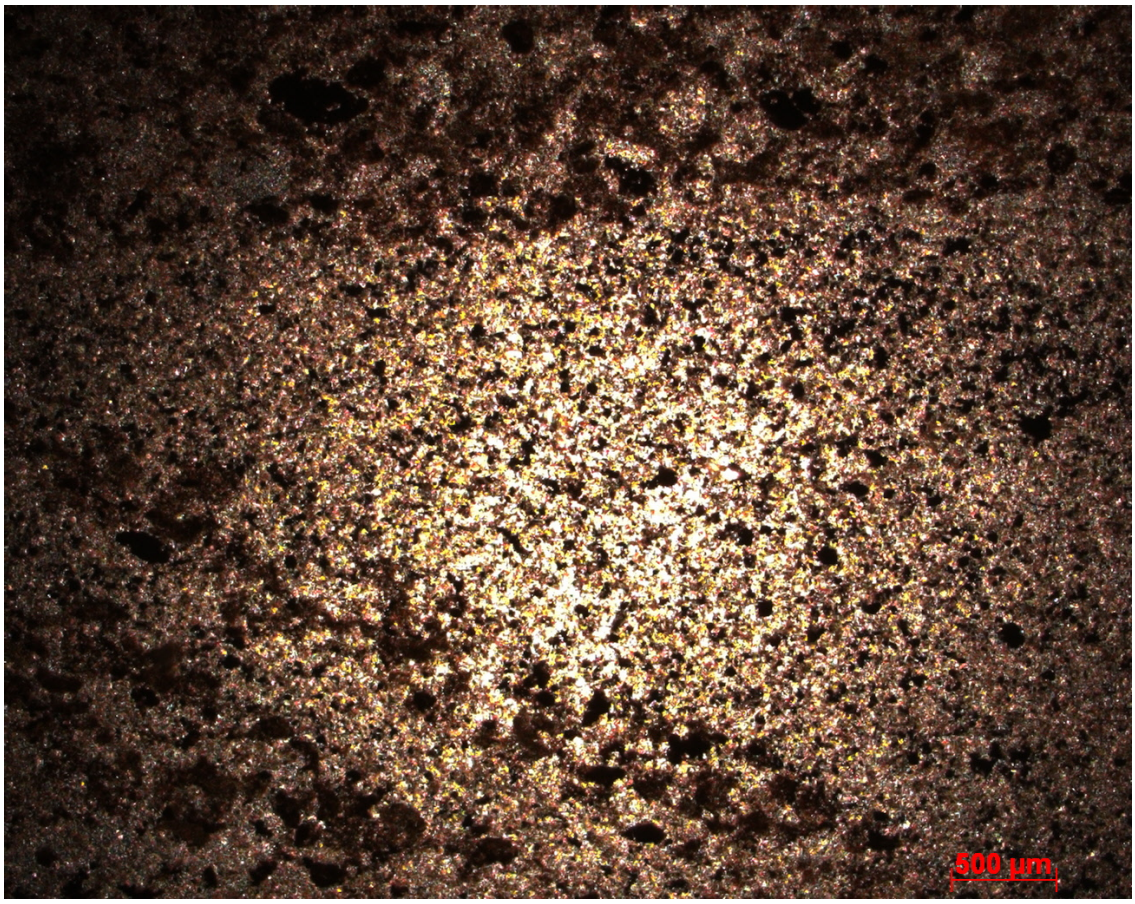

Sample: MC1-40

Height Above Buda: 40 ft

<u>Skeletal Grain Type Abundance</u>

Planktonic Foraminiferal: 70%

Calcispheres: 10%

Pellets 20%

Organics/mud: 60-70%

Other Diagenetic Features: Parallel to wavy lamination, cross bedding and erosional surface. 5% interparticle porosity

Rock Name: Foraminiferall calcareous packstone

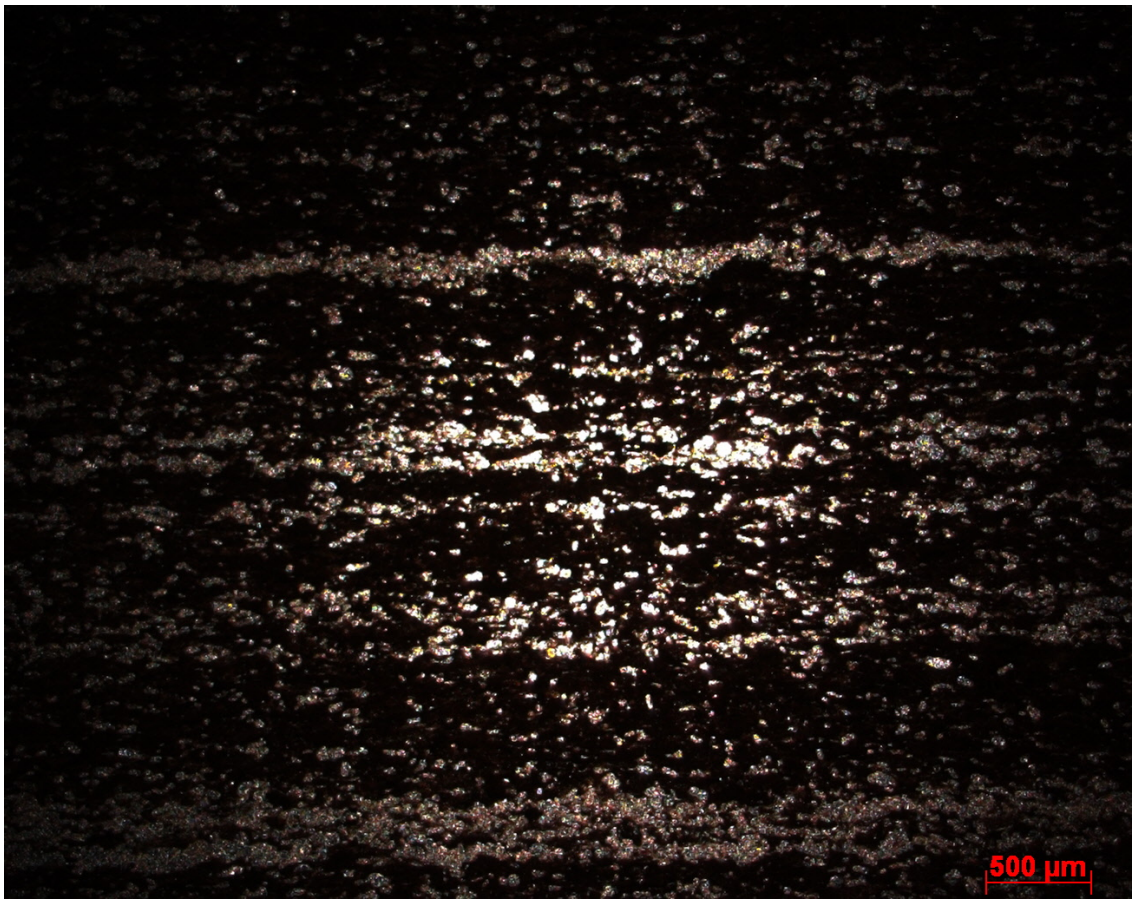

Sample: MC1-45

Height Above Buda: 45 ft

<u>Skeletal Grain Type Abundance</u>

Planktonic Foraminiferal: 70%

Calcispheres: 30%

Pellets 30%

Organics/mud: 80%

Other Diagenetic Features: Micritized biofragments.

Rock Name: Foraminiferall mudstone/wackestone

Sample: MC1-52.5

Height Above Buda: 52.5 ft

Skeletal Grain Type Abundance

Planktonic Foraminiferal: 70%

Calcispheres: 30%

Pellets 30%

Organics/mud: 80%

Other Diagenetic Features: Micritized biofragments.

Rock Name: Foraminiferall mudstone/siltstone

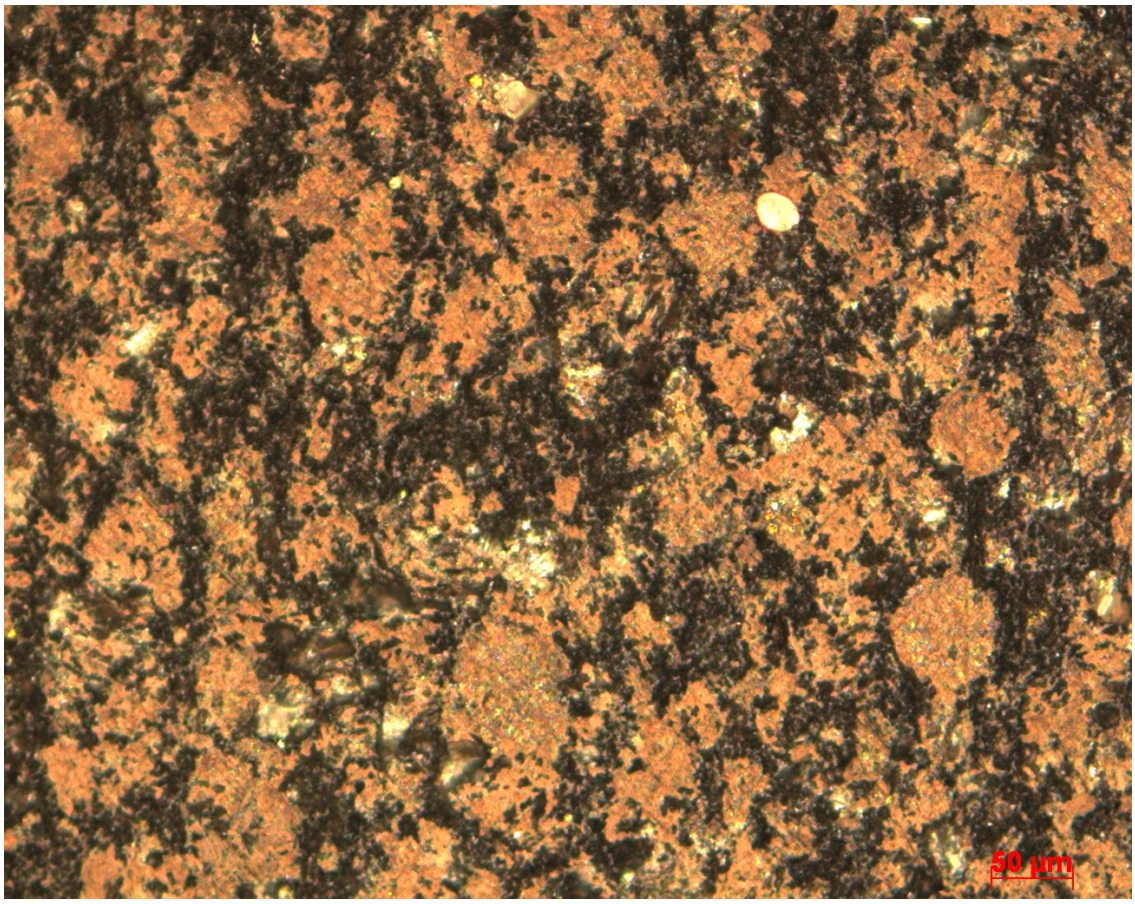

Sample: MC1-55

Height Above Buda: 55 ft.

<u>Skeletal Grain Type Abundance</u>

Planktonic Foraminiferal: 70%

Calcispheres: 35%

Pellets 50%

Organics: 30%

Other Diagenetic Features: Some calcite cement in fractures, highly micritized.

Rock Name: Foraminiferall calcareous wackestone

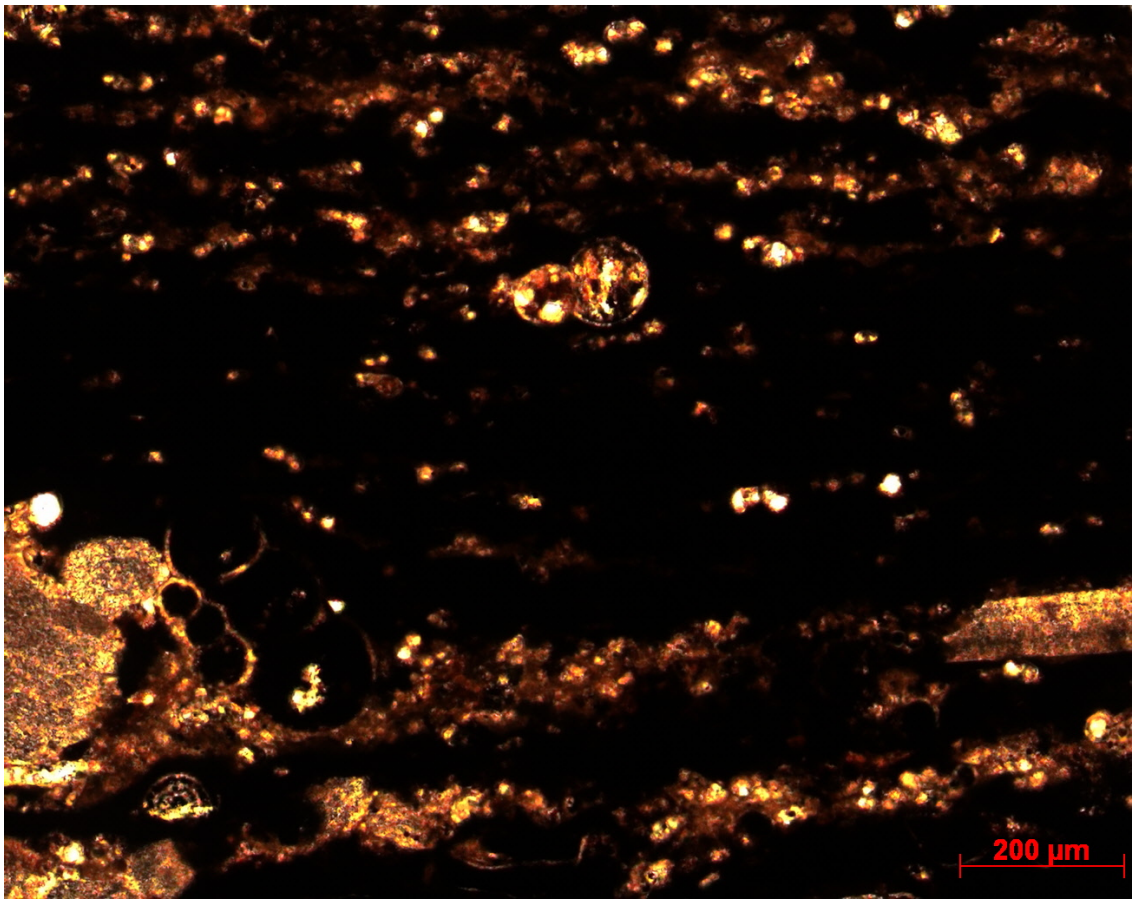

Sample: MC1-67.5

Height Above Buda: 67.5 ft

Skeletal Grain Type Abundance

Planktonic Foraminiferal: 20%

Calcispheres: 80%

Pellets: 5%

Organics/mud: 30-40%

Other Diagenetic Features: Parallel lamination some small fracutres, skeletal fragments have been micritized.

Rock Name: Foraminiferall calcareous siltstone/wackestone

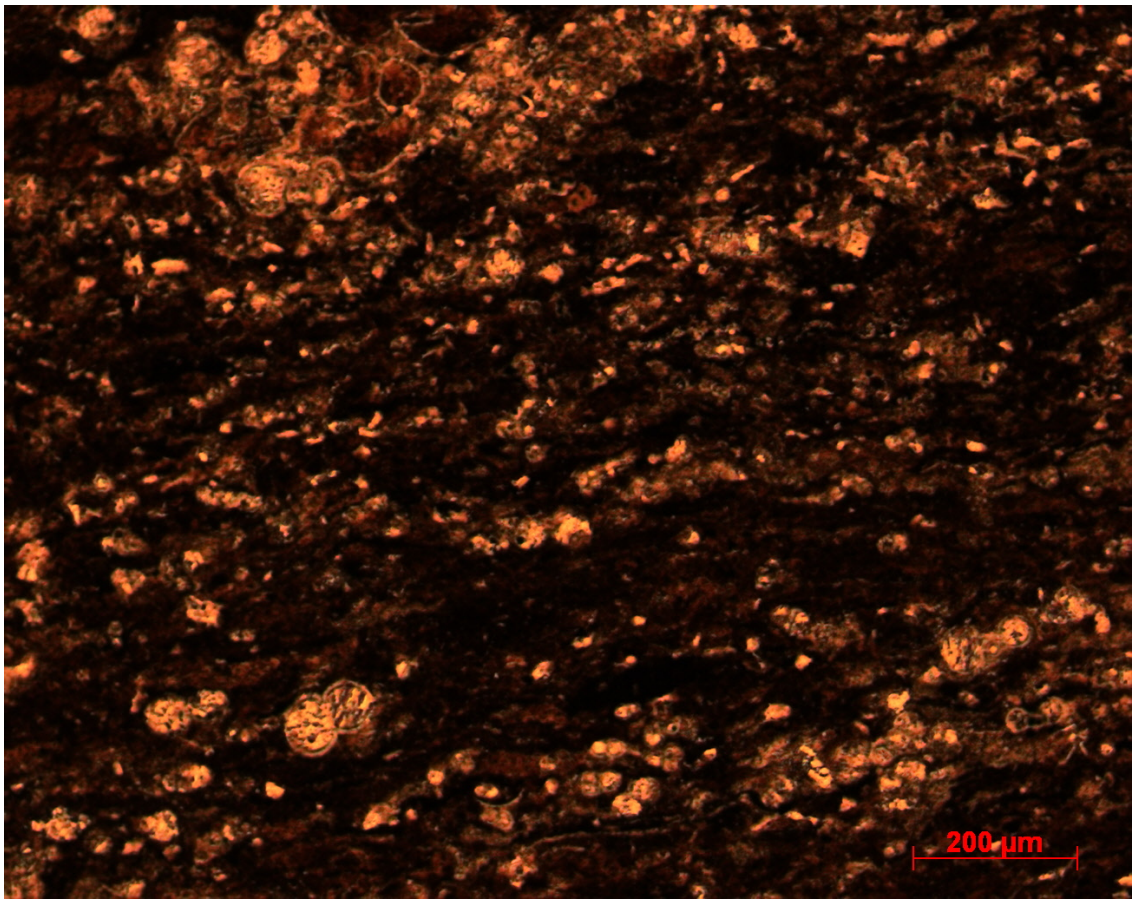

Sample: MC1-70

Height Above Buda: 70 ft

Skeletal Grain Type Abundance

Planktonic Foraminiferal: 70%

Calcispheres: 30%

Pellets <5%

Organics/mud: 60%

Other Diagenetic Features: parallel laminations of black organics. Biomicrite in foraminiferall laminations. Some skeletal grains partially micritized. Some fractures.

Rock Name: Calcareous foraminiferall mudstone

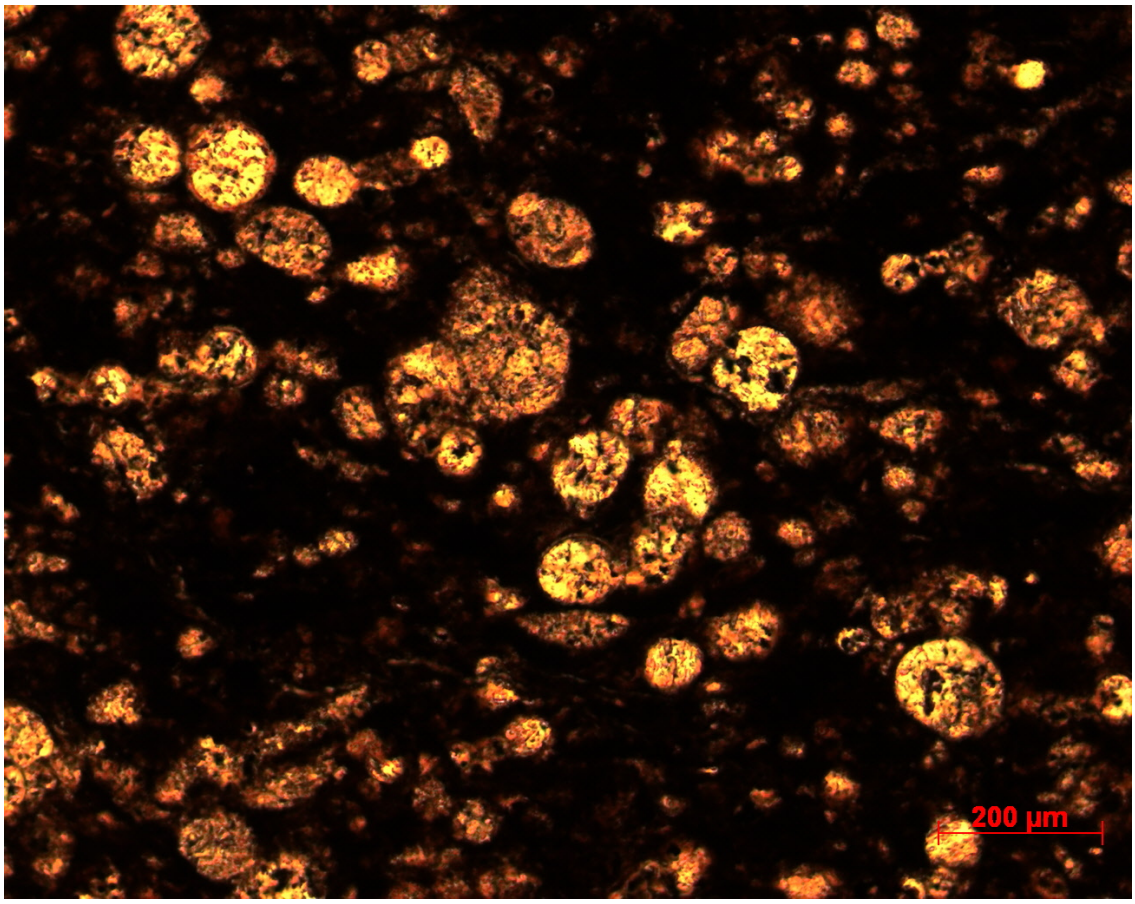

Sample: MC1-72.5

Height Above Buda: 72.5 ft

Skeletal Grain Type Abundance

Planktonic Foraminiferal: 80%

Calcispheres: 20%

Pellets 10%

Organics/mud: 40%

Other Diagenetic Features: Parallel laminations, micritized calcispheres and microfractures.

Rock Name: Calcareous foraminiferall mudstone/wackestone

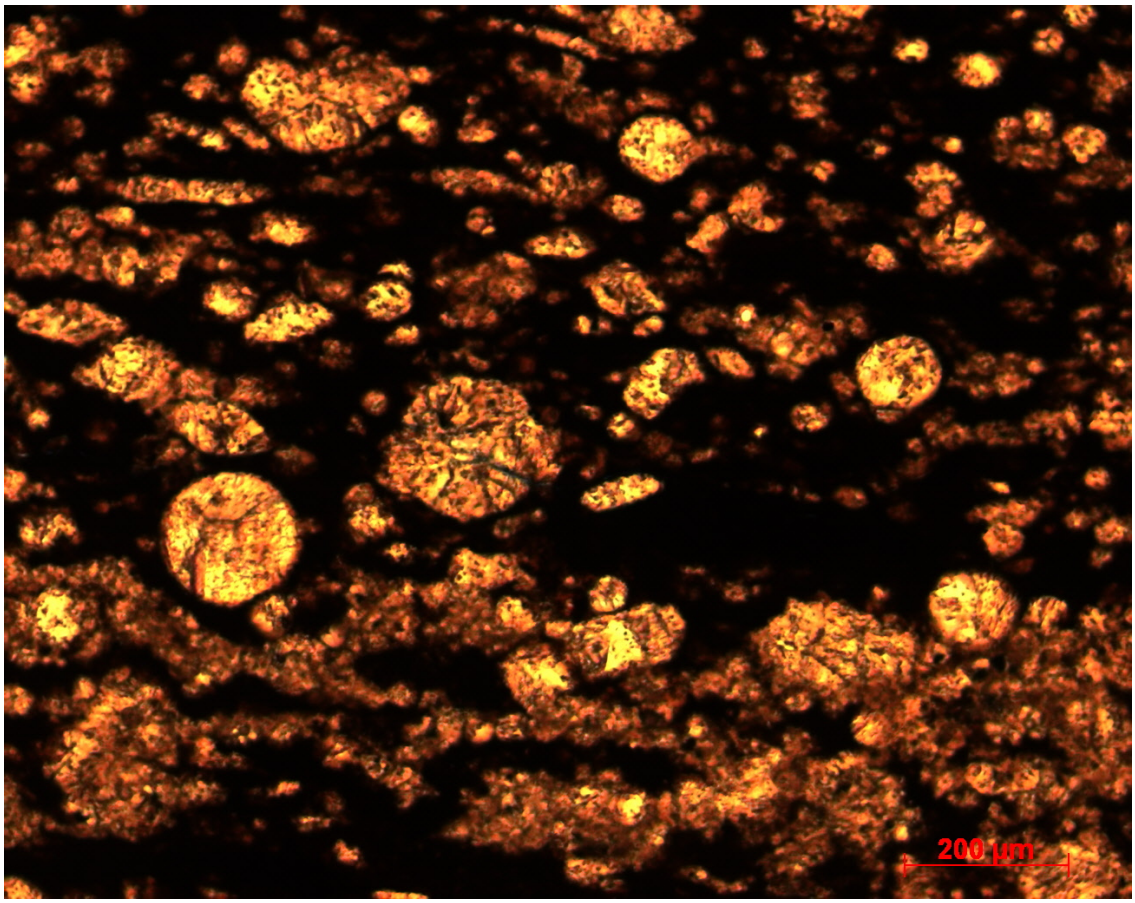

Sample: MC1-75

Height Above Buda: 75 ft

Skeletal Grain Type Abundance

Planktonic Foraminiferal: 30%

Calcispheres: 70%

Pellets 10%

Organics/mud: 80%

Other Diagenetic Features: Parallel laminations with micritized smaller calcispheres.

Rock Name: Foraminiferall calcareous mudstone

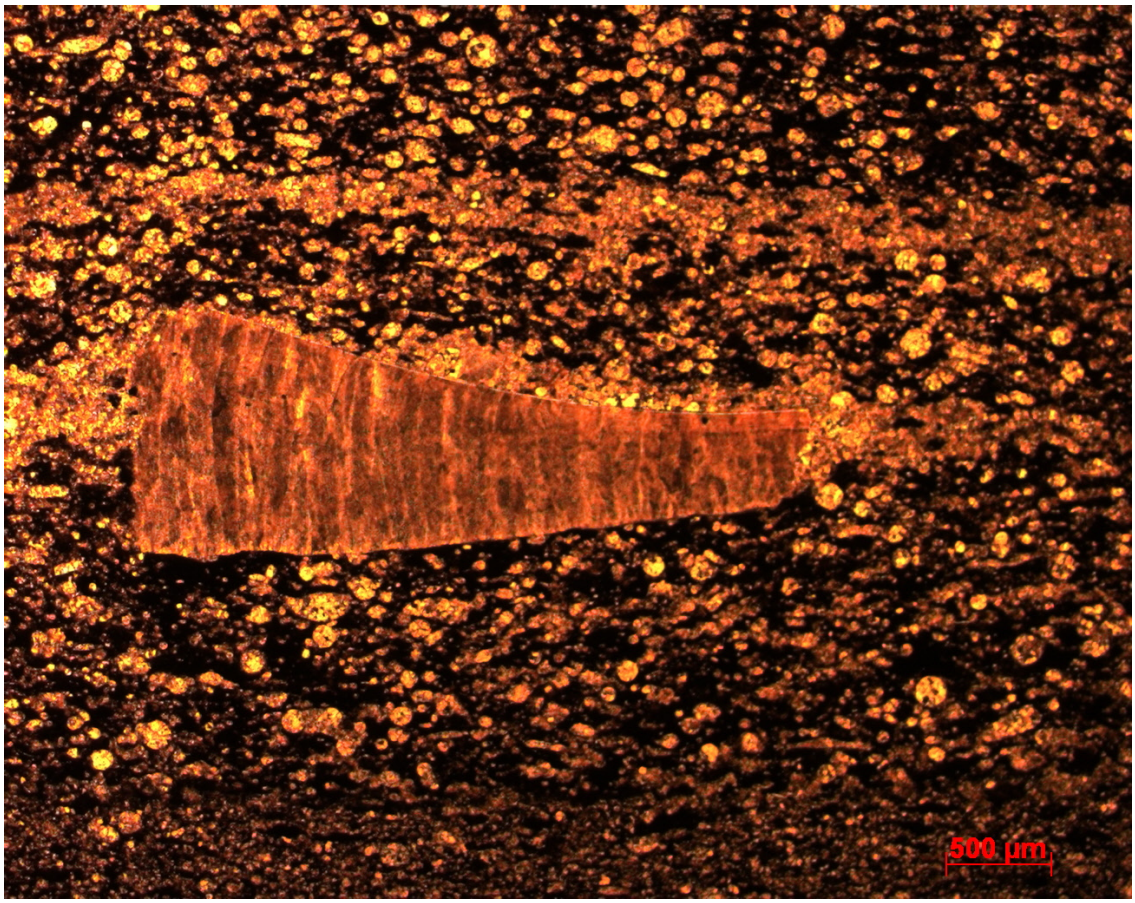

Sample: MC1-80

Height Above Buda: 80 ft

<u>Skeletal Grain Type Abundance</u>

Planktonic Foraminiferal: 60%

Inoceramids: 20%

Calcispheres: 20%

Pellets 40%

Organics: 30%

Other Diagenetic Features: Micritized biofragments.

Rock Name: Inoceramid foraminiferall calcareous wackestone

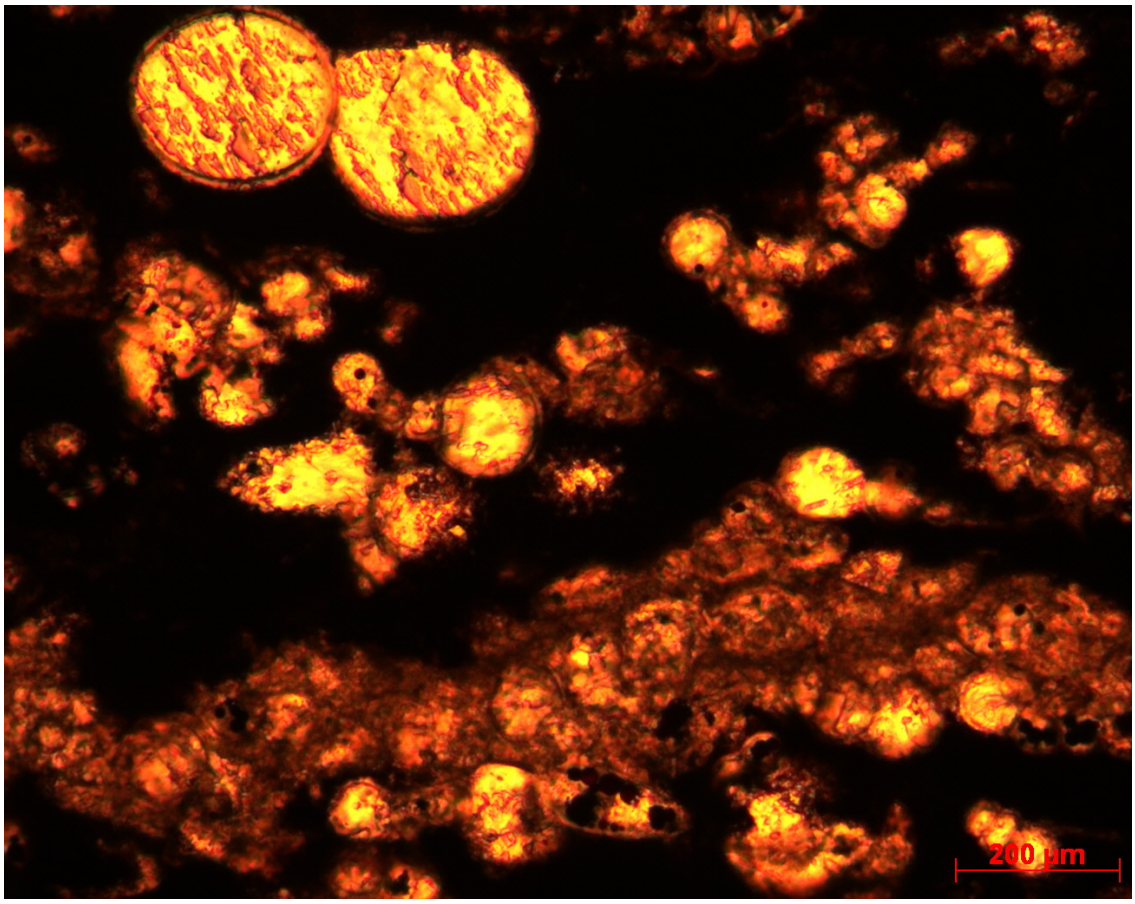

Sample: MC1-82

Height Above Buda: 82 ft

Skeletal Grain Type Abundance

Planktonic Foraminiferal: 60%

Calcispheres: 40%

Pellets 5%

Organics/mud: 70%

Other Diagenetic Features: Parallel lamination, micritized forams and calcispheres, possible dissolved bivalve fragments. Dissolution of skeletal fragments. Micritized boundaries.

Rock Name: Calcareous foraminiferall mudstone

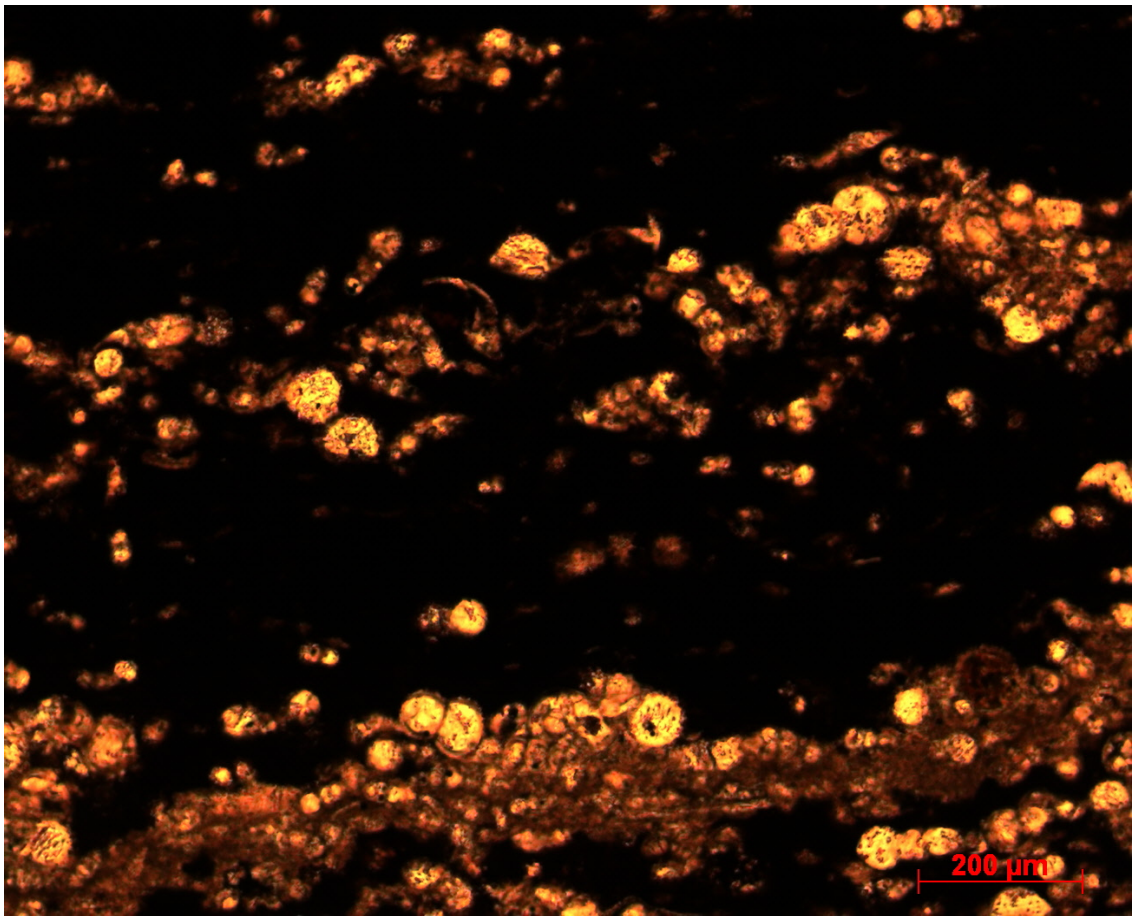

Sample: MC1-85

Height Above Buda: 85 ft

Skeletal Grain Type Abundance

Planktonic Foraminiferal: 60%

Calcispheres: 40%

Pellets 5%

Organics/mud: 70%

Other Diagenetic Features: Parallel lamination, micritized forams and calcispheres, possible dissolved bivalve fragments. Dissolution of skeletal fragments. Micritized boundaries.

Rock Name: Calcareous foraminiferall mudstone

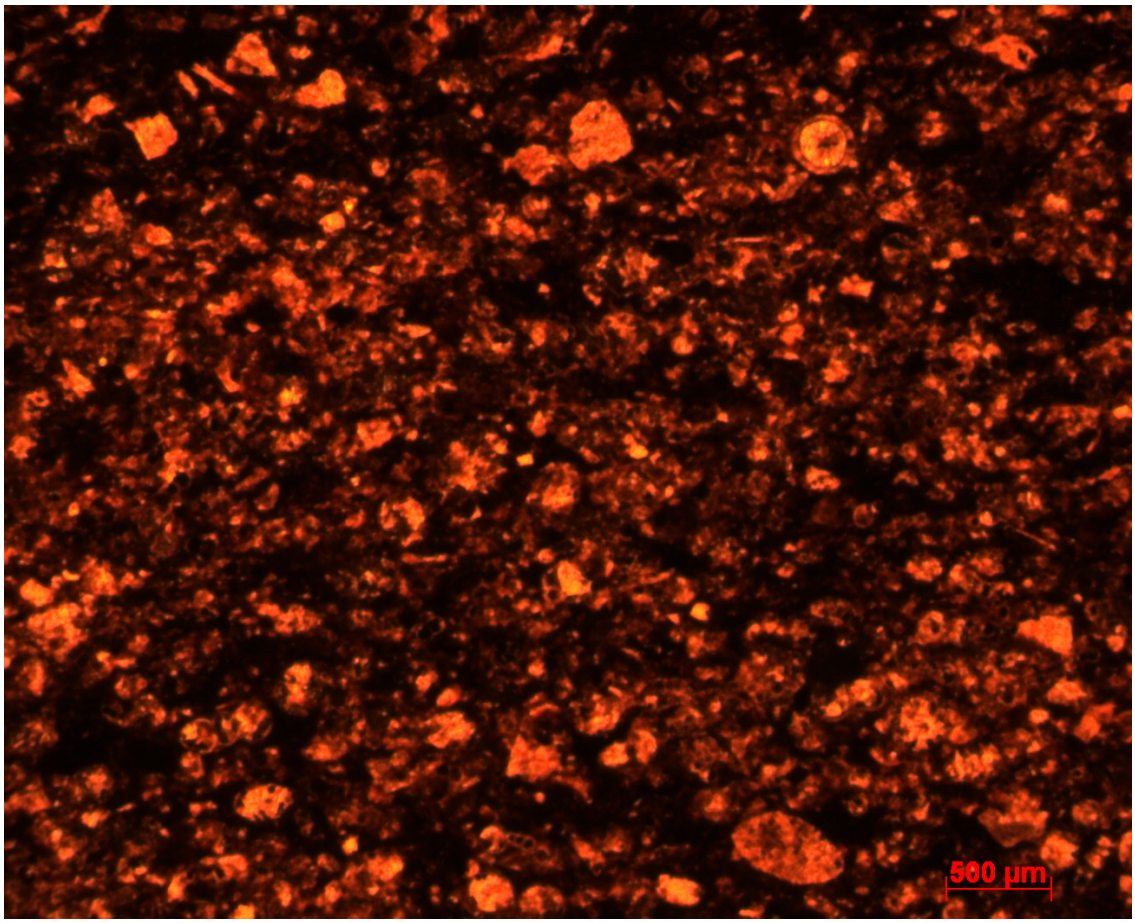

Sample: MC1-110

Height Above Buda: 110 ft

Skeletal Grain Type Abundance

Planktonic Foraminiferal: 30%

Inoceramids: 30%

Calcispheres: 20%

Unidentified 50%

Crinoid: <1%

Pellets 5-10%

Organics: 20-30%

Other Diagenetic Features: Micritized biofragments, wavy to parallel laminations.

Rock Name: Foraminiferall skeletal packstone

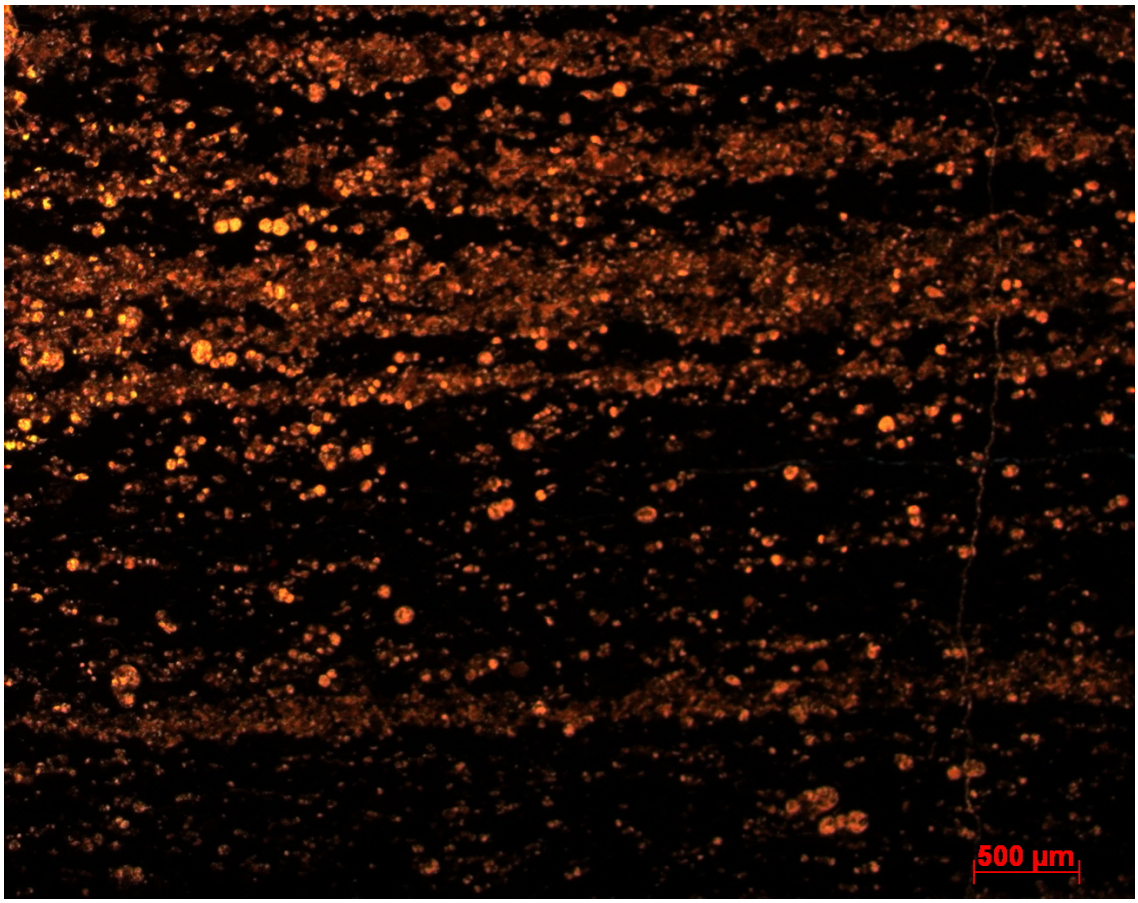

Sample: MC1-265

Height Above Buda: 265 ft

Skeletal Grain Type Abundance

Planktonic Foraminiferal: 60%

Calcispheres: 40%

Pellets 5%

Organics/mud: 70%

Other Diagenetic Features: Parallel lamination, micritized forams and calcispheres, possible dissolved bivalve fragments. Dissolution of skeletal fragments. Micritized boundaries.

Rock Name: Calcareous foraminiferall mudstone

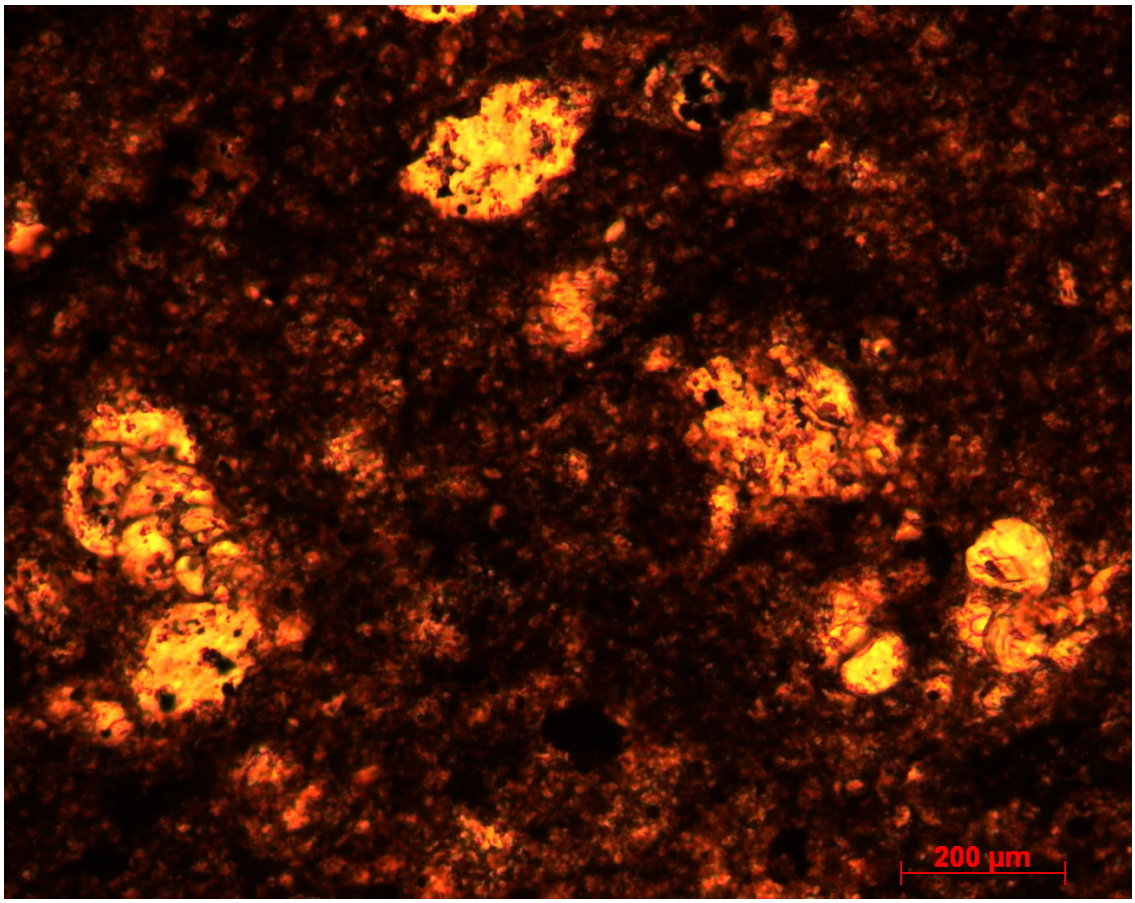

Sample: MC1-745

Height Above Buda: 745 ft

<u>Skeletal Grain Type Abundance</u>

Planktonic Foraminiferal: 30%

Calcispheres: 10%

Unidentified: 60%

Pellets 20%

Organics/mud: 80-90%

Other Diagenetic Features: Highly micritized and dissolved biofragments. Highly fractured with parallel laminations.

Rock Name: Foraminiferall mudstone

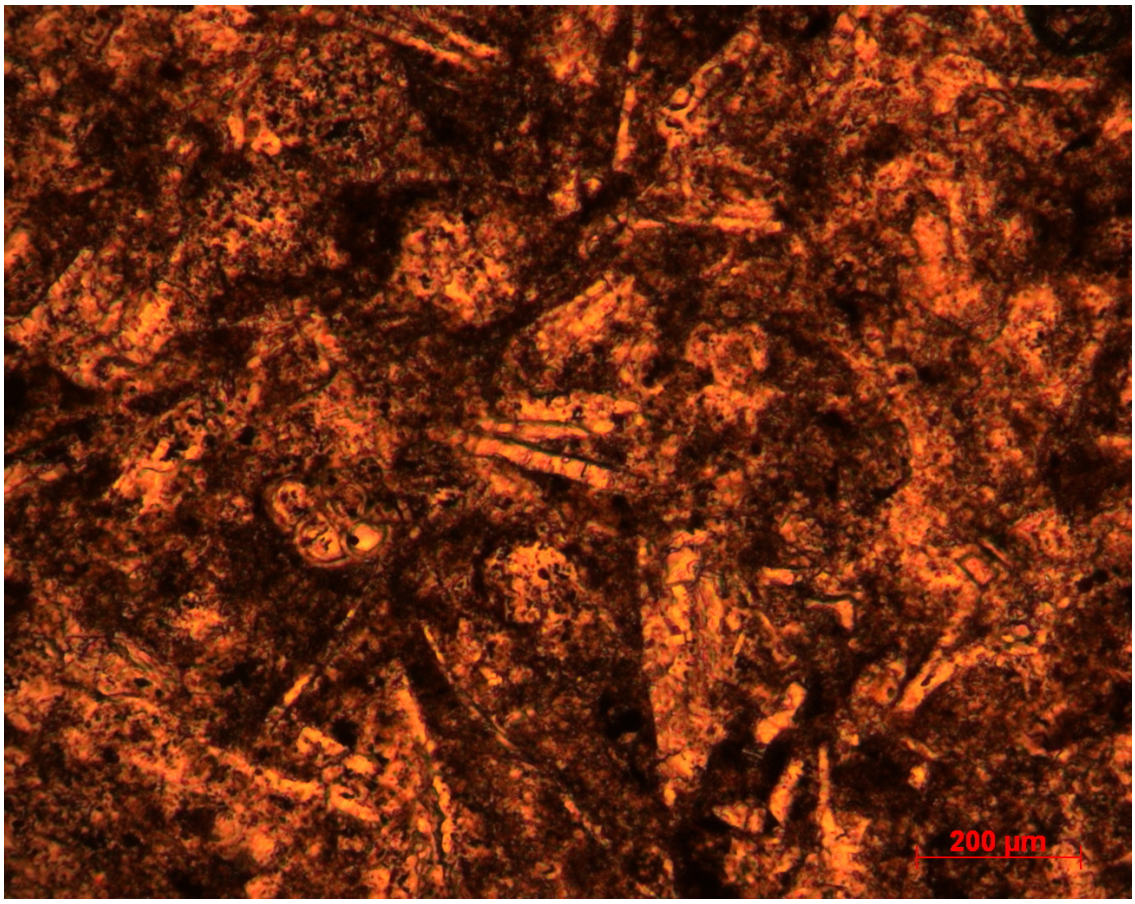

Sample: MC1-750

Height Above Buda: 750 ft

Skeletal Grain Type Abundance

Planktonic Foraminiferal: 10%

Calcareous sponge spicules: 90%

Pellets 5%

Organics/mud: 20%

Other Diagenetic Features: Micritized and dissolved biofragments. Highly fractured, post depositional.

Rock Name: Spiculitic Packstone

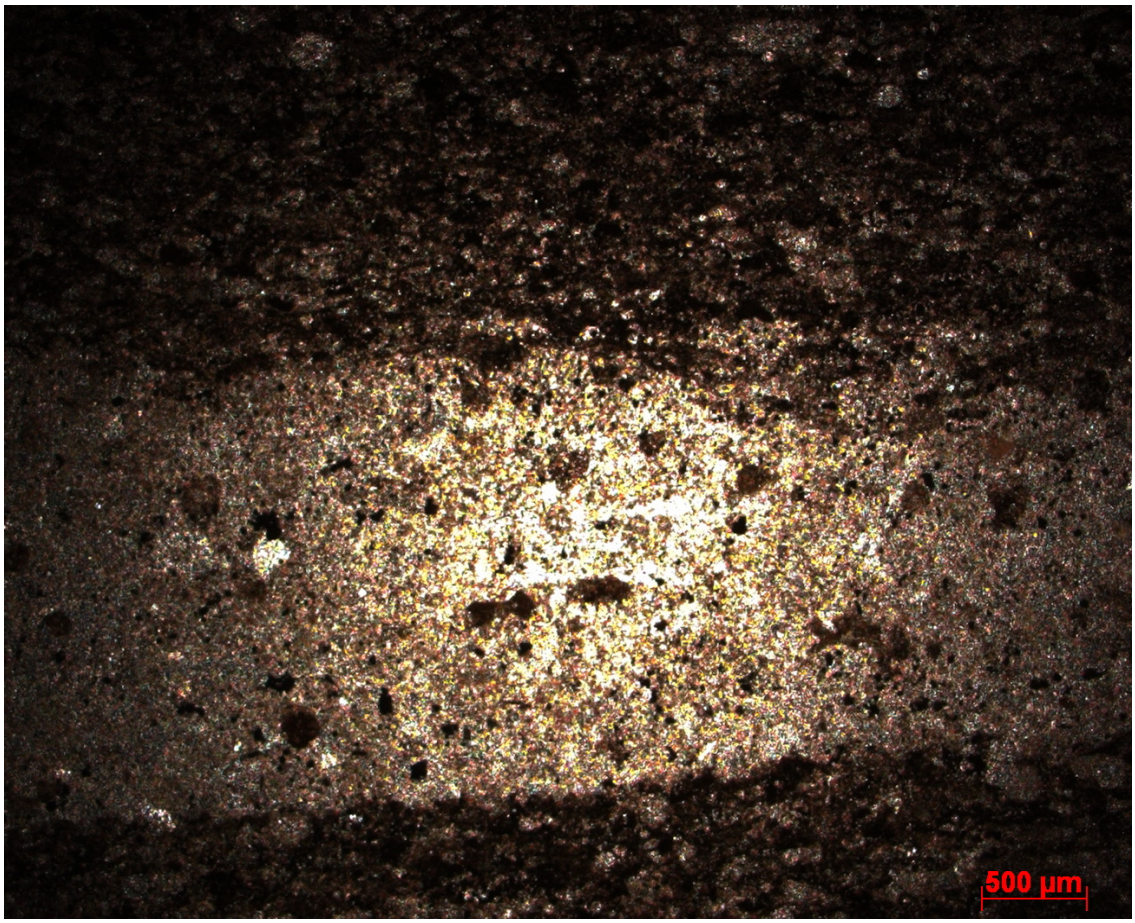

Sample: MC2-40

Height Above Buda: 40 ft

Skeletal Grain Type Abundance

Planktonic Foraminiferal: 60%

Calcispheres: 20%

Unidentified: 20%

Pellets 30%

Organics: 30-40%

Pyrite: 5%

Other Diagenetic Features: Highly micritized biofragments, parallel laminations and micrfaults.

Rock Name: Calcareous wackestone

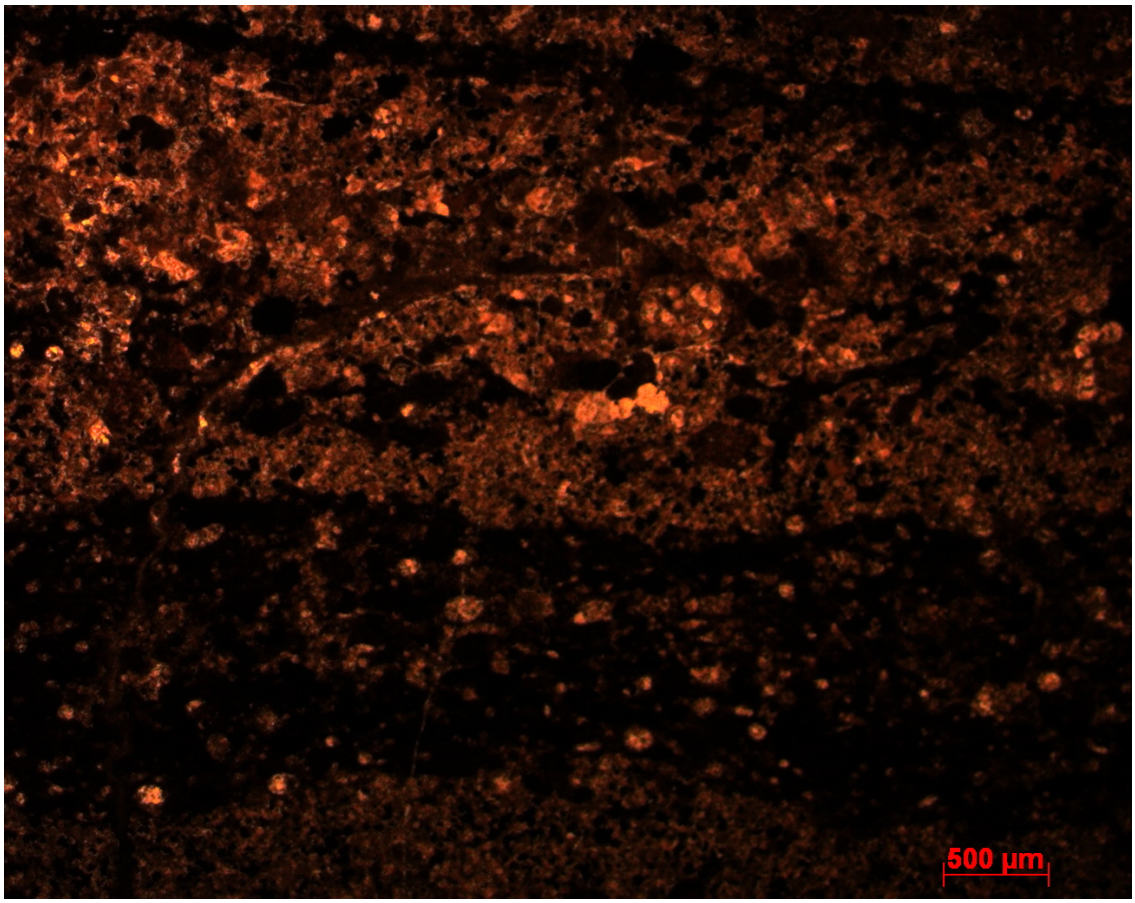

Sample: MC2-45

Height Above Buda: 45 ft

<u>Skeletal Grain Type Abundance</u>

Planktonic Foraminiferal: 60%

Calcispheres: 20%

Unidentified: 20%

Pellets 30%

Organics: 30-40%

Pyrite: 5%

Other Diagenetic Features: Highly micritized biofragments, parallel laminations and microfaults.

Rock Name: Calcareous wackestone

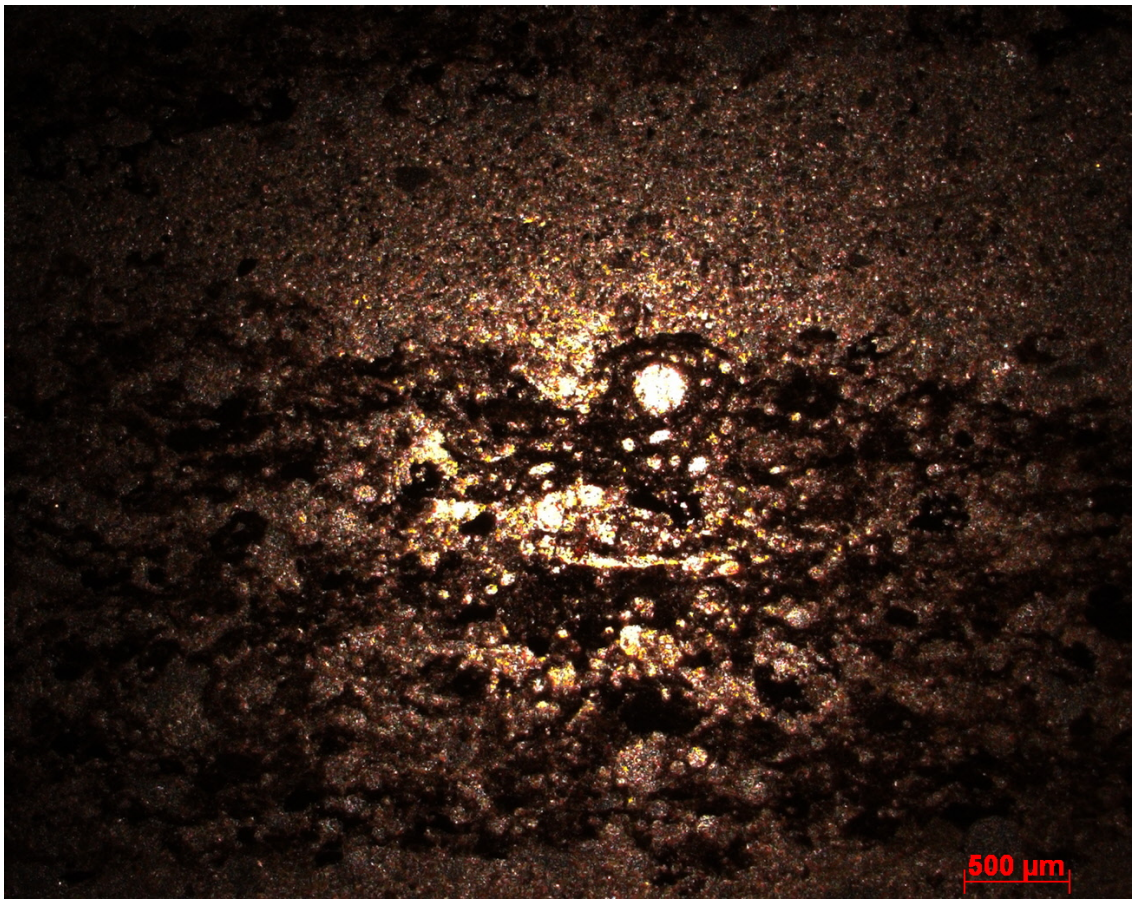

Sample: MC2-50

Height Above Buda: 50 ft

Skeletal Grain Type Abundance

Planktonic Foraminiferal: 90%

Calcispheres: 10%

Pellets 10%

Organics/mud: 70%

Other Diagenetic Features: Parallel lamination, calcite cement around calcispheres. Some small fractures.

Rock Name: Calcareous wackestone/packstone

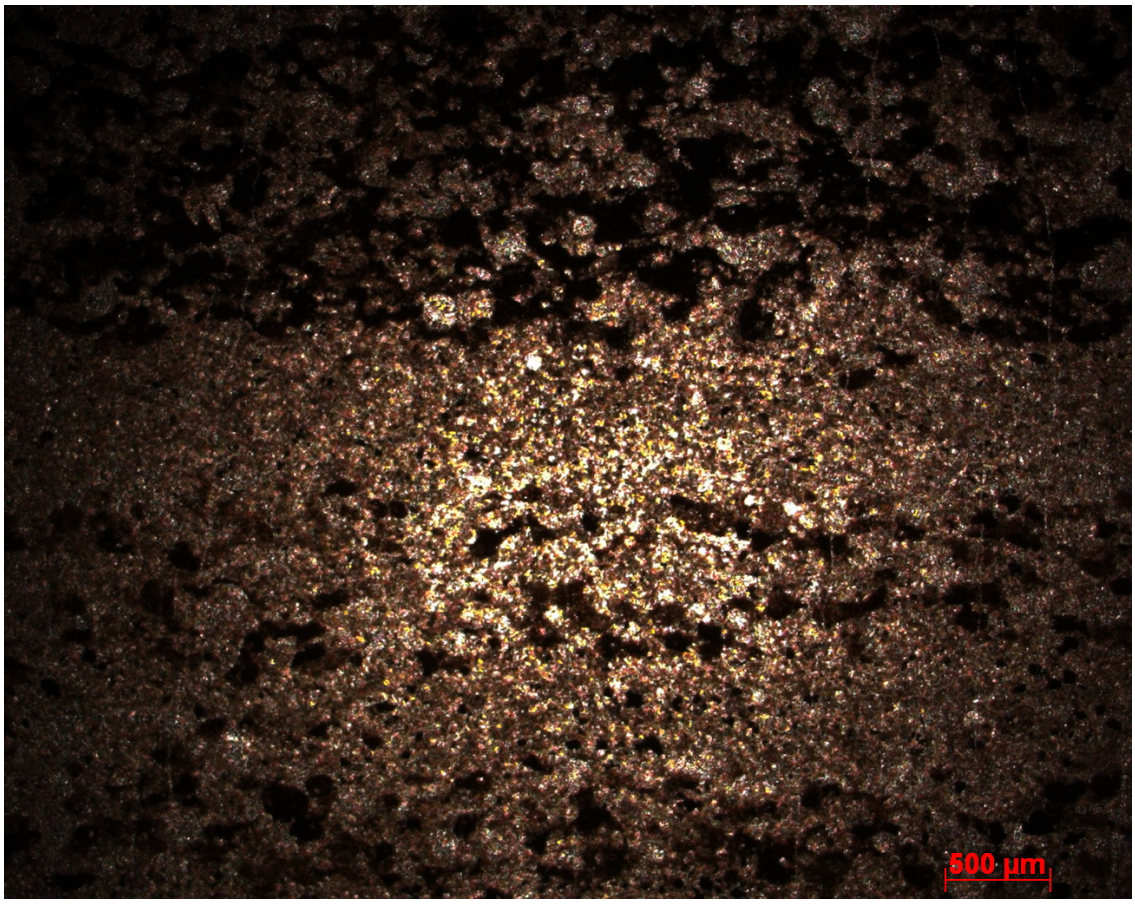

Sample: MC2-55A

Height Above Buda: 55 ft

Skeletal Grain Type Abundance

Planktonic Foraminiferal: 70%

Calcispheres: 15%

Pellets 30%

Organics/mud: 40%

Other Diagenetic Features: Micritized biofragments and calcite cement. Parallel laminations.

Rock Name: Calcareous mudstone/wackestone

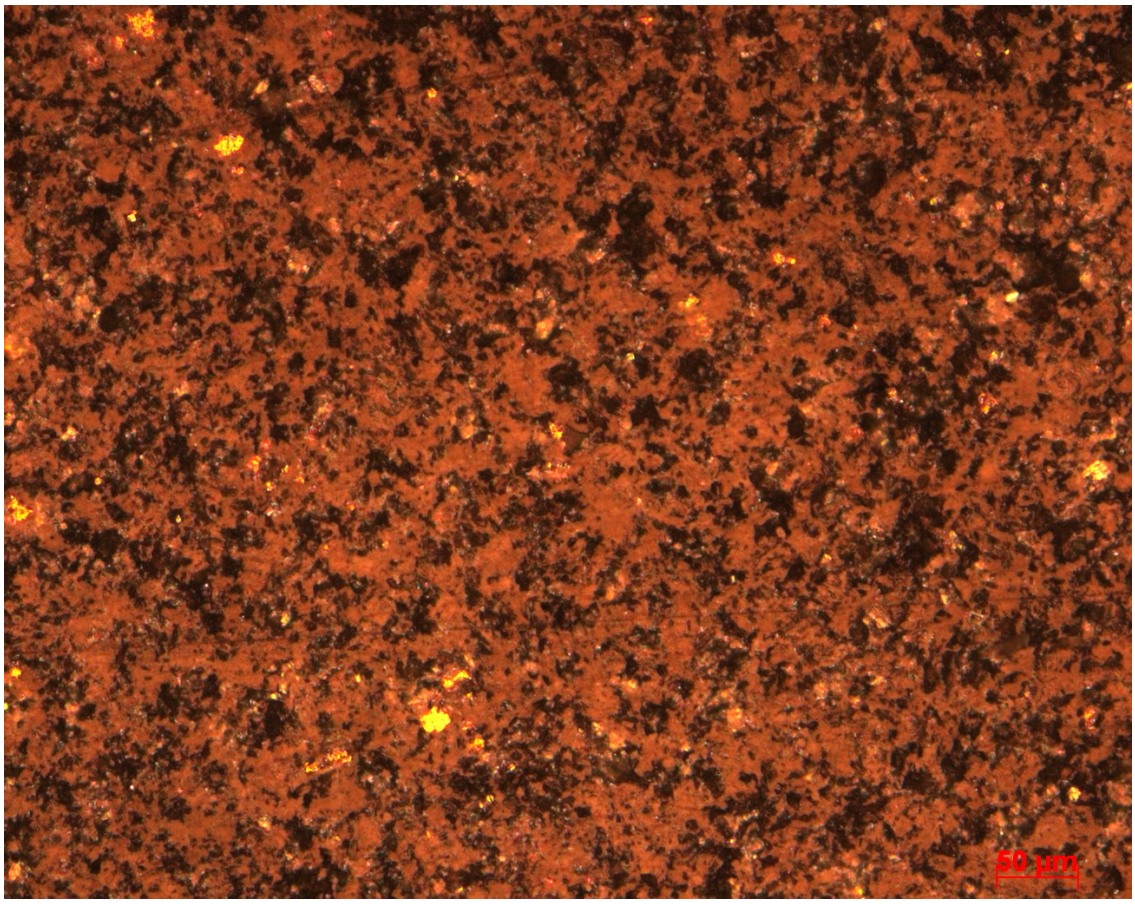

Sample: MC2-55 B

Height Above Buda: 55 B ft

Skeletal Grain Type Abundance

Planktonic Foraminiferal: 20%

Calcispheres: 10

Pellets 30%

Organics/mud: 40%

Other Diagenetic Features: Micritized biofragments and calcite cement. Parallel laminations.

Rock Name: Calcareous mudstone/wackestone

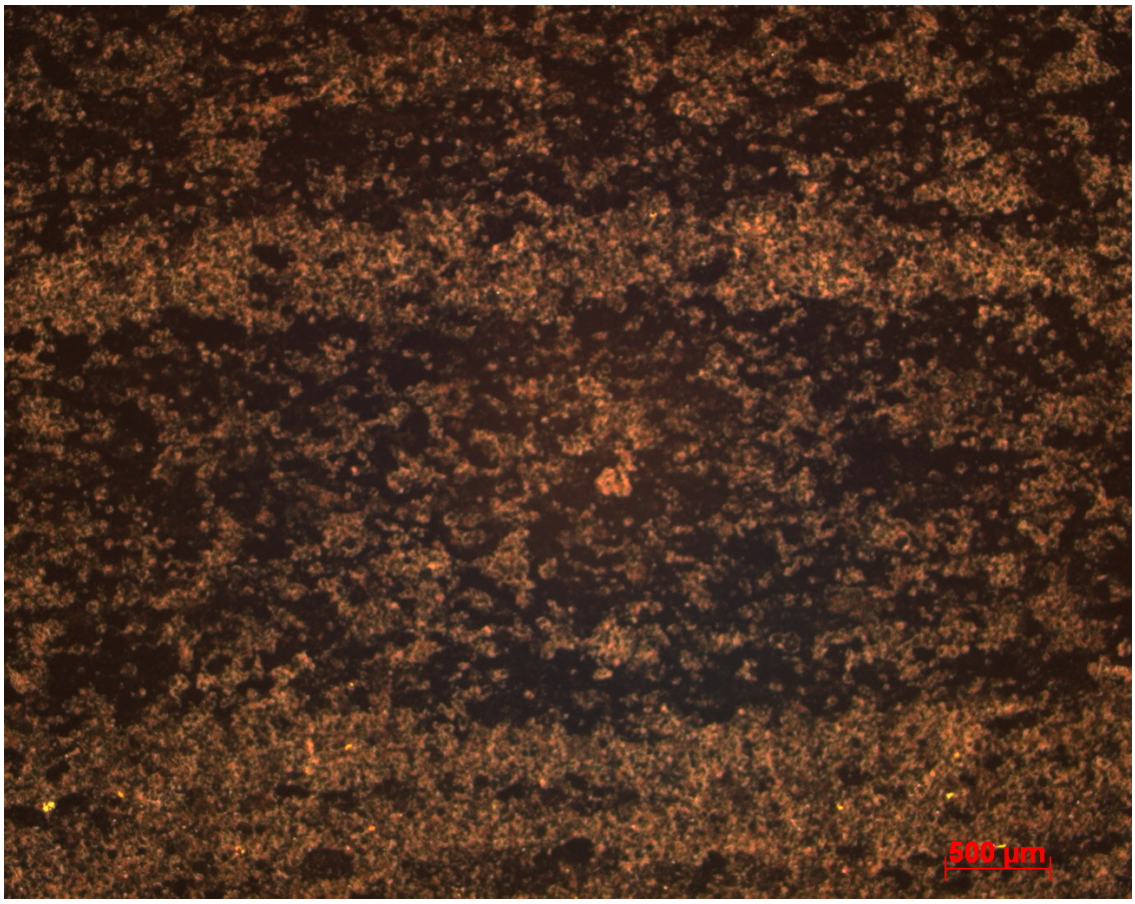

Sample: MC2-57.5

Height Above Buda: 57.5 ft

Skeletal Grain Type Abundance

Planktonic Foraminiferal: 60%

Calcispheres: 20%

Unidentified: 20%

Pellets 30%

Organics: 30-40%

Pyrite: 5%

Other Diagenetic Features: Highly micritized biofragments, parallel laminations and micrfaults.

Rock Name: Calcareous wackestone

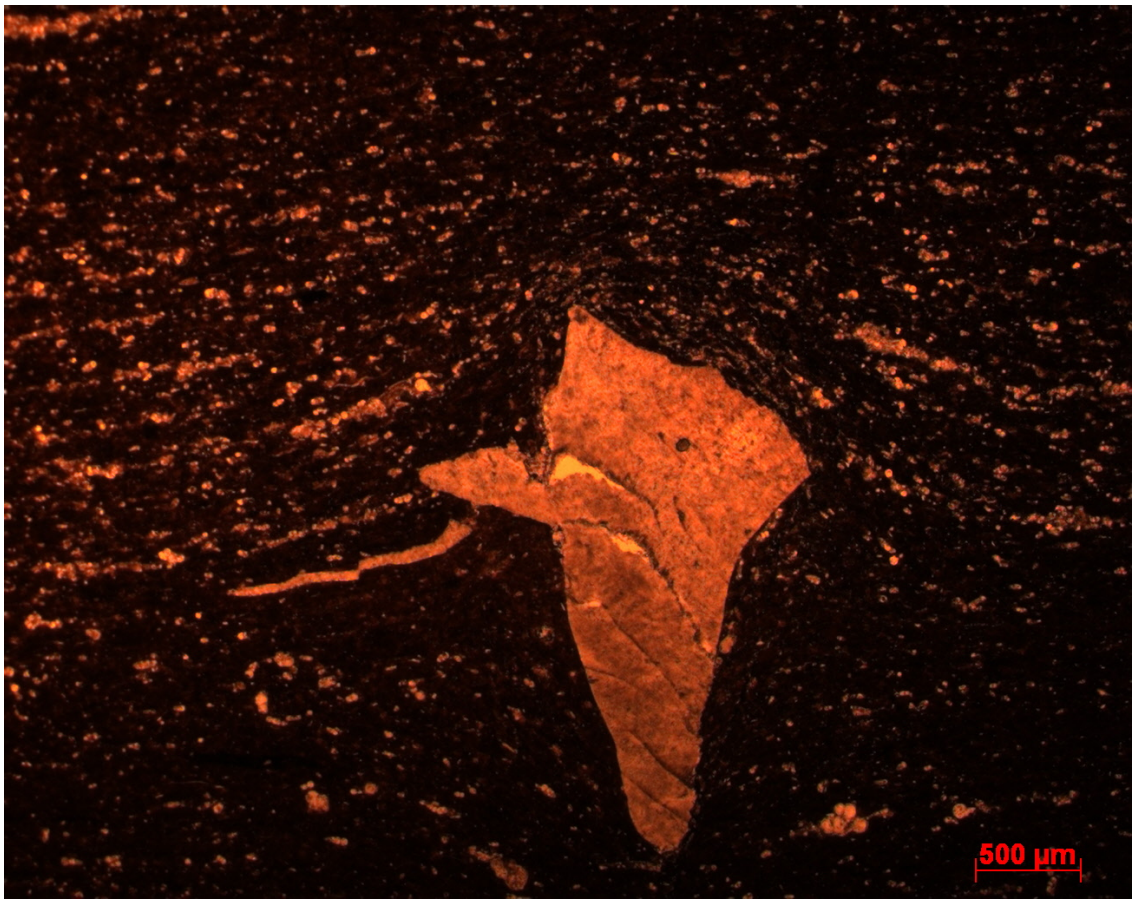

Sample: MC2-60

Height Above Buda:60 ft.

Skeletal Grain Type Abundance

Planktonic Foraminiferal: 40%

Calcispheres: 55%

Inoceramids: 5%

Pellets 40%

Organics: 30%

Other Diagenetic Features: Some calcite cement in fractures, highly micritized.

Rock Name: Foraminiferall calcareous wackestone

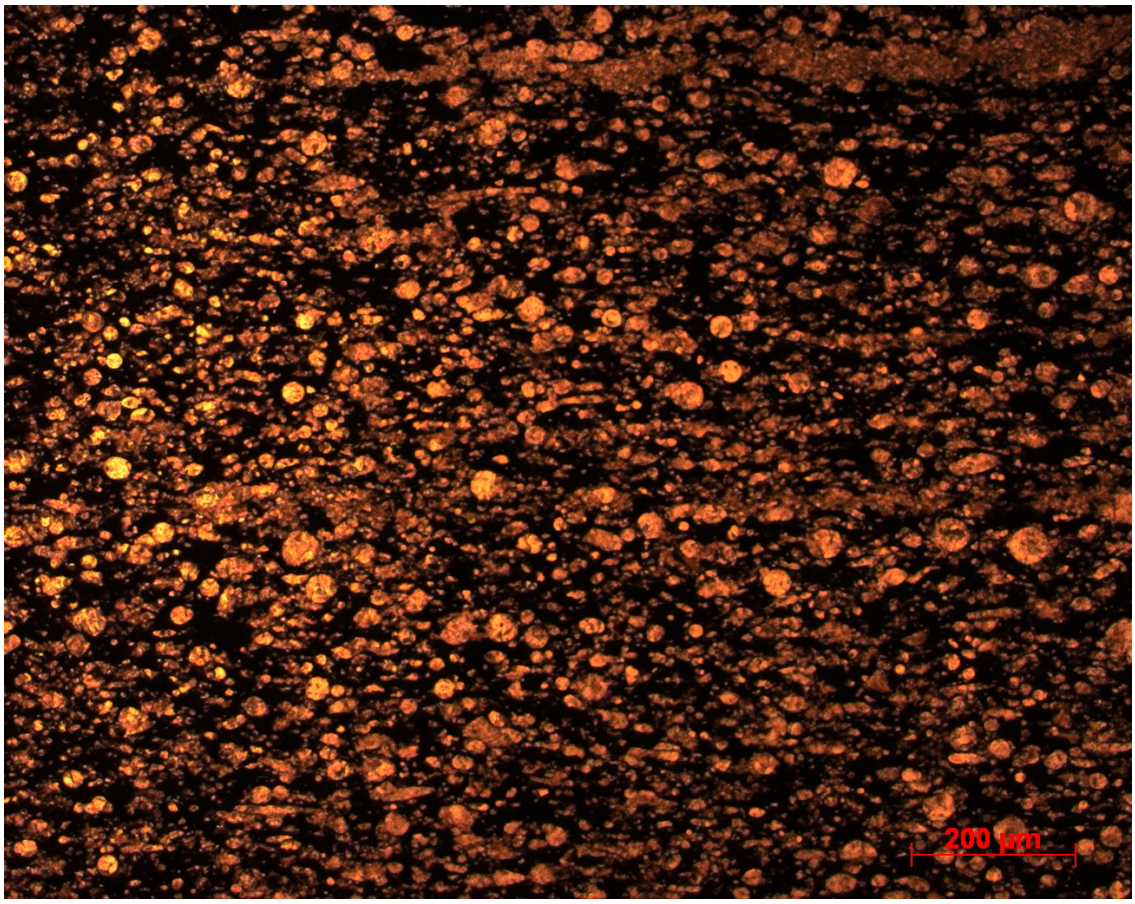

Sample: MC2-67.5

Height Above Buda: 67.5 ft

Skeletal Grain Type Abundance

Planktonic Foraminiferal: 60%

Calcispheres: 20%

Pellets: 5%

Organics/mud: 30-40%

Other Diagenetic Features: Parallel lamination some small fractures, skeletal fragments have been micritized.

Rock Name: Foraminiferall calcareous siltstone/wackestone

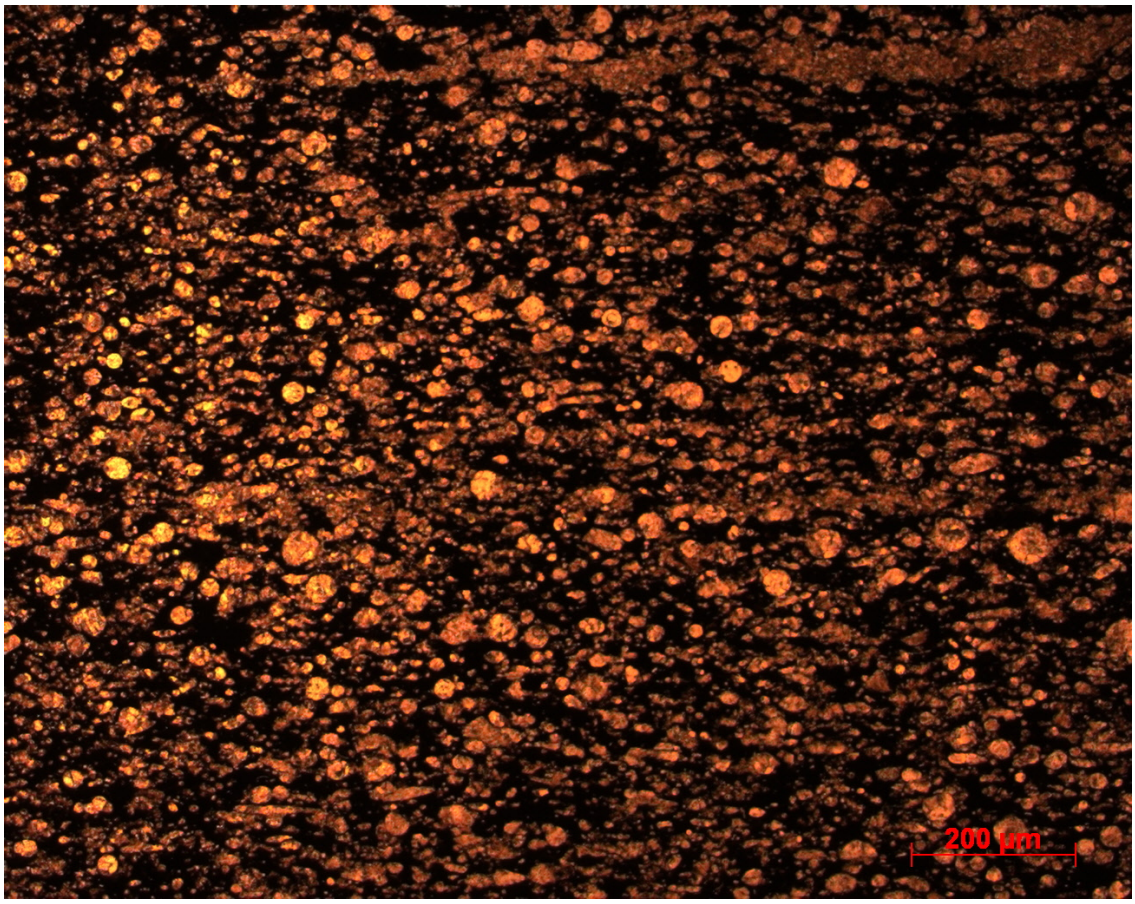

Sample: MC2-67.5

Height Above Buda: 67.5 ft

Skeletal Grain Type Abundance

Planktonic Foraminiferal: 70%

Inoceramids: 10%

Calcispheres: 20%

Pryite: 5%

Pellets: 20%

Organics/mud: 60%

Other Diagenetic Features: Partially or completely micritized biofragments with the exception of large bivalve fragments. Micrite in parallel laminations with foraminiferal.

Rock Name: Inoceramid skeletal mudstone/wackestone

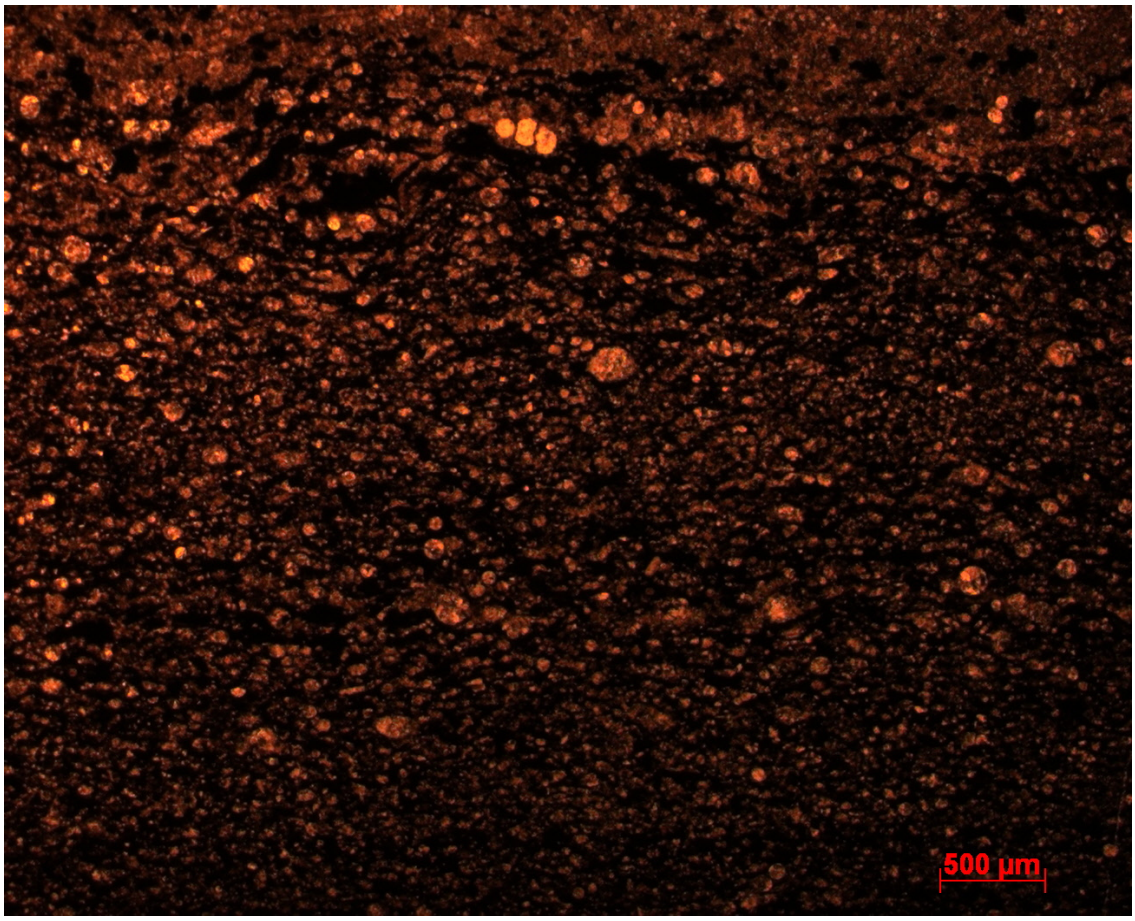

Sample: MC2-70

Height Above Buda: 70 ft

Skeletal Grain Type Abundance

Planktonic Foraminiferal: 70%

Calcispheres: 30%

Pellets 10%

Organics/mud: 80%

Other Diagenetic Features: Micritized calcispheres, gypsum filled fractures. Parallel laminations.

Rock Name: Calcareous mudstone

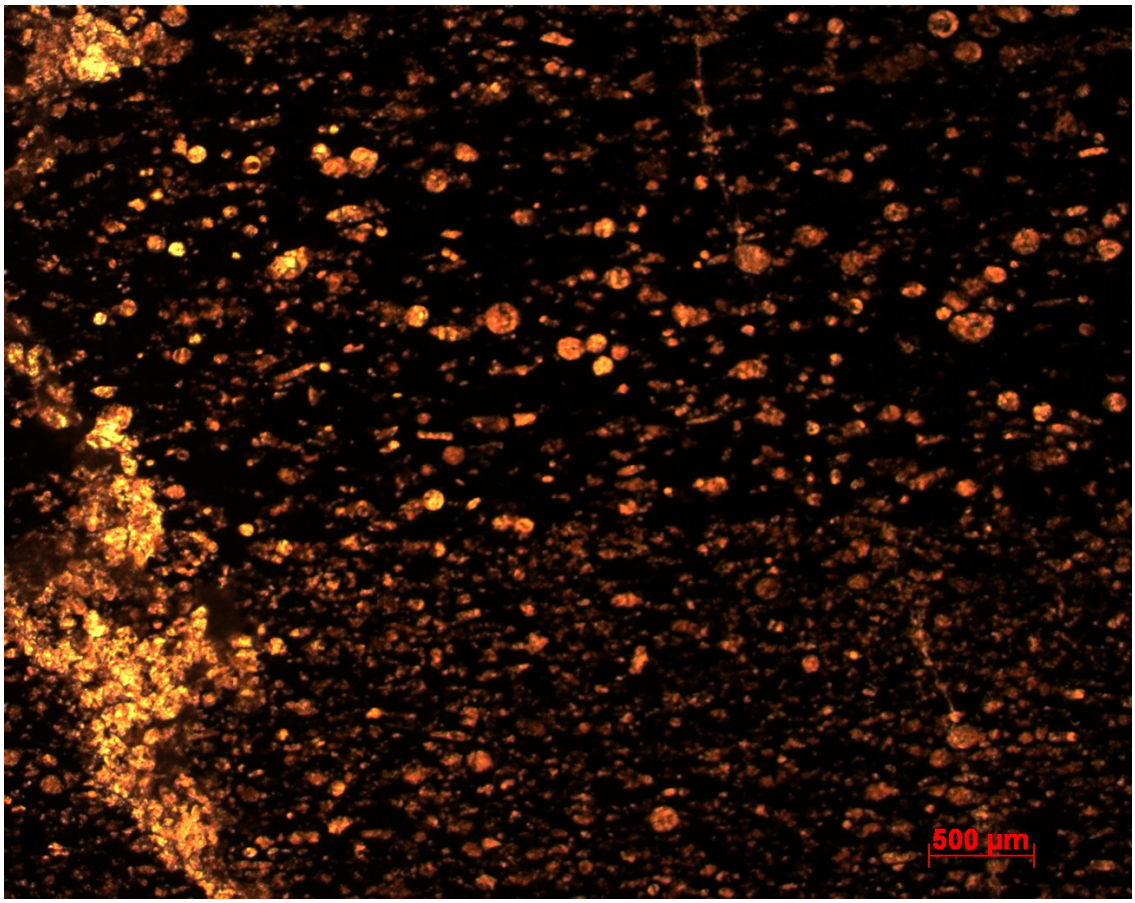

Sample: MC2-72.5

Height Above Buda: 72.5 ft

Skeletal Grain Type Abundance

Planktonic Foraminiferal: 70%

Calcispheres: 30%

Pellets 10%

Organics/mud: 80%

Other Diagenetic Features: Micritized calcispheres, gypsum filled fractures. Parallel laminations.

Rock Name: Calcareous mudstone

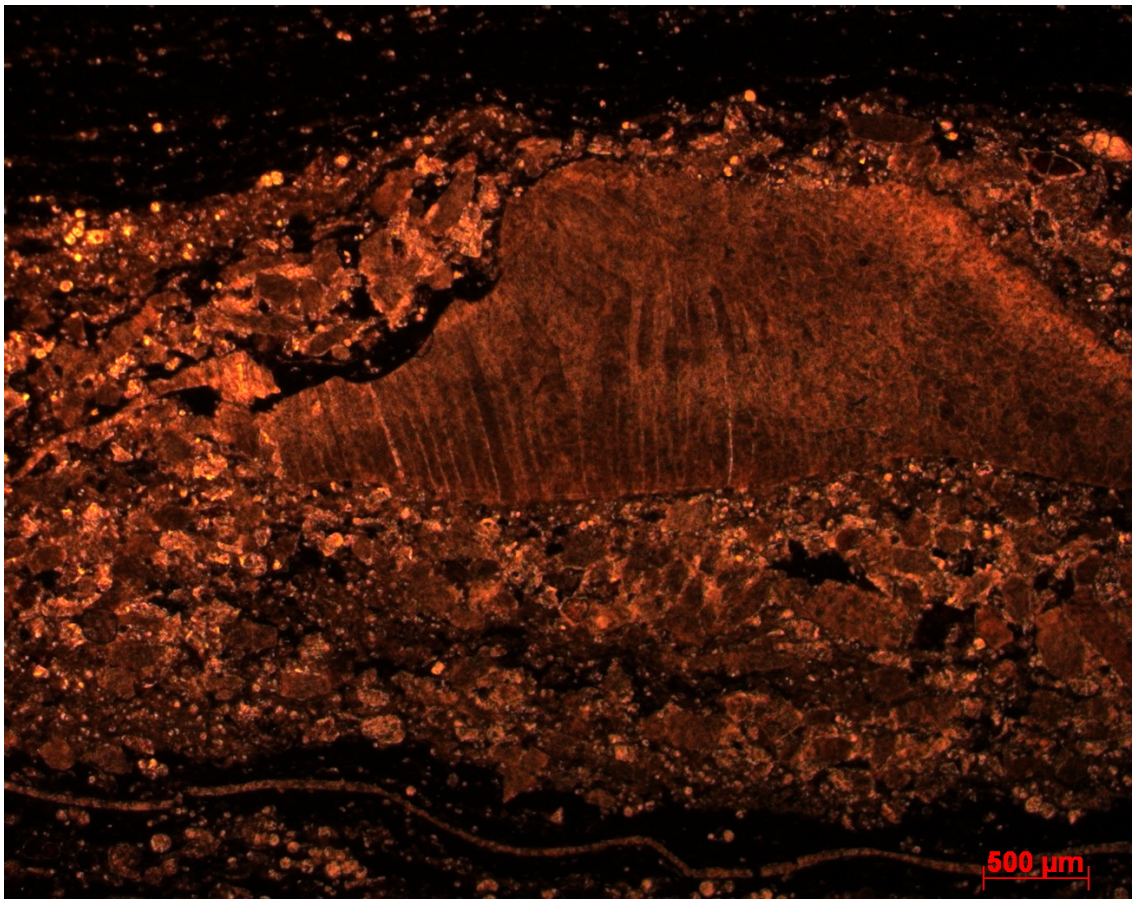

Sample: MC2-75

Height Above Buda:75 ft.
Skeletal Grain Type Abundance
Planktonic Foraminiferal: 40%
Calcispheres: 55%
Inoceramids: 5%
Pellets 40%
Organics: 30%
Other Diagenetic Features: Calcite cement in fractures, highly micritized.
Rock Name: Foraminiferall calcareous wackestone

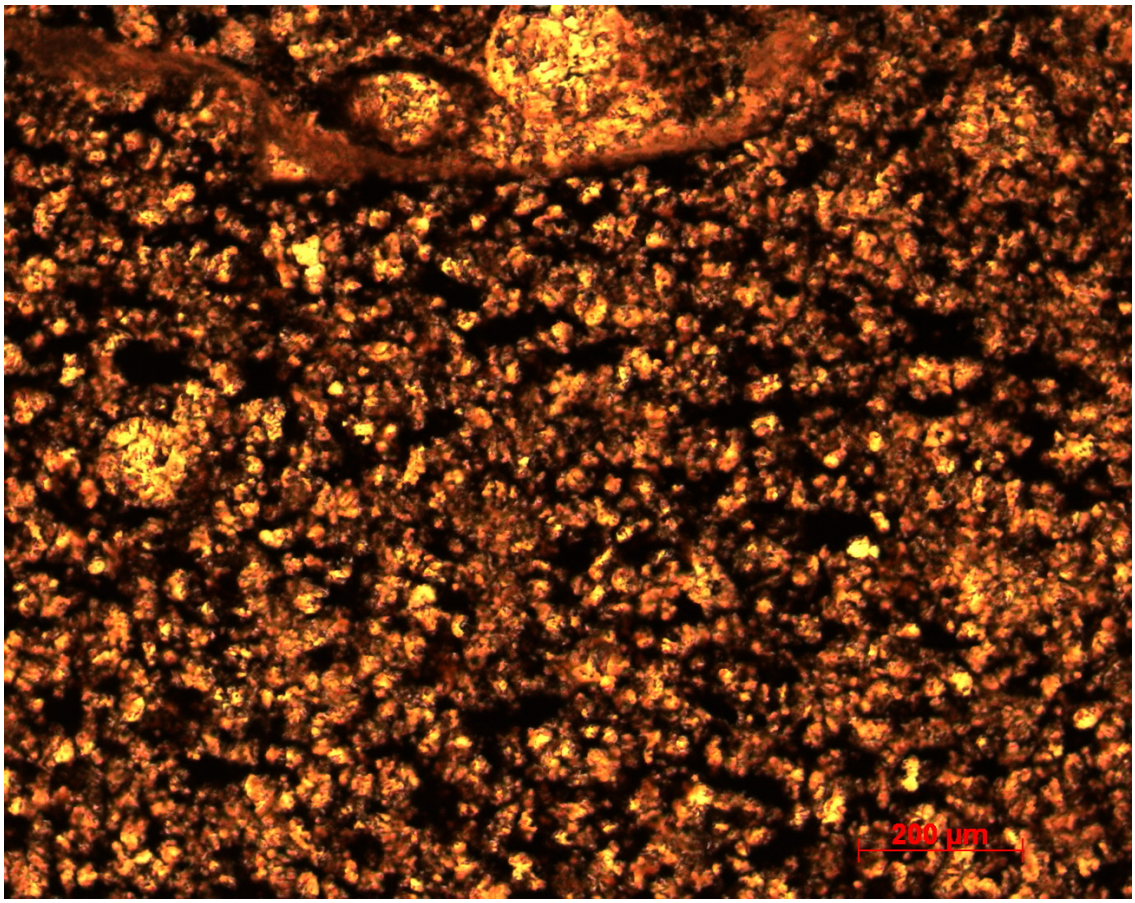

Sample: MC2-77.5

Height Above Buda: 77.5 ft

Skeletal Grain Type Abundance

Planktonic Foraminiferal: 90%

Inoceramids: 1%

Calcispheres: 10%

Pellets: 5%

Organics/mud: 30%

Other Diagenetic Features: Parallel laminations with fracture porosity and calcite infilling fractures. Smaller calcispheres and bivalve fragments micritized.

Rock Name: Calcareous mudstone/wackestone